Cooperative Wideband OFDM Communication

Proefschrift

ter verkrijging van de graad van doctor
aan de Technische Universiteit Delft,
op gezag van de Rector Magnificus Prof. ir. K. C. A. M. Luyben,
voorzitter van het College voor Promoties,
in het openbaar te verdedigen
op woensdag 6 februari 2013 om 15:00 uur

door

Hao LU

Master of Engineering, Jilin University, China,
geboren te Longyan City, Fujian Province, China.

Dit proefschrift is goedgekeurd door de promotor:

Prof. dr. ir. L.P. Ligthart

Copromotor: Dr. H. Nikookar

Samenstelling promotiecommissie:

Rector Magnificus, voorzitter

Prof. dr. ir. L.P. Ligthart,	Technische Universiteit Delft, promotor
Dr. H. Nikookar,	Technische Universiteit Delft, copromotor
Prof. Dr. E. Fledderus,	Technische Universiteit Eindhoven
Prof. Dr. H. Brezet,	Technische Universiteit Delft
Prof. Dr. R. Prasad,	Aalborg University
Prof. Dr. H. Rohling,	Technische Universitat Hamburg-Harburg
Prof. Dr. M. Ruggieri,	University of Rome Tor Vergata, Italy
Prof. P. van Genderen,	Technische Universiteit Delft, reservelid

ISBN 978-94-6186-112-2

Printed by: Proefschriftmaken.nl II Uitgeverij BOXPress

Cooperative Wideban OFDM Communication.
Thesis Delft University of Technology.

To my family

ABSTRACT

Cooperative communication means wireless nodes can help each other for communication. In this thesis, we study cooperative wideband Orthogonal Frequency Division Multiplexing (OFDM) communication, and propose a cooperative tall Toeplitz scheme for the cooperative OFDM communication system. Our scheme guarantees full cooperative diversity, outage diversity and multipath diversity, and simultaneously combats the Carrier Frequency Offsets (CFOs), by using low complex Linear Equalizers (LEs), only. Next, we investigate how to select relays and to allocate resources for improving the communication performance, and propose a hybrid OFDM cooperative strategy for multi-node wireless networks employing both Amplify-and-Forward (AF) and Decode-and-Forward (DF) relaying. The compact and closed-form Bit-Error Rate (BER) expression proposed for the hybrid AF-DF system can easily provide an insight into the results and can be a heuristic help for the design of future cooperative wideband systems. We also present a dynamic optimal selection strategy for optimal relay selection, which maximizes the BER performance of the whole system. Localization capabilities are considered as important research aspects in cooperative communication networks as well. We propose a trigger relay based cooperative localization technique with high resolution, low complexity and bandwidth efficiency. Compared to its counterparts AF and DF relays, trigger relay achieves a better performance in terms of system complexity and Time Difference of Arrival (TDOA) accuracy.

Summary

In this thesis, major attention is paid to cooperative diversity as an alternative way to achieve spatial diversity when the multiple antenna structure is not an option. By adopting the cooperative relay nodes to forward information, we can mitigate the fading effects, increase the capacity, lower the bit-error rate, increase the achievable transmission range, and without sacrificing time and bandwidth efficiency.

Orthogonal Frequency Division Multiplexing (OFDM) is a popular multicarrier modulation technique in the modern wireless communications, since it possesses the advantages of frequency parallel transmission, high speed communications and efficient spectrum usage. In this Ph.D. thesis OFDM transmission into the cooperative communication domain is investigated. The diversity gains from both spatial domain and frequency domain are combined and so cooperative communication can further enhance the reliable, high speed transmission, and enable the spectrum efficiency. We propose a cooperative OFDM tall Toeplitz scheme, which guarantees full cooperative diversity, taking outage diversity and multipath diversity into account; in addition it easily combats Carrier Frequency Offsets (CFOs), using Linear Equalizers (LEs) only. Compared to the conventionally used Maximum-Likelihood Equalizers (MLEs), the system complexity is reduced significantly.

There are mainly two relaying protocols in cooperative relay networks: Amplify-and-Forward (AF) and Decode-and-Forward (DF). In the research on relay selection and resource allocation issues in cooperative communications, we propose a dynamic optimal combination strategy for the hybrid DF-AF cooperative OFDM communications and removing unsuitable AF relays. Subsequently, we propose relay selection and resource allocation and optimization schemes for cooperative wireless communication networks with interference based on the so called Stackelberg game approach. This approach is a proper game model for solving the relay selection and power allocation problem in a distributed manner, when pricing and power allocation of the relay both are taken into account. As an extension of our research on cooperative wideband communication, we study wideband scale-lag channels as well,

present in many ultra-wideband communication applications. In our research, cooperative relaying communication network is set for multi-scale and multi-lag wideband channels. We also provide a dynamic optimal selection strategy for relay selection to take advantage of the multi-relay, multi-scale and multi-lag diversity and maximize the system Bit-Error Rate (BER) performance.

Cooperative localization research is growing when larger wireless networks are deployed and more applications are developed which require accurate position information. Therefore, cooperative locationing research becomes an important part of this Ph.D. research on cooperative wideband OFDM communications. In this research, we propose a trigger relay based cooperative localization technique. Because the trigger relay only needs to be switched on by the incoming signal, and to be sent as a simple pilot to the receiver, our technique gains from the easy processing together with noise and interference immunity of the base station to relay link. Compared to AF relay and DF relay Time Difference of Arrival (TDOA) estimation cases, the trigger relay reduces the system complexity. Meanwhile, trigger relay enables the bandwidth efficient TDOA, since it significantly reduces the amount of data for transmission. Furthermore, by exploiting cooperative-multipath diversity, the improved signal detection further contributes to a better TDOA estimation.

Samenvatting

In dit proefschrift wordt voornamelijk aandacht besteed aan ‘coöperatieve diversiteit’ als een alternatief voor het gebruik van ‘ruimtelijke diversiteit’ wanneer een meervoudige antennestructuur geen optie is. Middels coöperatieve relay knooppunten om informatie door te sturen kan het fading effect worden ingeperkt, waardoor de capaciteit kan worden verhoogd, de bit error rate verlaagd, het haalbare zendbereik vergroot en dat zonder verlies van tijd- en bandbreedte efficiency.

Orthogonal Frequency Division Multiplexing (OFDM) is een populaire multi-carrier modulatie techniek in moderne draadloze communicatie, omdat het beschikt over de voordelen van parallelle frequentie transmissie, hoge data communicatie snelheden en efficiënt gebruik van het spectrum. In dit proefschrift wordt OFDM transmissie in het domein van coöperatieve communicatie onderzocht. Profijt van diversiteit in het ruimtelijke domein en frequentie domein wordt gecombineerd, waardoor coöperatieve communicatie verbetering geeft aan betrouwbare hoge snelheid transmissie en spectrum efficiëntie. Wij stellen een coöperatieve OFDM hoge Toeplitz regeling voor, die volledige coöperatieve diversiteit waarborgt, rekening houdend met uitval van diversiteit en multi-pad diversiteit; daarnaast is het gemakkelijk om draagfrequentie offsets (CFOs) te bestrijden met behulp van alleen lineaire equalizers (LEs). Vergeleken met de gebruikelijke Maximum-Likelihood Equalizers (MLEs), wordt de complexiteit van het systeem aanzienlijk verminderd.

Er zijn hoofdzakelijk twee relay protocollen in coöperatieve relay netwerken: Amplify-and-Forward (AF) en Decode-and-Forward (DF). In het onderzoek naar relay selectie en problemen met het alloceren van de ‘resources’ in coöperatieve communicatie, komen wij met een dynamisch geoptimaliseerde combinatie strategie voor hybride DF-AF coöperatieve OFDM communicatie en met het verwijderen van de ongeschikte AF relays. Vervolgens stellen wij relay selectie, resource allocatie en optimalisatie schema’s van coöperatieve draadloze communicatienetwerken voor met een aanpak voor interferentie op basis van het zogenaamde Stackelberg spel. Deze aanpak is geschikt als spelmodel voor het oplossen van relay selectie en het probleem van vermogenstoewijzing op een gedistribueerde wijze, indien zowel het kostenaspect en als het vermogen ter plaatse van de relays in overweging

worden genomen. In het verlengde van ons onderzoek naar coöperatieve breedband communicatie, bestuderen we ook breedband 'scale-lag' kanalen, aanwezig in vele ultrabreedband communicatie toepassingen. In ons onderzoek is het coöperatieve relay communicatie netwerk opgezet voor 'multi-scale' en 'multi-lag' breedband kanalen. We geven ook een dynamisch geoptimaliseerde strategie voor relay selectie om te profiteren van multi-relay, multi-scale en multi-lag diversiteit alsmede voor het maximaliseren van de Bir-Error Rate (BER) systeem prestaties.

Coöperatieve lokalisatie onderzoek groeit als grotere draadloze netwerken worden opgezet en meer toepassingen nauwkeurige positie-informatie vereisen. Daarom is coöperatieve lokalisatie een belangrijk onderdeel geworden in dit proefschrift over coöperatieve breedband OFDM communicatie. In dit onderzoek komen wij met een voorstel voor trigger relay als coöperatieve lokalisatie techniek. De trigger relay hoeft alleen te worden ingeschakeld door het inkomende signaal. Vervolgens hoeft alleen een eenvoudige 'piloot toon' naar de ontvanger te worden versturen. De door ons voorgestelde techniek heeft als voordeel eenvoudige processing alsmede ruis- en interferentie immuniteit tussen het basisstation en de relay verbindingen. Uit vergelijking van AF relay en DF relay (TDOA) met de geschatte van tijdsverschillen van aankomst bepaald. De trigger relay reduceert de complexiteit van het systeem en verbetert de bandbreedte TDOA efficiëntie, daar de hoeveelheid data gegevens voor overdracht aanzienlijk minder is. Bovendien, door gebruik te maken van coöperatieve multi-pad diversiteit wordt de signaal detectie verbeterd en draagt zo verder bij aan een betere TDOA schatting.

Contents

Chapter 1

Introduction

1.1 Research background

In the past decades, wireless communication has benefited from a variety of technology advancements and it is considered as the key enabling technique of innovative future consumer products. As shown in Fig. 1.1, in order to satisfy the requirements of various applications from generation to generation, many kinds of innovations in wireless technologies and devices have been developed and utilized in our daily life. In future, significantly technical achievements are required to ensure that wireless communications have appropriate architectures suitable for supporting a wider range of services and higher speed data transmission delivered to the users.

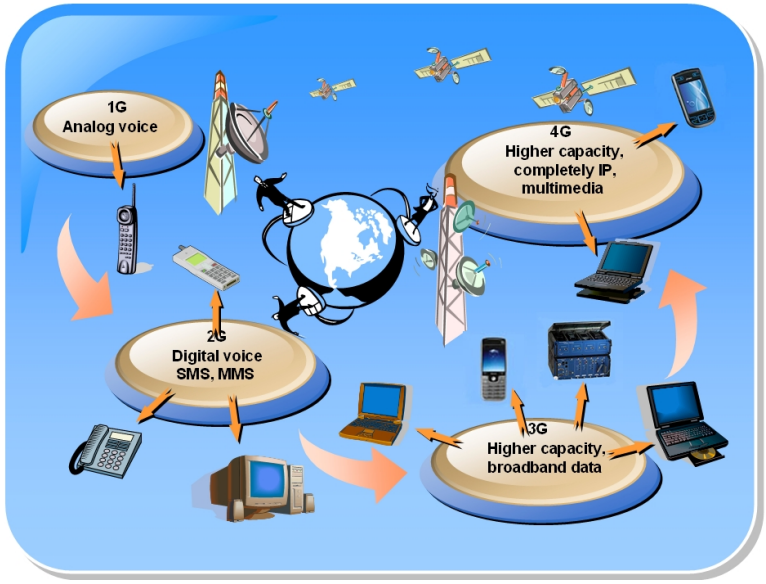

Fig. 1.1. Wireless communications require transmission of more and more sophisticated, high-speed wireless data.

In the foreseeable future, the large-scale deployment of wireless devices and the requirements of high bandwidth applications are expected to lead to tremendous new challenges in terms of efficient

exploitation of the achievable spectral resources. The coming wireless personal communication systems are expected to provide ubiquitous, high-quality, and high-rate mobile multimedia transmission. However, in order to achieve this objective, various technical challenges need to be overcome. Signal fading due to multi-path propagation is one of the major impairments to meet the demands of next generation wireless networks for high data rate services. To mitigate the fading effects, time, frequency, and spatial diversity techniques or their combinations can be used. Among different types of diversity techniques, spatial diversity is of a special interest as is does not incur the system losses in terms of delay and bandwidth efficiency. Spatial diversity has been studied intensively in the context of Multiple-Input-Multiple-Output (MIMO) systems [1]. It has been shown that utilizing MIMO systems can significantly improve the system throughput and reliability [2]. However, MIMO gains hinge on the independence of the paths between transmit and receive antennas, for which one must guarantee antenna element separation several times the wavelength, a requirement difficult to meet with the small-size terminals. To overcome this problem, and to benefit from the performance enhanced by MIMO systems, cooperative diversity schemes for the relay transmission have been introduced in [3-5].

Recently, the research on cooperative communication is extremely active [6]. In Europe, the Enhanced Wireless Communication Systems Employing COperative DIVersity [7] and NEWCOM++ [8] are two famous international projects; include a lot of state of the art on the cooperative communication research.

1.1.1 Cooperative relaying techniques

In cooperative communication, the two most common cooperative relaying protocols are decode-and-forward (DF) and amplify-and-forward (AF). In AF, the received signal is amplified and retransmitted to the destination. The advantage of this protocol is its simplicity and low-cost implementation. However, the noise is also amplified at the relay. In DF, the relay attempts to decode the received signals. If successful, it re-encodes the information and retransmits it. If some relays cannot fully decode the signal, they will be discarded.

Recently, there is another new relaying protocol, which is called Compress-and-Forward (CF), some scholars classified it into the DF protocol [6]. CF attempts to generate an estimate of the received signal. This is then compressed, encoded, and transmitted with the hope that the estimated value may assist in decoding the original code word at the destination. The tradeoff between the time-consuming decoding for a better cooperative transmission and finding the optimum hybrid cooperative relaying schemes, that include both DF and AF for different situations, is an important issue for the cooperative communication networks design.

1.1.2 Cooperative Orthogonal Frequency Division Multiplexing (OFDM) communication

Among the existing air-interface techniques, OFDM is a promising technique for high-bit-rate wireless communications [9]. It possesses the advantages of frequency parallel transmission, high speed communication and efficient spectrum usage. By introducing OFDM transmission into the cooperative communication domain, the gains from both sides are combined. When transmitted through the multipath channel, OFDM can help that cooperative communication gain from multipath diversity.

Most conventional OFDM-based wireless communication systems append Cyclic Prefix (CP) to provide robustness against multipath effects. However, the same multipath robustness can be obtained by adopting a Zero-Padding (ZP) prefix instead of CP [10, 11]. When ZP takes the place of CP in OFDM symbols, the transmitted power can be reduced usually up to 25% and the ripples in the Power Spectral Density (PSD) can be reduced significantly. This is a prominent advantage for future green wireless communication with low power transmission. Furthermore, ZP-OFDM systems provide advantages over CP-OFDM in terms of more accurate blind time synchronization, better blind channel estimation and elimination of the frequency response channel null problem, i.e., ZP-OFDM guarantees full symbol recovery and regardless if the zeros are located at the discrete channel's frequency response. Therefore, how to improve the cooperative ZP-OFDM communication performance in terms of diversity, capacity and complexity is of great importance.

1.1.3 Relay selection and resource allocation

Relay selection and resource allocation play important roles in cooperative communication. When the channel between the source node and the destination node suffers from severe fading, the direct transmission from the source node to the destination node will have poor performance. By using the cooperative relaying scheme, the source node can find relay nodes which have better channels to the destination node. Adopting these better relays to forward the signal to the destination node, the cooperative communication increases the reliability of the whole transmission. Selecting the relay nodes closer to the source node, it can also save battery power, since the source node does not have to transmit at high power and can use the relays' power to perform the transmission instead. The saving of the power by relay selection in cooperative communication can contribute in this way to the so called "green communication" with low power transmission.

After the relay selection, the resource allocation is another optimization issue in the cooperative communication network. Allocating the optimal resource to the proper relay nodes with different objectives in the system is required to obtain best performance from the cooperative communication network. In a cooperative communication network, because both relay nodes and source node hope to maximize their own benefits through resource allocation and optimization, it will have a more complicated resource allocation and optimization process than where the objective is only to maximize the source node benefit.

The so called "game theory" in solving problems for wireless communication has been gaining a lot of attention recently. In the field of cooperative communication, the game theory approach has been used in many aspects, especially in resource optimization and managing the relay nodes behavior. The game theory approach is used because it can model the behavior of nodes in real world situations, and perform multi-objective optimization. In this thesis work, we attempt to formulate the relay selection criterion and resource allocation and optimization which fulfill the practical situation and obtain optimal results in the system performance using the game theory approach.

1.1.4 Cooperative wideband localization

Nowadays, wireless network systems (with their ability to support mobility) are widely deployed to provide different services. It has been recognized that the location awareness is a cornerstone for future wireless network for Ubiquitous Computing. RF-based positioning built on existing wireless infrastructures can provide cost-effective implementations.

Generally, in the Line-of-Sight (LOS) scenario, high-accuracy positioning can be achieved using high-power base stations or a high-density base station deployment, both of which are cost prohibitive and impractical in realistic settings [3]. A practical way to address this need is through a combination of cooperative localization and wideband transmission, which is investigated in this thesis.

1.2 Research motivation

1.2.1 Application of cooperative mobile communication

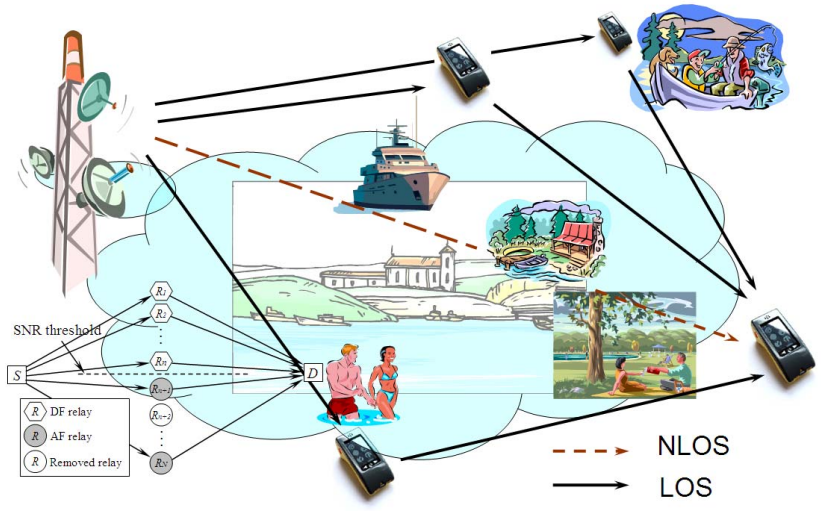

Fig. 1.2. Application of cooperative relay (mobile handset) communication.

The application of cooperative mobile communication can be illustrated as in Fig. 1.2. The mobile handsets, which have a cooperative capability, form a cooperative relay network. These relays decode and forward or amplify and forward the data to the target, when the direct transmission cannot perform so well. The mechanism of this cooperative

communication is theoretically represented as a hybrid DF-AF network, as shown in the left down corner of Fig. 1.2. In cooperative mobile communication, the broadcast nature, long considered as a significant waste of energy causing interference to others, is now regarded as a potential resource for possible assistance. Such a new viewpoint has brought various new communication applications that improve communication capacity, speed, and performance, reduce battery consumption and extend network lifetime, increase the throughput and stability region for multiple access schemes, expand the transmission coverage area and provide a cooperative tradeoff in source-channel coding schemes for multimedia communication.

1.2.2 Cooperative communication for Internet of Things

The Internet of Things as shown in the Fig. 1.3 [12] is a term for a wireless network between objects, such as sensors, automation controllers, cars, and household appliances to communicate via Machine-to-Machine (M2M) protocols to automate their functions without human intervention. If all powered things (as coffee makers, thermostats, cameras) are equipped with small Internet-capable radios and an automation system is built to report their status, location, and receive control commands, human life will undergo a vast technological transformation.

Fig. 1.3. Internet of Things for the Future.

In this massive and complex wireless system, the interference caused

by different signals will become very severe. Meanwhile, the transmission speeds for different applications are quite different, e.g., sending a video stream to the handset monitor needs a data rate up to Mega bits/s, while the state information of equipment only requires several bits. Therefore, in the future Internet of Things, cooperative communication technology will become a promising solution. The nodes in the self-organized cooperative network can help each other to improve the communication capacity and transmission performance, can reduce battery consumption and extend network life time, can increase the throughput and stability region, can expand the transmission coverage area, and can enhance the localization capability.

1.2.3 Cooperative networks for wireless tracking systems

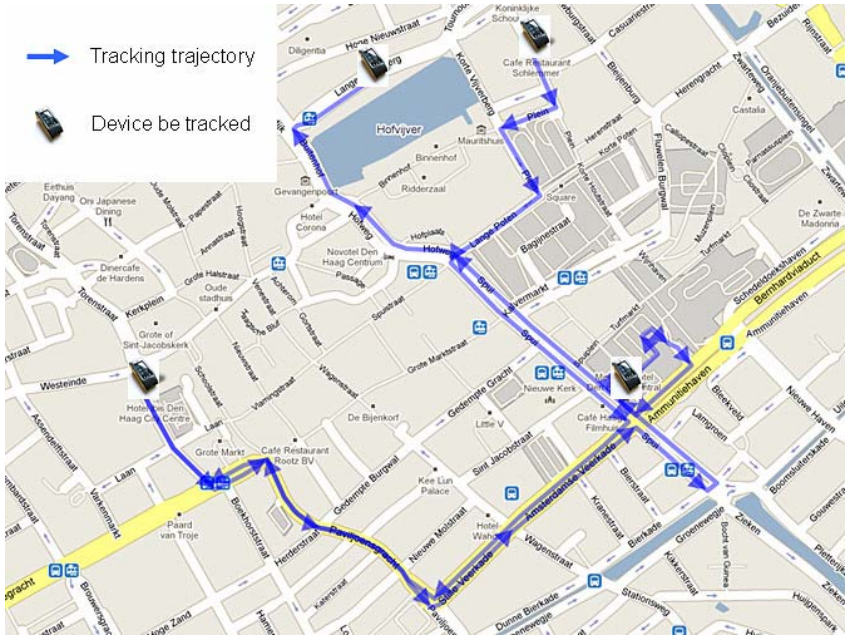

Fig. 1.4. Tracking wireless devices and illustrating their trajectories.

If cooperative localization can be implemented in future wireless systems, many compelling new applications can be enable. It is very useful to track mobile handsets over time and over a wide range, as shown in Fig. 1.4. Such tracking can answer questions about the holder's behavior, speed, and interaction with others. Using current practices, tracking is a difficult, expensive process that requires bulky tags which rapidly run out of energy. A typical practice is GPS, but these tags are

limited by cost concerns and offer only a short lifetime due to high energy consumption. Using multi-hop routing of location data through the wireless sensor networks can dramatically improve the abilities of localization and enable low transmit powers. Furthermore, inter-handset distances, which are of particular interest to localization and tracking, can be estimated using pair-wise measurements and cooperative localization method without resorting to GPS.

Switching from outdoor positioning to indoor positioning is an important challenge for the future wireless tracking system as well, as shown in the Fig. 1.5. In the indoor environment, GPS can not work properly, but the cooperative network can still provide accurate positioning information.

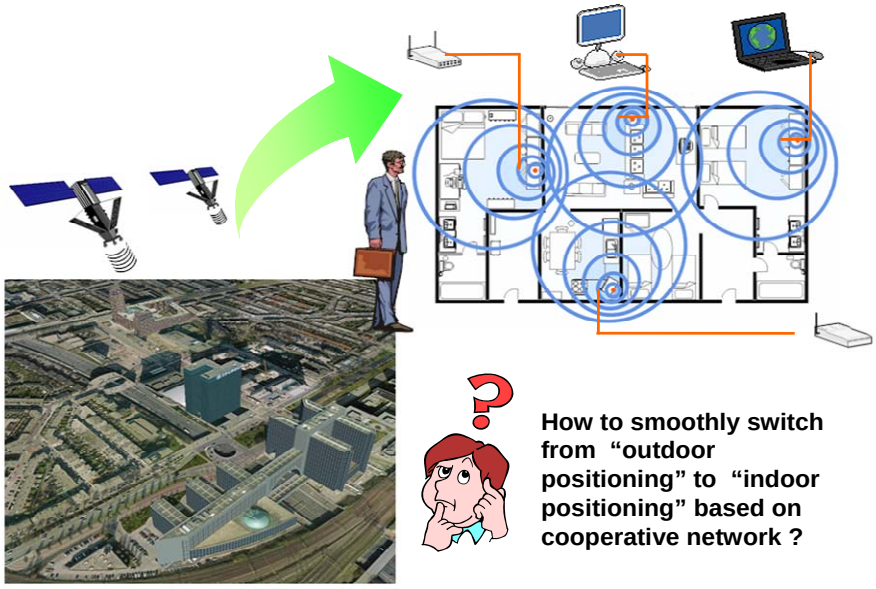

Fig. 1.5. Switching from outdoor position to the indoor position by cooperative networks.

A similar technology can be extended to animal tracking for the purpose of biological research.

1.2.4 Cooperative wireless sensor networks for manufacturing and logistics

As an example in logistics, we consider the deploying of a cooperative wireless sensor network in an office building, manufacturing floor, and warehouse.

Sensors already play a very important role in manufacturing and logistics. The monitoring and control of machinery has traditionally been wired, but making these sensors wireless reduces the high cost and weight of cabling and makes the usage more flexible. Deploying a cooperative wireless sensor network in an office building, manufacturing floor, and warehouse will make that future manufacturing and logistics become more intelligent and need lower power consumption. An automatic localization capability of these cooperative sensors will further increase automation as well.

Radio-Frequency Identification (RFID) tags, such as those required by Wal-Mart on pallets and cartons entering its warehouses, represent a first step in warehouse logistics. RFID tags are only located when they pass within a few feet of a reader, thus remaining out of access most of their time in the warehouse. RFID based on cooperative wireless sensors, however, can be queried and located as long as they are within range of the closest other wireless sensor, and can so improve the transmission reliability.

Furthermore, boxes and parts in a warehouse as well as in a factory and on office equipment can all be tagged with cooperative sensors. These sensors monitor storage conditions (temperature and humidity) and help to control the heating, ventilation, and air conditioning system. Sensors on mobile equipment report their location when the equipment is lost or needs to be found (e.g., during inventory), and even contact security if the equipment is about to “walk out” of the building. Knowing where parts and equipment are when they are critically required, reduces the need to have duplicates as backup, savings which could pay for the cooperative wireless sensor network itself.

1.3 Novelties and achievements

Recently, cooperative communication has received much attention and has been considered as a promising technique to use the broadcast nature of the wireless channels to make communicating nodes help each other to gain from the spatial diversity. The cooperative mechanism enlarges

the communication coverage, enhances the capacity and improves the transmission performance. OFDM possesses the advantages of frequency parallel transmission, high speed communication and efficient spectrum usage. By introducing OFDM transmission into the cooperative communication domain, the gains from both sides are combined. When transmitted through the multipath channel, OFDM can help cooperative communication to gain from multipath diversity. Therefore, in this thesis, we investigate cooperative wideband OFDM communication, and how to select the relay and to allocate the resources for improving the communication performance. The localization capability is another aspect in the cooperative communication network as well.

First, we focus on the performance of cooperative wideband communication based on ZP-OFDM. As mentioned before, the ZP-OFDM systems provide advantages over CP-OFDM in terms of transmission power saving, accurate blind time synchronization, better blind channel estimation and elimination of the frequency response channel null problem. In this research, we investigate the diversity, capacity and complexity issues of cooperative ZP-OFDM communication. We consider cooperative ZP-OFDM communication over a multipath Rayleigh channel and with multiple Carrier Frequency Offsets (CFOs) existing at different relays. We use a cooperative tall Toeplitz scheme to achieve full cooperative and multipath diversity, while simultaneously the CFOs can be combated. Importantly, this full diversity scheme only requires Linear Equalizers (LEs), such as Zero-Forcing (ZF) and Minimum Mean Square Error (MMSE) equalizers, an issue which reduces the system complexity when compared to Maximum-Likelihood Equalizers (MLE) or other near-MLEs. Theoretical analysis of the proposed cooperative tall Toeplitz scheme is provided on the basis of an analytical upper bound of the channel orthogonality deficiency derived in this thesis. Utilizing only low-complexity linear equalizers, theoretical analysis and simulation results show that the proposed Toeplitz scheme achieves full cooperative, multipath and outage diversity.

In this thesis, we also study relay selection and resource allocation issues in cooperative communication.

In this research, first, we propose a threshold scheme for the division

of DF and AF relays. Then, we propose a dynamic optimal combination strategy for the hybrid DF-AF cooperation and for removing unsuitable AF relays. The OFDM technique is utilized to resolve the multi-path in each cooperative link. Based on space-frequency coding, the hybrid cooperative OFDM can even gain from multi-path, and so obtains a multi-path diversity gain. In our research, a closed-form error probability expression for the suggested hybrid DF-AF cooperative OFDM network, under Rayleigh channel, is also provided. The resulting expression is general as it holds for an arbitrary number of cooperating DF-AF branches.

Subsequently, we propose relay selection and resource allocation and optimization schemes for cooperative wireless communication networks with interference using a game theoretical approach. We choose for a pricing game for such cooperative communication networks with interference based on the so-called Stackelberg game. Simulation results show that interference in the cooperative communication network can change the relay selection and resource allocation and optimization result, For this reason interference should not be neglected from the calculations; we can then predict the behavior of the system in an environment closer to real world situations, compared to the case that only noise is considered in the system. We found out that the pricing game for resource allocation and optimization, when the number of available nodes is high, can result in a high payment to relay nodes which will so highly reduce the source node utility function. Therefore, we propose an algorithm to limit the number of selected relay nodes to mitigate this problem. Using this algorithm, we chose for a number of relay nodes where the result of resource allocation and optimization is still beneficial for the value of source node utility function.

Wideband scale-lag channels can be found in many applications, including ultra-wideband communication and underwater acoustic communication. Signaling and reception schemes using the wavelet theory enable the multi-scale and multi-lag diversity in a wideband system. In our research, we design a cooperative wavelet scheme for the multi-relay, multi-scale and multi-lag diversity, which can be widely applied in the ultra-wideband communication and underwater acoustic communication. A cooperative relaying communication network has been set up for multi-scale and multi-lag wideband channels. Then, an analytical bit error rate (BER) expression for the cooperative wavelet

wideband communication system is presented, which can be used to predict the system performance. Based on this analytical BER expression, we also provide a dynamic optimal selection strategy for relay selection to take advantage of the multi-relay, multi-scale and multi-lag diversity and to maximize the system BER performance.

Location-awareness plays a crucial role in many wireless applications in commercial, public and military sectors. The performance of wireless positioning technology can be significantly improved via the use of cooperation between the wireless nodes. In our research, we investigate the cooperative relaying issue of the OFDM technique to estimate Time Difference of Arrival (TDOA) for locationing applications. Statistical features of OFDM blocks (symbols) are studied in this thesis to achieve a bandwidth efficient transmission and a low computational burden for TDOA estimation. In order to benefit from the easy processing of AF relay as well as the noise and interference cancellation of DF relay schemes, we introduce the so-called trigger relay technique for TDOA estimation. The trigger relay possesses the merit of bandwidth efficiency, since only a short pilot or preamble needs to be sent. Compared to its counterparts AF and DF relays, trigger relay achieves a better performance in terms of system complexity and TDOA accuracy. Gaining from cooperative-multipath diversity, the trigger relay TDOA resolution can be improved even further.

1.4 Outline of the thesis

The organization of this thesis is as follows:

Chapter 2 provides an overview of the fundamental background knowledge of our research in cooperative communication. The development history from MIMO to cooperative communication is introduced. It focuses on the infrastructure of the cooperative communication, but also the Amplify and Forward (AF) relay and Decode and Forward (DF) relay and their combination are reviewed. Orthogonal Frequency Division Multiplexing (OFDM), who is a favorite multicarrier modulation technique in modern communication, possesses the advantage of frequency parallel transmission, high speed communication and efficient spectrum usage. By integrating OFDM into cooperative communication, the gains from both are combined. Cyclic

Prefix (CP)-OFDM and its counterpart Zero Padding (ZP)-OFDM are briefly reviewed in this chapter. From the viewpoint of optimizing cooperative communication, conventional methods and Game theoretical approaches for relay selection and resource allocation are introduced. Cooperative localization as a new aspect in cooperative communication is reviewed in this chapter as well.

Chapter 3 describes our research on cooperative ZP-OFDM wideband communication. It first gives the system model of the DF protocol based cooperative ZP-OFDM communication system with a multipath channel and multiple CFOs. Then, it provides a cooperative tall Toeplitz scheme to illustrate the full diversity design. Different equalization schemes and the concept of channel orthogonality deficiency are shown in this chapter. This chapter also justifies the full cooperative and multipath diversity with CFOs and LEs by using the presented cooperative tall Toeplitz scheme. The upper bound of the channel orthogonality deficiency of the cooperative tall Toeplitz scheme is derived to elucidate the parameter's effect. In this chapter, we analyze and discuss the capacity and decoding complexity of different equalizers. Simulation results are illustrated to corroborate the theoretical claims.

In the Chapter 4, we study the relay selection and resource allocation in cooperative communication. Section 4.2 investigates the BER performance based relay selection for cooperative communication. Section 4.3 focuses on the Game theory based relay selection and resource allocation. Section 4.4 addresses the relay selection problem for cooperative communication over multi-scale and multi-lag wireless channels.

In chapter 5, we investigate the cooperative relaying issue of OFDM technique to estimate TDOA for cooperative localization applications. The conventional cooperative TDOA estimations based on AF relay and DF relay are reviewed. Then, the cooperative feature-based localization with DF relay is described, where the Peak to Average Power Ratio (PAPR) is proposed as the best feature for cooperative feature-based localization. A 2-step TDOA computation process to meet the different accurate localization requirements is proposed in this chapter. In order to combine the merits of AF relay and DF relay, the trigger relay TDOA estimation is introduced. The TDOA estimation performances of different relaying schemes are shown and analyzed. Results illustrate

that the trigger relay TDOA has advantages in bandwidth efficiency, system complexity and resolution. Cooperative multi-path diversity design for cooperative TDOA with trigger relay is illustrated in this chapter as well.

Chapter 6 summarizes all main results of the thesis, draws overall conclusions and gives some recommendations for future works.

Chapter 2

Theoretical backgrounds of cooperative wideband radio communication

2.1 Introduction

Signal fading due to the non-wired propagation is one of the major impairments to meet the demands of next generation wireless networks for reliable and high data rate services. To mitigate the fading effects, time, frequency, and spatial diversity techniques or their combinations can be used. Among different types of diversity techniques, spatial diversity is of special interest as it does not incur system losses in terms of delay and bandwidth efficiency.

Recently, cooperative diversity in wireless network has received great interest and is regarded as a promising technique to mitigate signal fading, which results in signal loss or fluctuation in the amplitude of the received signal. Cooperative communication is a new communication paradigm which generates independent paths between the user and the base station by introducing a relay channel. The relay channel can be thought of as an auxiliary channel to the direct channel between the source and destination. The basic idea behind cooperation is that several users in a network pool their resources in order to form a virtual antenna array which creates spatial diversity [3-5]. Since the relay node is usually at several or more wavelengths distant from the source, the relay channel is guaranteed to fade independently from the direct channel, which introduces a full-rank Multiple-Input-Multiple-Output (MIMO) channel between the source and the destination. This cooperative spatial diversity leads to improvement of the communication performance in terms of Bit-Error-Rate (BER) performance and channel capacity [6].

In this chapter, an overview of fundamental background knowledge of our research in cooperative communication is provided. In Section 2.2, the development history from MIMO to cooperative communication is introduced. In Section 2.3, we focus on the infrastructure of the cooperative communication, but also the Amplify and Forward (AF) relay and Decode and Forward (DF) relay and their combination are reviewed. Orthogonal Frequency Division Multiplexing (OFDM), which

is a favorite multi-carrier modulation technique in modern communications, possesses the advantage of frequency parallel transmission, high speed communication and efficient spectrum usage. By integrating OFDM into cooperative communication, the gains from both are combined. In Section 2.4, Cyclic Prefix (CP)-OFDM and its counterpart Zero Padding (ZP)-OFDM are briefly reviewed. From the viewpoint of optimizing cooperative communication, conventional methods and Game theoretical approaches for relay selection and resource allocation are introduced in Section 2.5,. Cooperative localization as a new aspect in cooperative communication is reviewed in Section 2.6. Finally, Section 2.7 concludes this chapter.

2.2 History: From MIMO to cooperative communication

For spatial diversity, high data rates and reliable wireless transmissions can only be achieved for full-rank[1] MIMO users [6]. To overcome the limitations of achieving MIMO gains in future wireless networks, we must think of a new technology beyond the traditional point-to-point communication. This brought us to what is known as cooperative communication and networking, which allows different users or nodes in a wireless network to share resources and to create collaboration by means of distributed transmission, in which each user's information is transmitted not only by the user but also by collaborating users [13]. Cooperative communication and networking is a new communication paradigm that promises significant capacity and multiplexing gain increases in wireless networks [14, 15]. It realizes a new form of spatial diversity to combat the detrimental effects of severe fading by mimicking the MIMO, while getting rid of the drawbacks of MIMO such as size limitation and correlated channels [3-5].

MIMO system designs comprise of multiple antennas at both the transmitter and receiver to offer significant increases in data throughput and link range without additional expenditure in frequency and time domain. Spatial diversity has been studied intensively in the context of MIMO systems. It has been shown that utilizing MIMO systems can significantly improve system throughput and reliability [2].

[1]If the channel matrix of the MIMO users is an m by n matrix $\mathbb{H}$, Full rank means a minimum number of independent rows or columns of $\mathbb{H}$, i.e., $\text{rank}(\mathbb{H}) = \min(m,n)$.

In the MIMO system, high data rates and reliable wireless communications are guaranteed by full-rank MIMO users. More specifically, full-rank MIMO users should have multiple antennas at the mobile terminal, and these antennas should see independent channel fades to the multiple antennas located at the base station. In practice, not all users can guarantee such high rates because they either do not have multiple antennas installed on their small-size devices, or the propagation environment cannot support MIMO because, for example, there is not enough independent scattering. In the latter case, even if the user has multiple antennas installed, full-rank MIMO is not achieved because the paths between several antenna elements are not uncorrelated.

The traditional view of a wireless system is that it is a set of nodes trying to communicate with each other. From a different viewpoint, and by considering the broadcast nature of the wireless channel, we can regard those nodes as a set of antennas geographically distributed in the wireless network. By adopting this point of view, nodes in the network can cooperate together for distributed transmission and for processing the information. The cooperating node acts as a relay node for the source node. Since the relay node is usually at several or more wavelengths distant from the source, the relay channel is guaranteed to fade independently from the direct channel. In this way, a full-rank MIMO channel between the source and the destination is obtained. In the cooperative communication setup, there is a-priori constraint for cooperative nodes receiving useful energy that has been emitted by the transmitting node. The new paradigm in user cooperation is that, by implementing the appropriate signal processing algorithms at the nodes of the network, multiple receiving terminals can process the transmissions coming from other nodes and can enhance the radio performance by relaying information for each other. The relayed information is subsequently combined at a destination node so as to create spatial diversity. This creates a network that can be regarded as a system implementing a distributed multiple antenna where collaborating nodes create diverse signal paths for each other [6]. Therefore, we study next the cooperative relay communication system, and consequently, the AF relay, DF relay, as well as their combination protocol are described.

2.3 Infrastructure: relays in cooperative communication

Cooperative relay communication is a new paradigm shift for the next

generation wireless system that will guarantee high data rates to all users in the network. It is anticipated to be the key technology aspect in the fifth generation wireless networks [6].

In terms of research ascendance, the communication based on cooperative relays can be seen as related to research on the relay channel and on MIMO systems. The concept of user cooperation itself was introduced in two parts [4, 5]. In these works, Sendonaris *et al.* proposed a two-user cooperation system, in which pairs of terminals in the wireless network are coupled to help each other forming a distributed two-antenna system. Cooperative communication allows different users or nodes in a wireless network to share resources and to create collaboration through distributed transmission and processing, in which each user's information is sent out not only by the user but also by the collaborating users [13]. Cooperative relay communication promises a significant capacity and multiplexing gain increase in the wireless system [14, 15]. It also realizes a new form of space diversity to combat the detrimental effects of severe fading. There are mainly two relaying protocols: AF and DF.

2.3.1 Amplify and forward (AF) protocol

In AF, the received signal is amplified and retransmitted to the destination. The advantage of this protocol is its simplicity and low cost implementation. But the noise is also amplified at the relay.

The AF relay channel can be modeled as follows. The signal transmitted from the source x is received at both the relay (r) and destination (D) as

$$y_{S,r} = \sqrt{E_S} h_{S,r} x + n_{S,r} ,$$

$$\text{and} \quad y_{S,D} = \sqrt{E_S} h_{S,D} x + n_{S,D} , \qquad (2\text{-}1)$$

where $h_{S,r}$ and $h_{S,D}$ are the channel gains between source and relay and source and destination, respectively; they are modeled as Rayleigh flat fading channels. The terms $n_{S,r}$ and $n_{S,D}$ denote the additive white Gaussian noise with zero-mean and variance N_0, E_S is the transmission energy per bit at the source node. In this protocol, the relay amplifies the

signal from the source and forwards it to the destination ideally to equalize the effect of the channel fading between the source and the relay. The relay does that by simply scaling the received signal by a factor A_r that is inversely proportional to the received energy and is denoted by

$$A_r = \sqrt{\frac{E_S}{E_S h_{S,r} + N_0}}, \qquad (2\text{-}2)$$

The destination receives two copies from the signal *x* through the source link and relay link. There are different techniques to combine the two signals at the destination. The optimal technique that maximizes the overall Signal-to-Noise Ratio (SNR) is the Maximal Ratio Combiner (MRC). Note that the MRC combining requires a coherent detector that has knowledge of all channel coefficients, and the SNR at the output of the MRC is equal to the sum of the received signal-to-noise ratios from all branches.

2.3.2 Decode and forward (DF) protocol

Another protocol is termed as a decode-and-forward scheme, which is often simply called DF protocol. In DF, the relay attempts to decode the received signals. If successful, it re-encodes the information and retransmits it. Although the DF protocol has the advantage over the AF protocol in reducing the effects of additive noise at the relay, the system complexity will be increased to guarantee correct signal detection.

Note that the decoded signal at the relay may be incorrect. If an incorrect signal is forwarded to the destination, the decoding at the destination is meaningless. It is clear that for such a scheme the diversity achieved is only one, because the performance of the system is limited by the worst link from the source-relay and source-destination [3].

Although DF relaying has the advantage over AF relaying in reducing the effects of noise and interference at the relay, it entails the possibility of forwarding erroneously detected signals to the destination, causing error propagation that can diminish the performance of the system. The mutual information between the source and the destination is limited by the mutual information of the weakest link between the source-relay and the combined channel from the source-destination and relay-destination.

Since reliable decoding is not always available, it also means that the DF protocol is not always suitable for all relaying situations. The trade off between the time-consuming decoding, and a better cooperative transmission, finding the optimum hybrid cooperative schemes, that include both DF and AF for different situations, is an important issue for the cooperative wireless network design.

2.3.3 Hybrid DF/AF protocol

Hybrid DF/AF protocol means a cooperative network that includes both DF relay and AF relay. We consider a hybrid DF/AF cooperative strategy as shown in Fig. 2.1, where we transmit data from source node S to destination node D through R relays, without the direct link between S and D. This relay structure is called 2-hop relay system, i.e., first hop from source node to relay, and second hop from relay to destination. The channel fading for different links are assumed to be identical, statistically independent, and quasi-static, i.e., channels are constant within several transmitted symbol durations. This is a reasonable assumption as the relays are usually spatially well separated and in a slowly changing environment. We assume that the channels are well known at the corresponding receiver sides. All the Additive White Gaussian Noise (AWGN) terms have equal variance N_0.

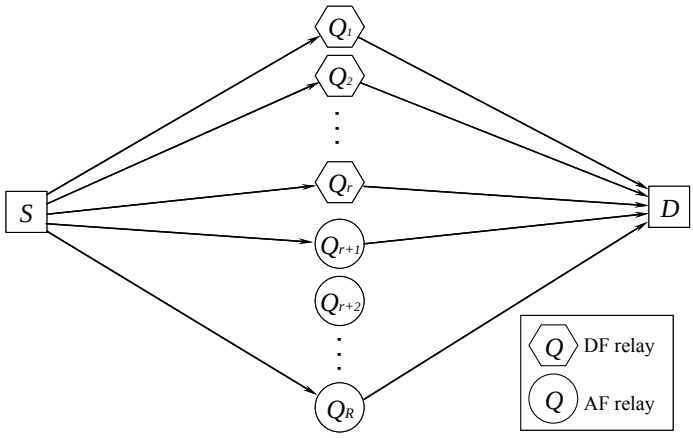

Fig. 2.1. Hybrid cooperation with DF/AF relays (S: Source, D: Destination, Q_r: r-th Relay).

We suppose the DF relays can fully decode the signal from the source. The received SNR at the destination in the hybrid DF/AF cooperative relay network can be denoted as [16, 17],

$$\gamma_h = \sum_{Q_i \in \mathrm{DF}} \frac{E_Q h_{Q_i,D}}{N_0} + \sum_{Q_j \in \mathrm{AF}} \frac{\dfrac{E_S h_{S,Q_j}}{N_0} \dfrac{E_Q h_{Q_j,D}}{N_0}}{\dfrac{E_S h_{S,Q_j}}{N_0} + \dfrac{E_Q h_{Q_j,D}}{N_0} + 1}, \tag{2-3}$$

where $h_{Q_i,D}$ denotes the power gain of the channel from the *i*-th relay to the destination in the DF protocol, h_{S,Q_j} denotes the power gain of the channel from the source node to the *j*-th relay in the AF protocol, and $h_{Q_j,D}$ denotes the power gain of the channel from the *j*-th relay to the destination in the AF protocol, respectively. E_S and E_Q in Eq. (2-3) are the transmission energy per bit at the source node and at the relays, respectively. By choosing the amplification factor A_{Q_j} in the AF protocol as:

$$A_{Q_j}^2 = \frac{E_S}{E_S h_{S,Q_j} + N_0}, \tag{2-4}$$

and forcing E_Q in DF equal to E_S, it will be convenient to maintain constant transmission energy at relays, equal to the original transmitted energy at the source node.

It is apparent that at high SNR, the last term in the denominator of Eq. (2-4) is negligible, and thus Eq. (2-3) reduces to

$$\gamma_h = \sum_{Q_i \in \mathrm{DF}} \frac{E_S h_{Q_i,D}}{N_0} + \sum_{Q_j \in \mathrm{AF}} \frac{\dfrac{E_S h_{S,Q_j}}{N_0} \dfrac{E_S h_{Q_j,D}}{N_0}}{\dfrac{E_S h_{S,Q_j}}{N_0} + \dfrac{E_S h_{Q_j,D}}{N_0}}. \tag{2-5}$$

According to the general parameterization method, which has been rigorized in [18, 19], we can obtain a general asymptotic average error

probability expression P_e for the hybrid cooperative network under Ricean fading

$$P_e \approx \frac{C(R)(K+1)^{R+1}}{k^{R+1}} \prod_{Q_i \in \mathrm{DF}} \frac{1}{\frac{E_S h_{Q_i,D}}{N_0}} \prod_{Q_j \in \mathrm{AF}} \left(\frac{1}{\frac{E_S h_{S,Q_j}}{N_0}} + \frac{1}{\frac{E_S h_{Q_j,D}}{N_0}} \right). \qquad (2\text{-}6)$$

In this expression, K is the so-called specular factor; for Rayleigh fading links $K = 1$, [19]; parameter k is determined by specific constellations; for Binary Phase Shift Keying (BPSK) modulation $k = 2$; for M-PSK $k = 2\sin^2(\pi/M)$ and for M-Quadrature Amplitude Modulation (QAM) $k = 3/(M\text{-}1)$. In Eq. (2-6),

$$C(R) = \left(\prod_{r=1}^{R+1} (2r-1) \right) \Big/ \left(2(R+1)!\, r^{(R+1)} \right) \qquad (2\text{-}7)$$

is a constant that depends on the number of cooperating branches R. Its first values are $C(1) = (3/4)$, $C(2) = (5/4)$, and $C(3) = (35/16)$.

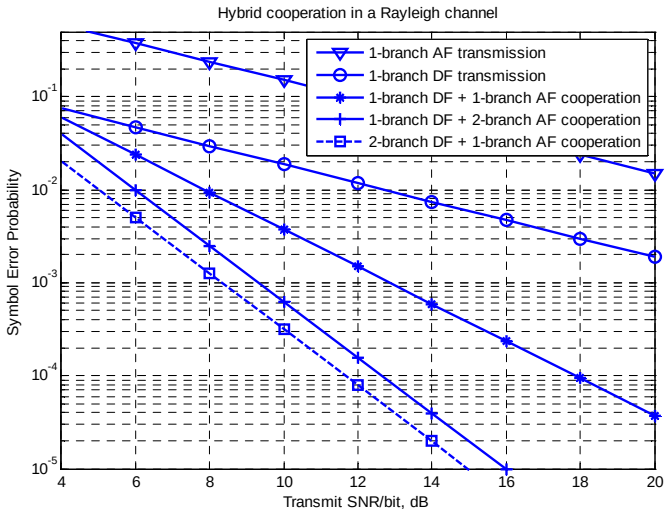

Fig. 2.2.Asymptotic error probability performance for hybrid cooperation in a Rayleigh channel.

We show in Fig. 2.2 an example to demonstrate the hybrid DF/AF cooperation, where we adopt BPSK modulation (k = 2), Rayleigh fading (K = 1), and R= 1, 2, 3. The resulting average error probabilities were plotted against the transmit SNR defined as SNR = E_s/N_0. We assume that $h_{Q_i,D} = h_{S,Q_j} = h_{Q_j,D} = 1$, for all branches. It can be seen from the figure that, in hybrid cooperative networks with reliable decoding, DF plays a more important role than AF. We formulate this characteristic of the DF/AF hybrid cooperation by the following theorem:

Theorem 2.1: For an L-hops relay link, with full decoding in the DF protocol, and as long as the SNR of the last hop is larger than $1/L$ times of the arithmetic mean of the whole link SNR, DF always plays a more important role than AF in improving the error probability performance. The proof of this theorem is given in Appendix 2.1.

In this thesis, we investigate different types of relay techniques in the cooperative communication, focus on the hybrid DF/AF relaying networks, and propose a selection scheme to pick up the proper DF and AF relays and improve the BER performance of the hybrid DF/AF relaying networks.

In this research, we consider a hybrid cooperative strategy for multi-node wireless networks employing both DF and AF relaying. Fully decoding is guaranteed by simply comparing SNRs at relay nodes to the SNR threshold, which is more efficient than utilizing conventional cyclic redundant checking code. The lower bound and the upper bound of the SNR threshold are provided as well. After correct decoding, the DF protocol outperforms the AF protocol in terms of BER performance, which can be seen from Monte Carlo simulation as well as analytical results. These results justify that the DF protocol dominates the hybrid cooperation strategy. For the suggested hybrid DF-AF cooperation protocol, we also represent a dynamic optimal combination strategy for the optimal AF selection. The closed-form BER expression of the hybrid cooperation in Rayleigh fading channel can be derived. The agreement between the analytical curves and numerical simulated results (as illustrated in Fig. 4.10 and Fig. 4.11) shows that the derived closed-form BER expression is suitable for the DF-dominant hybrid cooperation protocol. The compact and closed-form BER expression can easily provide an insight into the results as well as a heuristic help for the

design of future cooperative wireless systems.

2.4 Multi-carrier modulation: OFDM

In the modern wireless communication, OFDM technology has been widely used due to its spectral efficiency and inherent flexibility in allocating power and bit rate over distinct subcarriers which are orthogonal to each other. Different from serial transmission, OFDM is a multi-carrier block transmission, where, as the name suggests, information-bearing symbols are processed in blocks at both the transmitter and the receiver.

In particular, thanks to the Inverse Fast Fourier Transform (IFFT) precoding and the insertion of the so-called guard interval at the transmitter, the OFDM signals are not only orthogonal in the frequency domain, but also temporally orthogonal to each other. At the receiver side, the guard interval is discarded to avoid Inter-Symbol Interference (ISI); each truncated OFDM symbol is Fast Fourier Transformed (FFT) — an operation converting the frequency-selective channel into parallel flat-faded independent subchannels. Since the subchannel gains equal to the channel's frequency response value on the FFT grid, each subchannel can be easily equalized by a single-tap equalizer using a scalar division.

Utilizing the OFDM technique in cooperative communication, and transmitting the data in parallel, reliable high speed transmission can be achieved. Meanwhile, because of the OFDM technique the deleterious effect of fading is spread over many bits, and therefore instead of a few adjacent bits are completely destroyed by the fading, each bit is slightly affected by the fading. Another important advantage of OFDM is the performance of orthogonal sub-carriers, which enables efficient spectrum usage and interference-immunized sub-carrier resource allocation. Furthermore, similar to the MIMO-OFDM system, cooperative OFDM can gain from multi-path diversity. Therefore, in our research works [17, 21, 24, 25], we focus on the OFDM issues in cooperative communication.

For the conventional OFDM technology, a Cyclic Prefix (CP) is exploited to eliminate the Inter-Symbol-Interference (ISI) due to multi-path. With CP adding and removing, the linear convolution

channel is transformed into a circular convolution channel, and the ISI can be easily resolved. Meanwhile, the channel equalization is also simplified, due to the channel matrix diagonalization. However, the cyclic prefix is not the only way to combat the multi-path. Zero Padding (ZP) has already been proposed as an alternative to the CP in OFDM transmissions [20] and particularly for Cognitive Radio [21]. As will be shown in Section 3.2, one of the advantages of using ZP over CP is its lower spikes in the Power Spectral Density (PSD), because the ZP signal has a more random structure than the CP signal. A Multi-Band (MB) ZP-OFDM-based approach to design Ultra Wide Band (UWB) transceivers has been recently proposed in [11] and [22] for an IEEE Standard. In Dec. 2008, the European Computer Manufacturers Association (ECMA) adopted ZP-OFDM for the latest version of the High-rate UWB Standard [23]. Because of its advantage in the low power transmission, ZP-OFDM will have the potential to be used in other low power wireless communication systems.

2.4.1 Cyclic Prefix (CP)-OFDM

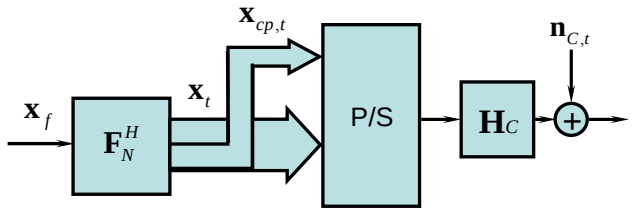

(A). transmitter & channel

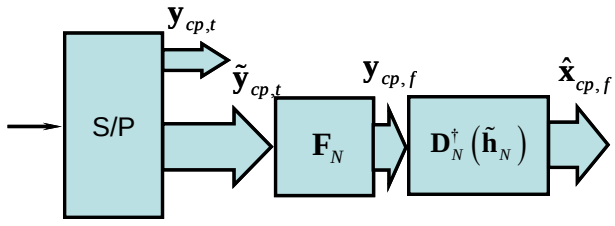

(B). receiver

Fig. 2.3. Discrete-time block equivalent models of CP-OFDM.

A number of benefits that OFDM brings to cooperative relay systems originate from basic features that OFDM possesses. To appreciate those, we first outline CP-OFDM's operation using the discrete-time baseband

equivalent block model of a single-transceiver system as depicted in Fig. 2.3, Fig. 2.3 (A) represents the transmitter and channel of a CP-OFDM system, while Fig. 2.3 (B) illustrates the receiver. The vector $\mathbf{x}_f = [x_0, \cdots, x_{N-1}]^T$ is the so-called frequency signal for one OFDM time symbol duration. Then it will be transferred to $\mathbf{x}_t$ in time-domain by the *N*-point Inverse Fast Fourier Transform (IFFT) matrix $\mathbf{F}_N^{-1} = \mathbf{F}_N^H$ with the (*n*, *k*)-th element of this matrix equals to $\exp(j2\pi nk/N)/\sqrt{N}$, i.e., $\mathbf{x}_t = \mathbf{F}_N^H \mathbf{x}_f$. $\mathbf{F}_N$ is the *N*-point Fast Fourier Transform (FFT) matrix, and *n*, *k* denote the index in frequency and time-domain, respectively. For better description, we use subscript *f* to indicate the signal vector in frequency domain, and use subscript *t* to indicate the signal vector in time domain. The blocks P/S and S/P in Fig. 2.3 denote the parallel to serial and serial to parallel operations respectively.

By applying the triangle inequality to the *N*-point IFFT definition it can be shown that the entries of $\mathbf{F}_N^H \mathbf{x}_f$ have magnitudes that can exceed those of $\mathbf{x}_f$ by a factor as high as *N*. In other words, IFFT processing can increase the Peak to Average Power Ratio (PAPR) by a factor as high as the number of subcarriers (which in certain applications can exceed 1000). Then a CP of length L_C is inserted between each $\mathbf{x}_t$ to form the redundant OFDM symbols $\mathbf{x}_{cp,t}$, which are sequentially transmitted through the channel. The total number of time domain signals in each OFDM symbol is, thus, $C = N + L_C$. If we define $\mathbf{F}_{cp} := [\mathbf{F}_D, \mathbf{F}_N]^H$ as the $C \times N$ expanded IFFT matrix, where $\mathbf{F}_D$ is characterized by the last L_C columns of $\mathbf{F}_N$, the redundant OFDM symbol to be transmitted can also be expressed as $\mathbf{x}_{cp,t} = \mathbf{F}_{cp} \mathbf{x}_f$. Then the received symbol $\mathbf{y}_{cp,t}$ can be written as:

$$\mathbf{y}_{cp,t} = \mathbf{H}_C \mathbf{F}_{cp} \mathbf{x}_f + \mathbf{H}_{ISI} \mathbf{F}_{cp} \mathbf{x}_{p,f} + \mathbf{n}_{C,t}, \qquad (2\text{-}8)$$

In Eq. (2-8), $\mathbf{H}_C$ is the $C \times C$ lower triangular Toeplitz filtering matrix with first column $[h_1 \cdots h_L \quad 0 \cdots 0]^T$, where *L* is the channel order (i.e., $h_l = 0, \ \forall\, l > L$, h_l denotes the *l*-th path gain), $\mathbf{H}_{ISI}$ is the $C \times C$ upper triangular Toeplitz filtering matrix with first row $[0 \cdots 0 \quad h_L \cdots h_2]$, which

captures Inter-Symbol Interference (ISI), $\mathbf{n}_{C,t}$ denotes the Additive White Gaussian Noise (AWGN) vector with variance N_0=1 and Length *C*. After removing the CP at the receiver, ISI is also discarded, and Eq. (2-8) can be rewritten as:

$$\mathbf{y}_{cp,t} = \mathbf{C}_N(\mathbf{h})\mathbf{F}_N^H \mathbf{x}_f + \mathbf{n}_{N,t}, \tag{2-9}$$

where $\mathbf{C}_N$ (**h**) is the $N \times N$ circulant matrix with first row $[h_1 \quad 0\cdots 0 \quad h_L \cdots h_2]$, and $\mathbf{n}_{N,t}$ is a vector formed by the last *N* elements of $\mathbf{n}_{C,t}$.

The procedure of adding and removing CP forces the linear convolution with the channel impulse response to resemble a circular convolution. Equalization of CP-OFDM transmissions ties to the well known property that a circular convolution in time domain, is equivalent to a multiplication operation in frequency domain. Hence, the circulant matrix can be diagonalized by post- (pre-) multiplication by (I)FFT matrices, and only a single-tap frequency domain equalizer is sufficient to resolve the multi-path effect on the transmitted signal. After demodulation with the FFT matrix, the received signal is given by:

$$\begin{aligned} \mathbf{y}_{cp,f} &= \mathbf{F}_N \mathbf{C}_N(\mathbf{h})\mathbf{F}_N^H \mathbf{x}_f + \mathbf{F}_N \mathbf{n}_{N,t} \\ &= \mathrm{diag}\left(H_1 \cdots H_N\right)\mathbf{x}_f + \mathbf{F}_N \mathbf{n}_{N,t} \\ &= \mathbf{D}_N\left(\tilde{\mathbf{h}}_N\right)\mathbf{x}_f + \mathbf{n}_{N,f}. \end{aligned} \tag{2-10}$$

In this expression, $\tilde{\mathbf{h}}_N = \left[H_1 \cdots H_N\right]^T = \sqrt{N}\mathbf{F}_N \mathbf{h}$, with

$$H_k \equiv H\left(2\pi k / N\right) := \sum_{l=1}^{L} h_l e^{-j2\pi kl/N} \tag{2-11}$$

denoting the channel's transfer function on the *k*-th subcarrier, $\mathbf{D}_N\left(\tilde{\mathbf{h}}_N\right)$ stands for the $N \times N$ diagonal matrix with $\tilde{\mathbf{h}}_N$ on its diagonal, and $\mathbf{n}_{N,f} := \mathbf{F}_N \mathbf{n}_{N,t}$.

Eq. (2-10) and Eq. (2-11) show that an OFDM system which relies on *N* subcarriers to transmit the symbols of each block $\mathbf{x}_f$, converts an

Finite Impulse Response (FIR) frequency-selective channel to an equivalent set of N flat fading subchannels. This is intuitively reasonable since each narrowband subcarrier that is used to convey each information-bearing symbol per OFDM block "sees" a narrow portion of the broadband frequency-selective channel which can be considered frequency flat. This scalar model enables simple equalization of the FIR channel (by dividing Eq. (2-10) with the corresponding scalar sub-channel $\tilde{\mathbf{h}}_N$) as well as low-complexity decoding across sub-channels [21]. Transmission of symbols over subcarriers also allows for a flexible allocation of the available bandwidth to multiple users operating with possibly different rate requirements imposed by multimedia applications, which may include communication of data, audio, or video. When Channel State Information (CSI) is available at the transmitter side, power and bits can be adaptively loaded per OFDM subcarrier, depending on the strength of the intended sub-channel. Because of orthogonality of OFDM subcarriers, the OFDM system exhibits robustness to the narrow band interference.

The price paid for OFDM's attractive features in equalization, decoding, and possibly adaptive power and bandwidth allocation is its sensitivity to subcarrier drifts and the high PAPR that IFFT processing introduces to the entries of each block transmitted. On the one hand, subcarrier drifts come either from the carrier-frequency and phase offsets between transmit-receive oscillators or from mobility-induced Doppler effects, with the latter causing a spectrum of frequency drifts. Subcarrier drifts cause Inter-Carrier Interference (ICI), which renders Eq. (2-10) invalid. On the other hand, high PAPR necessitates backing-off transmit-power amplifiers to avoid non-linear distortion effects [11].

2.4.2 Zero Padding (ZP)-OFDM

However, our previous research [24, 25] learned that the same multi-path robustness can be obtained by adopting ZP instead of CP. If the length of the zero-padding equals the length of CP, then the ZP-OFDM will achieve the same spectrum efficiency as CP-OFDM.

There are differences between the transmission part and receiver part of ZP-OFDM and CP-OFDM, as shown in Fig. 2.4. Fig. 2.4 (A) depicts the transmitter and channel of a ZP-OFDM system. Fig. 2.4 (B) and (C) illustrate the commonly used Overlap and Add (OLA) receiver and

FAST[2] receiver [20], respectively.

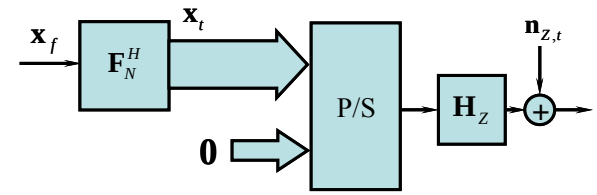

(A). transmitter & channel

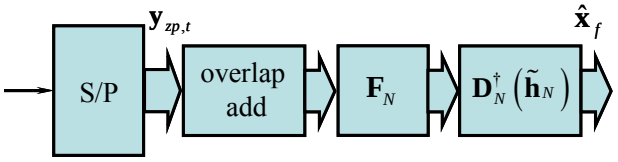

(B). OLA receiver

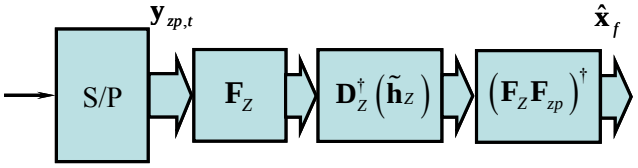

(C). FAST receiver

Fig. 2.4. Discrete-time block equivalent model of ZP-OFDM.

The differences between ZP-OFDM and CP-OFDM start from adding the Guard Interval for the time symbol. For the ZP-OFDM, a zero vector with length L_Z is appended at the end of the time symbol. If we define

$$\mathbf{T}_{ZP} = \begin{bmatrix} \mathbf{I}_N \\ \mathbf{0} \end{bmatrix}_{Z\times N}, \qquad (2\text{-}12)$$

where $\mathbf{I}_N$ is an $N \times N$ identity matrix and $Z = N + L_Z$, the transmitted OFDM symbol can be denoted as $\mathbf{x}_{zp,t} = \mathbf{T}_{ZP}\mathbf{F}_N^H\mathbf{x}_f$. The received symbol (i.e., $\mathbf{y}_{zp,t}$) is now expressed as:

$$\mathbf{y}_{zp,t} = \mathbf{H}_Z\mathbf{T}_{ZP}\mathbf{F}_N^H\mathbf{x}_f + \mathbf{H}_{ISI}\mathbf{T}_{ZP}\mathbf{F}_N^H\mathbf{x}_{p,f} + \mathbf{n}_{Z,t}, \qquad (2\text{-}13)$$

[2] This is so-called FAST because it is a fast version of the corresponding linear or non-linear equalizer based on channel matrix diagonalization.

where $\mathbf{H}_Z$ is the $Z \times Z$ lower triangular Toepliz filtering matrix with first column $[h_1 \cdots h_L \quad 0 \cdots 0]^T$, L is the channel order (i.e., $h_l = 0, \ \forall\, l > L$, h_l denotes the l-th path gain) and $\mathbf{H}_{ISI}$ is the $Z \times Z$ upper triangular Toeplitz filtering matrix with first row $[0 \cdots 0 \quad h_L \cdots h_2]$, which captures ISI from the previous symbol $\mathbf{x}_{p,f}$. In Eq. (2-13), $\mathbf{n}_{Z,t}$ denotes the AWGN vector with zero mean, variance N_o=1 and length Z.

To avoid ISI, we should have $L \le L_Z$. In this thesis, we assume $L = L_Z$. i.e., ZP exactly combats the ISI. Then, $\mathbf{H}_{ISI}\mathbf{T}_{ZP} = \mathbf{0}$, and Eq. (2-13) can be rewritten as:

$$\mathbf{y}_{zp,t} = \mathbf{H}_Z \mathbf{T}_{ZP} \mathbf{F}_N^H \mathbf{x}_f + \mathbf{n}_{Z,t} . \qquad (2\text{-}14)$$

The OLA receiver and FAST receiver, as shown in Fig. 2.4 (B) and (C), respectively, are elaborated in [20], for estimating $\hat{\mathbf{x}}_f$ from the observation $\mathbf{y}_{zp}$. $\mathbf{D}_N\left(\tilde{\mathbf{h}}_N\right)$ stands for the $N \times N$ diagonal matrix with vector $\tilde{\mathbf{h}}_N$ on its diagonal, while $\mathbf{D}_Z\left(\tilde{\mathbf{h}}_Z\right)$ denotes the $Z \times Z$ diagonal matrix with vector $\tilde{\mathbf{h}}_Z$ on its diagonal; $\tilde{\mathbf{h}}_N$ and $\tilde{\mathbf{h}}_Z$ are the N-point and Z-point frequency response of the channel's impulse response, respectively. $\mathbf{F}_Z$ stands for the Z-point FFT matrix, and $\mathbf{F}_{zp} = \mathbf{T}_{ZP}\mathbf{F}_N^H$. The OLA receiver is used to recast the ZP-OFDM as a CP-OFDM. Similar to the circular convolution property in CP-OFDM, the OLA receiver diagonalizes the channel, transfers the broadband frequency-selective channel to a multi-frequency (but per subcarrier flat-fading) channel, and enables the simple equalization of the ZP-OFDM channel. However, since the multi-path channel is transformed to the flat-fading channel, the OLA receiver loses the merit of multi-path diversity accordingly. As shown in the Fig. 2.3 (C), and by comparing with the OLA receiver we learn that although the extra two FFT matrices slightly increase the equalization complexity, the FAST receiver always holds the linear structure or the tall Toeplitz structure of the ZP-OFDM channel, i.e., $\mathbf{H}_{ZN} = \mathbf{H}_Z\mathbf{T}_{ZP}$. The tall Toeplitz structure can be illustrated by the $(L+M-1)$-row and M-column matrix $\mathcal{T}(\mathbf{v}, L, M)$ as follows:

$$\mathcal{T}\left(\mathbf{v},L,M\right)=\begin{bmatrix} v_1 & 0 & \cdots & 0 \\ v_2 & v_1 & \cdots & 0 \\ \vdots & \vdots & \ddots & \vdots \\ v_L & v_{L-1} & \cdots & 0 \\ 0 & v_L & \cdots & v_1 \\ \vdots & 0 & \cdots & v_2 \\ \vdots & \vdots & \ddots & \vdots \\ 0 & 0 & 0 & v_L \end{bmatrix}, \tag{2-15}$$

where $\mathbf{v}=\left[v_1,v_2,\cdots,v_L\right]^T$ is a non-zero column vector of length L. Both the OLA receiver and FAST receiver have their own application fields. Generally speaking, the OLA receiver with ZP-OFDM can mimic the conventional CP-OFDM to obtain a simple equalization, while the FAST receiver keeps the inherent merits of ZP-OFDM, and provides a relatively faster equalization.

In the ZP-OFDM, the tall Toeplitz structure of the equivalent channel matrix always guarantees its full rank (it only becomes rank deficient when the channel impulse response is identically zero, which is impossible in practice). In other words, the full rank property guarantees the detection of transmitted symbols. Nevertheless, the zero-padding and linear structure of ZP-OFDM outperforms CP-OFDM in the lower frequency spikes, as zero-padding replaces the cyclic prefix in OFDM symbols, and so significantly reduces the ripples in the PSD. Compared to CP, tailing zeros will save transmit power. Furthermore, by adopting proper filters, the ZP-OFDM will not give rise to out-of-band spectral leakage, either. In the blind channel estimation and blind symbol synchronization area, ZP-OFDM also has its advantage over CP-OFDM in reducing the system complexity, again due to its linear structure [26, 27].

In this thesis, we investigate diversity, capacity and complexity issues in cooperative ZP-OFDM communication. We design a cooperative tall Toeplitz scheme for the cooperative ZP-OFDM communication system, with different Carrier Frequency Offsets (CFOs) at different relays and over a multi-path Rayleigh channel, i.e., a doubly time-frequency selective channel. In the proposed cooperative tall Toeplitz scheme, the tall Toeplitz structure together with the frequency orthogonality of the channel matrix has a unique feature, which guarantees the full

cooperative and multi-path diversity, and easily combats the CFOs, only with the linear equalizers. We derived the upper bound of the channel orthogonality deficiency, which provides an insight into how the change of channel factors affects the system performance in terms of BER performance and capacity. According to the theoretical analysis and simulation results, only with linear equalizers, the cooperative tall Toeplitz scheme achieves full diversity, while the system complexity is reduced significantly.

2.5 Optimization: relay selection and resource allocation

Relay selection and resource allocation play important roles in cooperative communication. Considering a scenario that the channel between the source node and the destination node suffers from severe fading, the direct transmission from the source node to the destination node will have poor performance. By using the cooperative communication scheme, the source node can find relay nodes which have better channels to the destination node. By using these better relays to forward the signal to the destination node, the cooperative communication increases the reliability of the whole transmission. By selecting relay nodes closer to it, the source node can also save battery power, since it does not have to transmit at high power and can use the relays' power to perform the transmission instead. The saving of the power by relay selection in cooperative communication can also contribute to the so called "green communication" with low power transmission.

Since the source node in the cooperative communication scheme needs the help from relay nodes to forward the signal, relay selection becomes important in order to obtain optimal performance of the cooperative communication system. By choosing the proper nodes to relay the transmission, the system can achieve higher capacity and consume lower power.

After relay selection, resource allocation is the next optimization issue in the cooperative communication network. Allocating the optimal resource to the proper relay nodes with different objectives in the system is required to obtain best performance from the cooperative communication network. In a cooperative communication network,

because both relay nodes and source node hope to maximize their own gain through resource allocation and optimization, it will have a more complicated resource allocation and optimization process than where the objective is only to maximize the source node gain.

The so called “game theory” in solving problems for wireless communication has been gaining a lot of attention recently. In the field of cooperative communication, the game theory approach has been used in many aspects, especially in resource optimization and managing the relay nodes behavior. The game theory approach is used because it can model the behavior of nodes in real situations, and perform multi objective optimization.

This thesis work is an attempt to formulate the relay selection criterion and resource allocation and optimization which fulfills the practical situation and obtains optimal result in the system performance using the game theory approach.

2.5.1 Conventional methods

Relay selection is regarded as an effective mean to improve the performance of cooperative communication networks by selecting these nodes which more positively contributed to the transmission performance compared to other nodes available in the system. In some simple scenarios, for instance in a cooperative network where the source node has limited power, relay nodes which are closer to the source node or have a better source-relay link might have the potential to increase the performance of the transmission. In a cooperative communication network where identical power is transmitted at all relay nodes, improving the transmission performance can be done by choosing relay nodes with a better relay-destination channel coefficient.

Resource allocation and optimization is a process to allocate power, time-slot, bandwidth, or any other form of resources to each node in the network to improve the performance of the system with different objectives. The objective in the system can be BER performance of the system, transmission capacity, power consumption, etc.

Up to now, there have been many works in relay selection for cooperative communication networks. In the work by Zhao and Valenti

[28], the source node is assumed to have *a priori* knowledge about the channel model and the location of other nodes using GPS. This knowledge is then used to estimate the SNR between the links, the relay nodes closer to the destination will be chosen to forward the information. This work shows that the geographical location based relay selection is better than random relay selection or relay selection by the instantaneous SNR at the destination. The novelty in this works though, is not the relay selection criterion, but the application of a hybrid Automatic Repeat re-Quest (ARQ) in the cooperative communication. The relay nodes in this scenario keep the information which they forward to the destination node until they reach the acknowledgement (ACK) from the destination node. If the destination failed to obtain the information due to errors, the relay nodes can re-send the information without having the source node to re-transmit the information.

Zhao and Su [29] also worked on location based relay selection. They investigated two scenarios and proposed a relay selection scheme for each scenario. In the first scheme the relays are placed in a uniform distributed setting (all the relays have same distance to the source) and in the second scheme the source is assumed to know the location of the relays and choose a small subset of optimal relays to forward the data. Power allocation to the relay is also studied here. The power allocation is derived from estimation of the outage probability at the destination. These works show that the first scheme has better outage probability with a large number of users. The optimal power allocation for the distributed scheme is obtained by using half of the power to be transmitted to the destination, and half of the power is used to be transmitted to the relay nodes.

The multi-carrier system properties such as OFDM can also be exploited as relay selection criteria. Kaneko *et al* [30] proposed a relay selection scheme based on sub-carrier allocation in a cooperative communication network with OFDM. In this scheme, each node is transmitting in multiple OFDM subcarriers. The source node broadcasts information to all the available relay nodes. Then, different relay selection schemes based on multiple carriers was applied. In the first scenario, called All Participate All Sub-carrier (APAS), all relay nodes forward the information received from the source node to the destination sequentially. In the second scenario, called All Participate Rate Splitting (AP-RS), the relay nodes are dividing the information they need to

forward into a number of relay nodes, before transmitting each part to the destination node. The third scenario, called Average Best Relay Selection scheme (AvgBRS), is using the relay with the best average SNR from all the subcarriers to forward the information. In the Per Sub-carrier Best Relay Selection scheme (PSBRS), the relay nodes only transmit the subcarriers with the best SNR. The last scenario, called Random Based Selection (RBS), selects a random relay to forward information to the destination. The RBS is used as a reference to other relay selection scenario. Simulation results show that the PSBRS is the best scenario for relay selection, but this scenario is not practical for implementation since we need complete channel state information (CSI) on the SNR for each subcarrier. The AvgBRS on the other hand, provides a result approaching the NRBS result with less complicated implementation.

The relay selection criterion can also be based on interference. Selecting relay nodes based on the instantaneous SNR calculation in the destination node or in the relay node cannot guarantee the transmission performance since the effect of interference from other nodes might affect the system performance. In work done by Krikidis *et al* [31], the relay nodes are considered to receive interference, which change the result of the relay selection criterion.

From the above mentioned previous work, it is shown that in the field of cooperative communication, relay selection as well as resource allocation have become promising research areas. In the next paragraph, game theory basics and classification will be discussed as an introduction to its application in cooperative wireless communication. Game theory has become an important tool in cooperative communication network since the nodes in this network have different objectives. After the introduction, some literature study for game theoretical approach in cooperative communication network will be provided.

2.5.2 Game theoretical approaches in cooperative communication

Game theory is a mathematical model that analyzes how different players with different strategies interact with each other. It provides the necessary tool to model the situation and predict the output of the interaction. The concept of game theory can be traced back to Emile

Borel's research in his 1938 book Applications aux Jeux de Hazard [32], followed by the book Theory of Games and Economic Behavior [33] in 1944 by J. von Neumann and O. Morgenstern. In this book, J. von Neumann and O. Morgenstern laid the foundation of game theory by providing a method for finding mutually consistent solutions for two-persons zero-sum games. J. Nash developed a new concept known as Nash equilibrium in his research between 1950 [34] and 1951 [35]. It marked an important development in the game theory, by providing a method that can be applied to non-zero-sum games. After that, the researches in game theory continued with covering cooperative gaming, various kinds of equilibriums, and many game forms.

In wireless communication, especially in cooperative communication, game theory approaches are used to solve multi-objective problems. When transmitting information, the source node and the relay nodes may have different objectives. The source node may care about high quality of the transmission, and can increase the transmitted power accordingly, while the relay node hopes to save the power consumption. This problem of different objectives can be solved using a game theory approach and by allowing different players with different objectives to interact with each other in the objective optimization process until some equilibrium is reached [36].

Thus, the game theory became a popular and attractive tool in solving multi-objective problems in wireless communication, and can be used to model the behavior of nodes in a network as well. In the following paragraphs, game theory basics and principles such as components, types of games, and equilibrium definition will be provided. Applications of game theory in wireless communication and cooperative communication are provided as well as a view on how game theory works in cooperative communication is presented.

a. Game theory basics

From game theory point of view a game is composed by three elements: a set of players, a set of actions for each player, and payoff/utility functions. Players in a game can be a decision maker, individuals or groups of individuals which have the capabilities to make decision over a choice of actions. Players interact with each other using a set of actions available to them, resulting in payoff/utility function for each player.

In game theoretical modeling, there are assumptions about the characteristics of the players. Most important is the assumption that the players are rational, in the sense that each player understands the goal of the game, the consequences of every action it took towards the goal, and the ability to choose the action for optimization.

In short, a player i with rational decision capability will choose an optimal action a_i^* from action space A_i which will give $u\left(a_i^*\right) \geq u\left(a_{-i}\right)$ where $a_{-i} \in A_i$ is the complement of the action space A_i other than optimal action a_i^*, and $u(\cdot)$ stands for the utility function. Sometimes in a game theoretical model, the players will have to make a decision under an uncertainty condition, caused by imperfect information between players, uncertainty from the environment, and non-deterministic action behaviors of other players in the game. In this case, decisions are made based on a probabilistic approach, and the players will have to maximize the expected value of the objective functions.

b. Game theory classifications

Game theory basically can be divided into two main groups, the non-cooperative game theory and the cooperative game theory. Non-cooperative game theory has game models where the players in the game are individuals competing each other. In cooperative game theory, the players are groups of individuals. The actions in the game are taken as a group, and each group is competing on the objective functions. Most game models are based on a non-cooperative game group, although lately cooperative game theory has also gain popularity in research. Fig. 2.5 [36] provides a diagram of game theory classification.

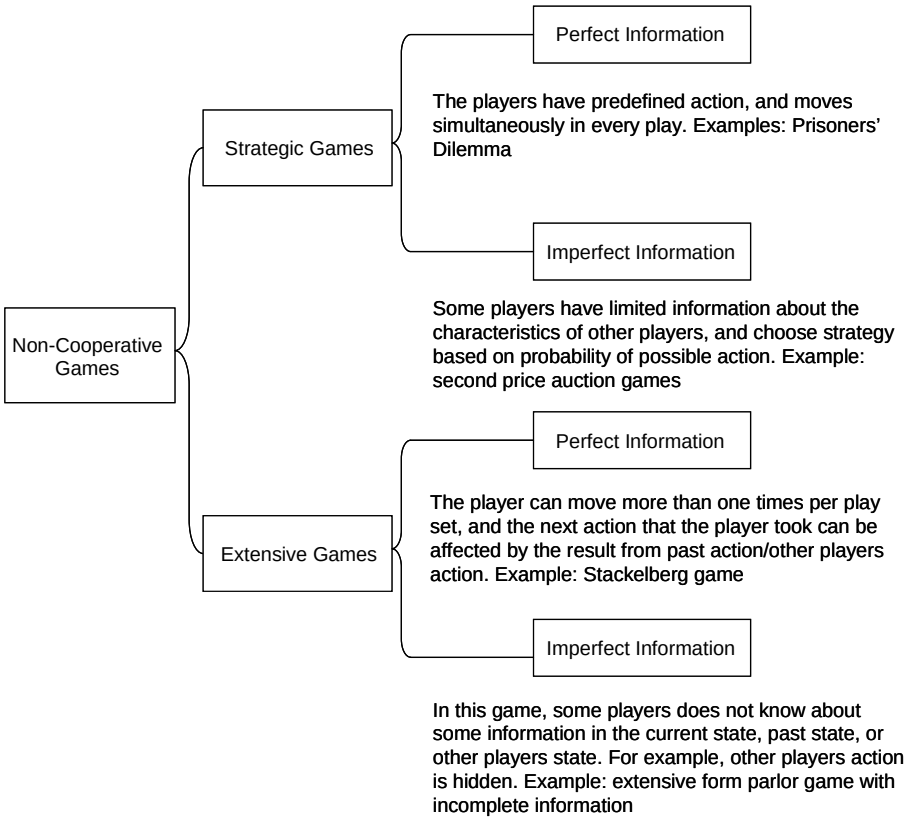

Fig. 2.5. **Game Theory Classification** [36].

c. Applications in cooperative communication

In the field of cooperative communication, the game theory approach has been used to model the nodes behavior in the cooperative communication network and to solve the relay selection and resource allocation problems.

One of the earliest works on game theory for cooperative communication is done by Ileri *et al.* [37], who introduce pricing into the cooperative communication network to encourage cooperation and to solve the resource allocation problems. From game theory approach, those relay nodes which want to optimize their utility functions might not join the cooperation without some benefit. By introducing pricing, the relay nodes will gain some benefit by joining the cooperative communication scenario, which encourages relay nodes to forward the information.

The work of Shastry *et al.* [38] basically extends the work of Ileri *et al*. The previous works on game theory for cooperative communication are mainly focusing on the network revenue, and under some conditions, the relay utility function for forwarding is lower than the non-forwarding case. This can discourage forwarding in the cooperative communication network since joining cooperation is not beneficial for the relay nodes. In paper [38], the authors suggest that the price for reimbursement should be decided by the source. Hence, the source will pay reimbursement to the forwarding user. The forwarding user will still pay to the Access Point (AP) for using the resource when forwarding the data but at the same price with sending its own data. The relay will gain profit from the difference between the price that the AP set and the reimbursement price from the source. The source and the relay will still have to reach "Nash equilibrium" by changing the power level and bandwidth, and then the result will be used by the source to recalculate the reimbursement price for the relay and is also used by the AP to recalculate the price for transmitting data to the AP to maximize its own utility.

In Wang *et al.*'s work [39], the scenario is that the nodes (both the source and relaying nodes) are trying to maximize their own utility function. The source node only pays for the power that the relay forwards to transfer the data to the destination. The equilibrium is only

controlled by how much power from the relay the source will use and at what price it will buy it from the relay. The price is set by the relay according to the channel quality, and the source can choose which relay it wants to use depending on the price. In paper [39], the result shows that the locations of the relays affect the channel quality, hence affecting the price. Comparison between the proposed protocol and a centralized approach shows that the proposed protocol could reach the same performance as the centralized approach.

Game theory is also used in the work done by Shi *et al.* [40] for optimized power control in a distributed manner within a cooperative communication network with interference. In this scenario, there are two source nodes which want to transmit information to their own destination nodes and two relay nodes which help to forward the information. Each source node will cause interference to the other relay nodes, and the relay nodes will cause interference to the destination nodes. Interference comes because of side lobe leakage in the transmission antenna beam width.

In cooperative communication networks, we have different types of nodes with different objectives. A source node wants to maximize its throughput, but the relay nodes might want to reserve its resources and to benefit more from the source node. Through literature study, the game theory has been shown to be a useful and powerful tool to solve multi-objective optimization in cooperative communication, especially in the field of relay selection and resource allocation. In chapter 4, we will use the game theory approach to solve relay selection and resource allocation problems in cooperative communication networks.

In this thesis, we propose relay selection and resource allocation and optimization schemes for cooperative wireless communication networks with interference using a game theoretical approach. We introduce a pricing game for relay selection and resource allocation and optimization in cooperative communication networks with interference based on the so called Stackelberg game. Simulation results show that interference in the cooperative communication network can change the relay selection and resource allocation and optimization result. This aspect should not be neglected from the calculations allowing us to predict the behavior of the system in an environment closer to real world situations, compared to the case when only noise is considered in the system. Then we learn

that the pricing game for resource allocation and optimization, when the number of available nodes is high, can result in high payment to relay nodes which will highly reduce the source node utility function. Therefore, we propose an algorithm to limit the number of selected relay nodes to mitigate this problem. Using this algorithm, we chose a number of relay nodes where the result of resource allocation and optimization is still beneficial for the value of source node utility function.

2.6 New aspect: cooperative localization

Wireless location information and wireless location-based services have been receiving a growing attention over the past decades. The reason is the remarkable business potential behind these kinds of applications, which encompass emergency, security, monitoring, tracking, logistics, mobile yellow pages, radio planning, cellular system management, etc.

Although the Global Positioning System (GPS) is still the most popular commercial localization solution, it has to be pointed out that GPS is not always the most suitable localization solution for all scenarios and locations [41]. GPS provides location information by exploiting Time of Arrival (TOA) measurements from downstream satellite links. As a technological consequence of market demands, third generation (3G) handsets have embedded GPS receivers. Therefore, they have got more flexibility, while sharing a higher number of systems and services. However, GPS requires Line-of-Sight (LOS) to multiple satellites. For GPS-denied scenarios [42], such as indoor, underground, in urban canyons, and under tree canopies, it then becomes difficult, if not impossible, to obtain adequate location information.

Thus, alternative methods of positioning and navigation are of interest, either as a backup or for use in areas unreachable by satellites. Beacon localization, on the other hand, relies on a terrestrial fixed infrastructure, such as WiFi Access Points (APs) or GSM base stations. This kind of localization is accomplished through the use of radio communication between mobile devices and base stations. Location information is provided by a database commonly placed on a remote server (e.g., managed by universities, WiFi clubs, war-driving activities, etc.), which needs to be constantly updated in order to provide valid and up-to-date position information. However, in less populated areas where network

coverage is sparse, the lack of WiFi APs or base stations may cause a lack of estimated positions, and consequently the localization errors can be unacceptably large [43].

Conventionally, high-accuracy localization can only be achieved using high-power base stations or a high-density base station deployment, both of which are cost prohibitive and impractical in realistic settings. Hence, there is a need for localization systems that can achieve high accuracy in harsh environments with power constraint and limited infrastructure. A practical way to address this need is through a combination of cooperative localization and wideband transmission.

2.6.1 Cooperative localization and cooperative communication

The technologies of cooperative communication in the wireless networks have gained tremendous research interests recently because of its inherent spatial diversity gains and bringing many advantages, such as increasing the capacity and coverage, reducing the outage probability and Bit Error Rate (BER). Similar to cooperative communication, cooperative localization can benefit from the spatial diversity as well. The cooperative scheme becomes an emerging paradigm that solves the needs for high-power, high-density base station deployment, and offers additional localization accuracy by enabling the mobile devices to help each other in estimating their positions [44]. The benefit of cooperative localization based on time domain measurements is illustrated in Fig. 2.6: mobile device 1 is not in the communication range of base stations 3 and 4, while mobile device 2 cannot communicate with base stations 1 and 2. Neither mobile device can trilaterate its position based solely on the information from its neighboring base stations. However, the cooperation between mobile devices 1 and 2 enables both mobile devices to be localized.

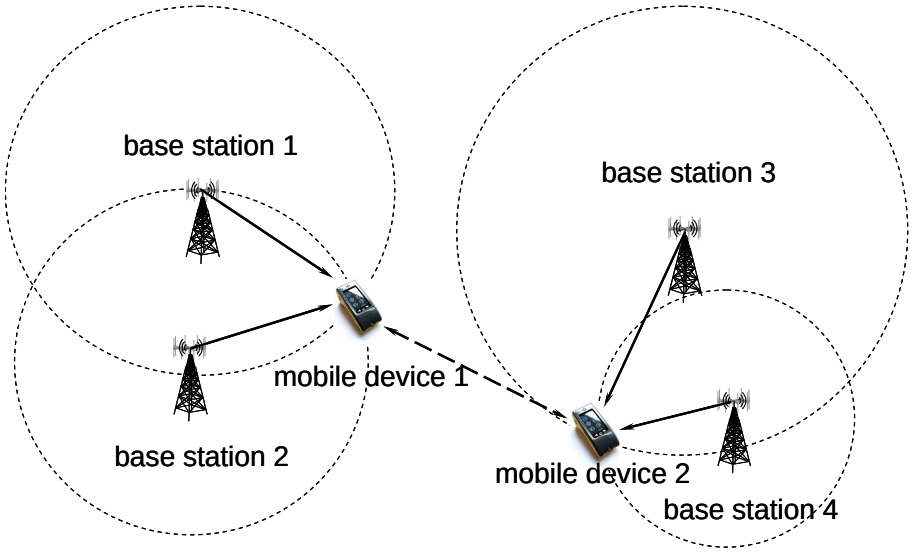

Fig. 2.6. Cooperation between the nodes benefits the conventional localization.

The cooperative localization procedure typically consists of two phases, i.e., measurement phase and location update phase [45]. In the measurement phase, the position relative information including the time of propagation, the Angle-of-Arrival (AOA) or the Received-Signal-Strength (RSS) should be measured. In the location update phase, the measurements are aggregated and used as the inputs to a localization algorithm, to determine the location of the mobile device. For instance, when a mobile device obtains distance estimates with respect to three base stations, the mobile device can infer its own position through trilateration, provided the mobile device knows the positions of the base stations. In order to achieve a high resolution of the cooperative localization, the accuracy in both measurement phase and location update phase should be enhanced.

2.6.2 Measurement phase

a. Signal strength measurement

RSS is measured by the received signal power, i.e., the squared magnitude of the signal strength. It exploits the relation between power loss and the distance between transmitter and receiver to determine the distance between the transceiver. The RSS measurement is simple, and it is attractive due to its low cost for the system designer. However, a RSS

measurement always includes a large error, and only provides accurate localization with dense nodes in the wireless networks.

b. Time measurement

Estimating the propagation time of the wireless signals usually provides a finer resolution in distance measurements, and it will be more useful with low-density nodes in wireless networks. Propagation time measurement techniques include Time-of-Arrival (TOA), Round-trip Time-of-Arrival (RTOA), and Time-Difference-of-Arrival (TDOA), which are all based on the cross-correlation of two separated signals. RTOA is a practical TOA scheme in a distributed manner, as it does not require a common time reference between nodes.

TDOA always means the time difference of signal propagation between the two transmission links received at one common receiver or two synchronized receivers. Therefore, there must be either two transmitters sending the same signal simultaneously to one receiver or two spatially separated synchronized receivers measuring the signal transmitted from one transmitter.

c. Angle measurement

Angle of Arrival (AOA) estimation determines the orientation of the received signal, and accordingly finds out the direction of the transmitter, when the receiver is equipped with antenna arrays. Naturally, the AOA positioning approach with antenna arrays requires more system costs.

d. Measurement in wideband localization

In wideband or UWB localization, due to the very large bandwidth, a very large number of paths can be seen, especially in the indoor scenarios. Therefore, accurate AOA estimation becomes very challenging due to much scattering from objects in the multi-path environment. Meanwhile, the very large bandwidth of UWB leads to a very high temporal resolution, making it ideal for high-precision time-based radiolocation applications. However, this unique characteristic of UWB, i.e., the very large bandwidth, is not exploited to increase the accuracy of the RSS approach. Although it is easier to estimate RSS than propagation time, the range information obtained

from a RSS measurement is very coarse compared to that obtain from the time measurement. Thus, time-based approaches are better motivated for wideband cooperative localization than the more costly AOA-based technique and lower accurate RSS-based technique.

2.6.3 Location update phase

In the second phase, measurements are aggregated and used to calculate the position of each mobile device, and to update the location information for each mobile device. While localization algorithms for positioning and navigation have a long history, in the cooperative scenarios there are some new characteristics for the cooperative localization algorithm.

a. Hybrid centralized-distributed

A cooperative localization algorithm is a hybrid algorithm that combines the advantages of centralized and distributed features. Centralized algorithms collect measurements at a central processor prior to calculation of the position; the position information is then transmitted by the central processor to corresponding mobile devices. Distributed algorithms require the mobile device to locate the position for it self, but iteratively. Mobile devices need to recalculate their locations for many times until convergence.

There are two reasons for the hybrid algorithms. First, centralized algorithms have no need to address the convergence issue as distributed algorithms, and likely save the energy cost. Second, for some applications, no central processor is available to process the calculation for all the mobile devices. Furthermore, when a large number of mobile devices forward all the measurement data to a central processor, there is a communication bottleneck for the central processor.

Therefore, it is wise to adopt hybrid centralized-distributed algorithms for cooperative localization. For those mobile devices near the base station, the centralized algorithms are adopted; in this case the base station plays the role of central processor, collects the measurements, and calculates the position for each mobile device. In general, when the number of hops for the mobile device to the base station exceeds the necessary number of iterations for convergence at the mobile device, the

distributed algorithms are adopted; otherwise, the centralized algorithms are adopted.

b. Cooperative and relative

Compared to the conventional localization algorithms, in the cooperative localization, the communication among the mobile devices removes the need for all mobile devices to be within the communication range of base stations. Therefore, a high base station density or large base station transmission range is no longer required. Since the mobile devices can obtain information from both base stations and other mobile devices, cooperation between the mobile devices can offer increased localization accuracy and provide positioning information to the remote mobile devices.

Cooperative localization algorithms can also use measurements (of range or angle) between pairs of unknown-location mobile devices, and so refer the mobile device to the neighborhood or local environment to obtain the relative positions of the mobile devices. By introducing the position information of the base station through communication between the base station and mobile devices, the relative position of the mobile device can be transferred into an absolute position. The challenge of cooperative localization is to allow mobile devices that are not in the range of any known-location device to be located and, further, to improve the location estimates of all mobile devices. Many cooperative location estimation algorithms have been proposed to determine the position of a device. Detailed reviews of these algorithms could easily cover many pages. Therefore, we direct the readers to two classic review papers, [46] and [47].

In this thesis, we investigate cooperative relaying schemes for ZP-OFDM TDOA estimation, while feature-based cooperative TDOA estimation to achieve bandwidth efficient transmission is analyzed. A trigger relay technique is proposed to gain from easy processing together with noise and interference immunity of the base station to the relay link. Compared to AF relay and DF relay TDOA estimation cases, the trigger relay reduces the system complexity. Meanwhile, trigger relay enables the bandwidth efficient TDOA, since it significantly reduces the amount of data for transmission. In terms of TDOA estimation error, among AF relay, trigger relay and DF relay with block feature, the trigger relay

achieves the best accuracy. Furthermore, by exploiting cooperative multi-path diversity, the improved signal detection at the primary receiver further contributes to trigger the relay with a more accurate TDOA estimation.

2.7 Conclusions

This chapter has given an overview of fundamental backgrounds of cooperative radio communication. First, the history of development from MIMO technology to cooperative communication is reviewed. Then, the infrastructure of the cooperative communication in terms of AF relay protocol, DF relay protocol and their combination are introduced.

OFDM is a favorite multi-carrier modulation technique in modern communication. By introducing OFDM into cooperative communication, the advantage of frequency parallel transmission, high speed communication and efficient spectrum usage possessed by OFDM can be utilized by a cooperative relay system. In this chapter, we have summarized own papers and reviewed own research on the famous CP-OFDM and its counterpart ZP-OFDM [17, 21, 24, 25].

In cooperative communication, and knowing that communication nodes are not cooperative by nature, a key question on how to get relays to join cooperation and to select relays to cooperate plays an important role in optimization of the radio performance. In this chapter, in the context of cooperative communication, conventional relay selection and resource allocation techniques and game theory approaches have been reviewed.

A new era of highly accurate ubiquitous location-awareness is on the horizon, which is enabled by the cooperation between wireless nodes. Cooperative localization researches will continue to appear since larger wireless networks are deployed and more applications require accurate position information. This chapter has provided an overview of the state of the art in wideband cooperative localization technology. Different cooperative localization techniques have been briefly introduced; their characteristics, challenges and future trends for development were unveiled.

Appendix 2.1

Proof of the *Theorem 2.1*:

According Eq. (2-5), the average error probability P_e is a decreasing function w.r.t. SNR of a DF link or an AF link. The SNR of a *L*-hop AF relay link, γ_{AF}, is the 1/*L* times of the harmonic mean of γ_i, $\forall i \in [1, L]$, i.e.[48],

$$\gamma_{\mathrm{AF}} = \frac{\gamma_1 \gamma_2, \ldots, \gamma_L}{\sum_{i=1}^{L} \gamma_1 \gamma_2, \ldots, \gamma_{i-1}\gamma_{i+1}, \ldots, \gamma_L}, \tag{A2-1}$$

where γ_i denotes the SNR of the *i*-th hop in AF relay link,

$$\gamma_i = \begin{cases} \dfrac{E_S h_{S,Q_1}}{N_0} & i = 1 \\ \dfrac{E_S h_{Q_{i-1},Q_i}}{N_0} & i \neq 1 \text{ or } L \\ \dfrac{E_S h_{Q_{L-1},D}}{N_0} & i = L \end{cases} \tag{A2-2}$$

where h_{S,Q_1} denotes the power gain of the channel from the source node to the first relay, i.e., first hop. h_{Q_{i-1},Q_i} denotes the power gain of the *i*-th hop, when $i \neq 1$ or L. $h_{Q_{L-1},D}$ denotes the power gain of the *L*-th hop, using the Pythagorean means theorem, where the harmonic mean is always smaller than the arithmetic mean.

For instance, for large AF SNR, the second term of Eq. (2-3) is approximated as the second term of Eq. (2-5), which is half the harmonic mean of the 2-hop SNR in the AF relay link. When we consider the DF case, i.e., replacing all (*L*-1) AF relays by DF relays, under the condition of correct decoding, it only needs to take into account the last hop relaying. Therefore,

$$\gamma_{DF} = \frac{E_S h_{Q_{L-1},D}}{N_0} \tag{A2-3}$$

In practice, it is easy for the last hop relay to achieve an SNR larger than $1/L$ times of the arithmetic mean of the whole link SNR; so we can only consider the last hop of the reliably decoded DF protocol. Therefore, under the condition of correct decoding, DF can more enhance the error probability performance than AF in the cooperative network.

Chapter 3

Performance analysis of cooperative ZP-OFDM: diversity, capacity and complexity

3.1 Introduction

We reviewed modern wireless communication technology in Chapter 2. In order to achieve high speed, low power and reliable wireless transmission, and to satisfy future wireless communication requirements, we must think of a new technology beyond the traditional point-to-point communications. This led us to what is known as cooperative communication and networking, which is a new communication paradigm that promises significant capacity and multiplexing gain increases in wireless networks [14, 15]. It realizes a new form of space diversity to combat the detrimental effects of severe fading by mimicking the Multiple-Input-Multiple-Output (MIMO), while getting rid of the drawbacks of MIMO such as size limitation and correlated channels.

Recently, cooperative communication has received much attention and has been considered as a promising technique to use the broadcast nature of wireless channels to make communicating nodes help each other gaining from the spatial diversity. Cooperative mechanism enlarges the communication coverage, enhances the capacity, and improves the transmission performance.

Cooperative techniques have already been considered for wireless and mobile broadband radio and Cognitive Radio (CR) [49]; they have also been under investigation in various IEEE 802 standards. A recent evolution of IEEE 802.11 using mesh networking, i.e., 802.11s considers the update of 802.11 MAC layer operations to self-configuration and multi-hop topologies. As an amendment to the 802.16 networks, IEEE 802.16j is concerned with multi-hop relay to enhance coverage, throughput, and system capacity [50].

As introduced in Chapter 2, there are mainly two relaying protocols: Amplify-and-Forward (AF) and Decode-and-Forward (DF). In AF, the

received signal is amplified and retransmitted to the destination. The advantage of this protocol is its simplicity and low-cost implementation. However, the noise is also amplified at the relay. In DF, the relay attempts to decode the received signals. If successful, it re-encodes the information and retransmits it. If some relays cannot fully decode the signal, they will be discarded. Recently, there is another new relaying protocol, which is called Compress-and-Forward (CF), some scholars classified it into the DF protocol [6]. CF attempts to generate an estimate of the received signal. This is then compressed, encoded, and transmitted with the hope that the estimated value may assist in decoding the original code word at the destination. In this chapter, we limit ourselves to the DF protocol, which will be explained later in Section 3.3.

Orthogonal Frequency Division Multiplexing (OFDM) possesses the advantages of frequency parallel transmission, high speed communication and efficient spectrum usage. By introducing OFDM transmission into the cooperative communication domain, the gains from both sides are combined. When transmitted through the multi-path channel, OFDM can help cooperative communication to gain from multi-path diversity.

As mentioned in the OFDM review in the last chapter, for the conventional OFDM technology, a Cyclic Prefix (CP) is exploited to eliminate the Inter-Symbol-Interference (ISI) due to multi-path. With CP adding and removing, the linear convolution channel is transformed into a circular convolution channel, and the ISI can be easily resolved. Meanwhile, the channel equalization is also simplified, due to the channel matrix diagonalization. However, the cyclic prefix is not the only way to combat the multi-path. Zero-Padding (ZP) has already been proposed as an alternative to the CP in OFDM transmissions [10] and particularly for Cognitive Radio, reported by us [21]. ZP-OFDM systems provide advantages over CP-OFDM in terms of the transmission power saving, accurate blind time synchronization, better blind channel estimation and elimination of the frequency null problem in the channel frequency response.

Average Bit Error Rate (BER) and capacity are two important criteria for quantifying the performance of different communication systems. The BER performance of wireless transmissions over fading channels is usually quantified by two parameters: diversity order and coding gain.

The diversity order is defined as the asymptotic slope of the BER curve versus Signal-to-Noise Ratio (SNR). It describes how fast the error probability diminishes with SNR, while the coding gain measures the performance gap between different schemes when they have the same diversity. The higher the diversity, the smaller the error probability is at high-SNR regimes. To cope with the deleterious effects of fading on the system performance, diversity-enriched transmitters and receivers have well-appreciated merits. Most of the existing diversity-enabled schemes adopt Maximum-Likelihood Equalizers (MLEs) or near-MLEs at the receiver to collect full diversity [51]. Although MLE enjoys the maximum diversity, its exponentially increased decoding complexity makes it unsuitable for certain practical systems. In order to reduce the system complexity, one may apply Linear Equalizers (LEs), such as Zero-Forcing (ZF) and Minimum Mean Square Error (MMSE) equalizers. It is a well-known fact that LEs usually lose capacity relative to those systems with MLE. However, with the proper design of the transceivers, LEs can still achieve the full diversity. The capacity is another important criterion to quantify the performance of a certain transmission strategy, and describes the maximum information rate for a transmission system with a certain equalizer employed at the receiver. In addition to the potential diversity loss, LEs also lose capacity when compared to systems with MLE.

In order to combine the advantages of both the MIMO systems and the OFDM, by concatenating a linear pre-coder with a layered space-time mapper, a full-diversity and full-rate Space Time Coding (STC) has been proposed for MIMO-OFDM system [52]. A Space Frequency Coding (SFC) MIMO-OFDM system, where two-dimensional coding is applied to distribute channel symbols across space (transmit antennas) and frequency (OFDM tones) within one OFDM block, has been developed to exploit the available spatial, time and frequency diversity [53]. Recently, several research activities on STC and SFC have addressed the full spatial and multi-path diversity issues for MIMO-OFDM system [54, 55]. The Digital Phase Sweeping (DPS) technique based on multiplying a permutation matrix with the time-domain transmitted symbol has been proposed to obtain the tall Toeplitz channel in order to guarantee maximum possible spatial and multi-path diversity in MIMO-OFDM system [56, 57].

Unlike the MIMO system, multiple relays transmissions in the

cooperative system may not be either time or frequency synchronized, i.e., signals transmitted from different relays arrive at the receiver at different time instances, and multiple Carrier Frequency Offsets (CFOs) exist due to the oscillator mismatching. Multiple CFOs introduce time selectivity into the wireless channel. This is similar to high-mobility terminals and scatterers inducing Doppler shifts and so introducing the time selectivity. This similarity can be explained by the resemblance between the multiple CFOs channel matrix and multiple Doppler shifts channel matrix. The time selective channel together with the frequency selective channel caused by the multi-path transmission give a so called doubly time-frequency selective channel. Unlike the conventional MIMO system, the existence of multiple CFOs in cooperative systems makes direct CFOs compensation hard if not impossible. To the best knowledge of authors, the cooperative ZP-OFDM system affected by a multi-path channel and CFOs is a subject that has not yet been addressed in literature. The channel orthogonality deficiency (*od*) [58], which will be defined in Section 3.4, determines the fundamental condition when LEs collect the same diversity as the MLE, i.e., meaning that full diversity can be achieved. To collect the same spatial and multi-path as MLE does, and to improve the system capacity only with LEs, the equivalent channel matrix needs some "modification" to upper bound the od by a constant less than 1. In this chapter, based on some new results proposed in [58] and [59], we will illustrate how to simultaneously achieve the full cooperative and multi-path diversity, to combat CFOs and to enable low system complexity only with LEs. We also show that, on the basis of the proposed cooperative tall Toeplitz scheme, the same outage diversity as that of MLE is attained by LEs.

Therefore, in this chapter, we first review the main characteristics of the ZP-OFDM, and explain why ZP-OFDM is a good candidate for cooperative wideband communication. Then, we investigate the diversity, capacity and complexity issues of cooperative ZP-OFDM communication. We consider cooperative ZP-OFDM communication over a multi-path Rayleigh channel and with multiple CFOs which may exist at different relays. We use a cooperative tall Toeplitz scheme to achieve full cooperative and multi-path diversity, while simultaneously combat the CFOs. Importantly, this full diversity scheme only requires LEs, such as ZF and MMSE equalizers, an issue which reduces the system complexity when compared to MLE or other near-MLEs. Theoretical analysis of the proposed cooperative tall Toeplitz scheme is

provided on the basis of the analytical upper bound of the channel orthogonality deficiency derived in this chapter. Utilizing only low-complexity linear equalizers, theoretical analysis and simulation results show that the proposed Toeplitz scheme achieves the full cooperative, multi-path and outage diversity.

The rest of the chapter is organized as follows. Section 3.2 reviews important features of ZP-OFDM. In Section 3.3, we first give the system model of the (on DF protocol-based) cooperative ZP-OFDM communication system with a multi-path channel and multiple CFOs. Then, we provide a cooperative tall Toeplitz scheme to illustrate the full diversity design. Different equalization schemes and the concept of channel orthogonality deficiency are shown in Section 3.4. In Section 3.5, we justify the full cooperative and multi-path diversity with CFOs and LEs by using the presented cooperative tall Toeplitz scheme. The upper bound of the channel orthogonality deficiency of the cooperative tall Toeplitz scheme is derived to elucidate the parameter's effect. In Section 3.6 and Section 3.7, we analyze and discuss the capacity and decoding complexity of different equalizers. Simulation results are illustrated in Section 3.8 to corroborate the theoretical claims, and finally Section 3.9 concludes the chapter.

3.2 Why ZP-OFDM for cooperative wideband communication

OFDM possesses the advantages of frequency parallel transmission, high speed communication and efficient spectrum usage. By introducing OFDM transmission into the cooperative communication domain, the gains from both sides are combined. When transmitted through the multi-path channel, OFDM can help for cooperative communication gain from multi-path diversity. The ZP-OFDM systems provide advantages over CP-OFDM in terms of transmission power saving, accurate blind time synchronization, better blind channel estimation and elimination of the null problem in the frequency response channel. Therefore, in this Section, we investigate the characteristics of ZP-OFDM, and analyze if ZP-OFDM is a good candidate for cooperative wideband communication.

3.2.1 Power consumption

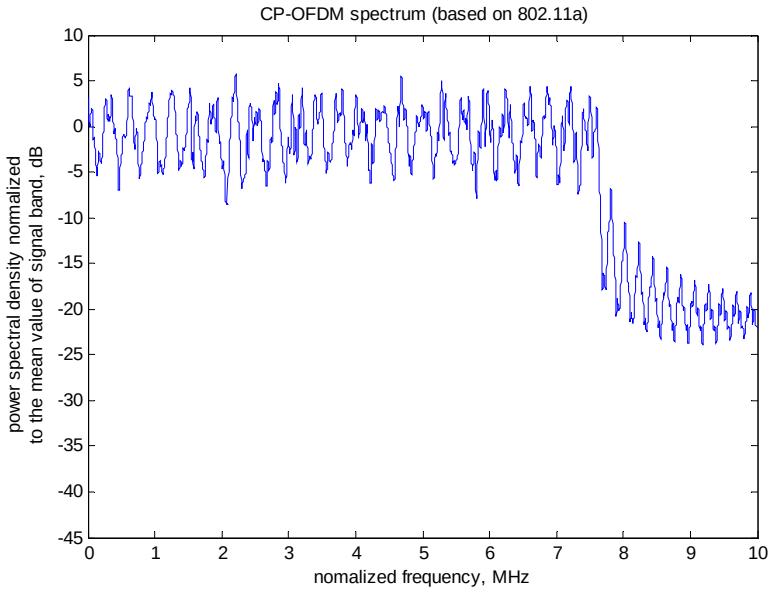

(A). CP-OFDM based on IEEE 802.11a

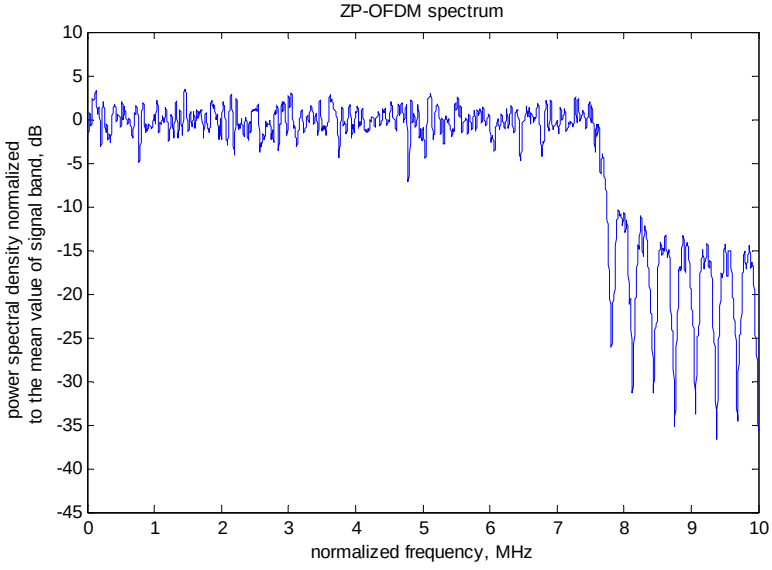

(B). ZP-OFDM

Fig. 3.1. PSD plots for CP-OFDM and ZP-OFDM.

One most important advantage why ZP-OFDM outperforms CP-OFDM

is its low power consumption for transmission. Since the linear structure of the channel matrix of ZP-OFDM, see Section 2.4 for the details, the frequency spikes are reduced, compared to the CP-OFDM case. Similar to silent periods in TDMA, trailing zeros will not pose problems to High-Power Amplifiers (HPA). Thanks to subsequent pulse-shaping, they will not give rise to out-of-band spectral leakage, either.

Next, we show an example to compare the ripples in the power spectral density (PSD) of CP-OFDM and ZP-OFDM cases. We consider the IEEE 802.11a standard, adopting 64 subcarrier OFDM, utilizing 52 subcarriers for data transmission, while CP and ZP both account for 25% of the OFDM symbol duration. Fig. 3.1 (A) illustrates the power spectrum at the transmission side according to IEEE 802.11a. If the CP is replaced by the ZP, the power spectral density is as shown in Fig. 3.1 (B), where ripples in the signal band are reduced. In Fig. 3.1, the PSD of the signal band in CP-OFDM exhibits more fluctuations than in the ZP case, which shows a clear indication of lower frequency spikes when using ZP-OFDM.

In the ZP-OFDM case, the transmitted signal has no longer any coherent structure, and is completely random. Thus, the ripples in the PSD can be reduced significantly by averaging, which consequently provides lower frequency spikes. In the CP-OFDM case, the redundancy in the signal structure is introduced into the transmitted signal. The correlation between the CP replica and the original OFDM symbol leads to the ripples. These ripples in the PSD require some power backup at the transmitter. In fact, the amount of power backup required is equal to the PAPR of the OFDM signal. For a multiband CP-OFDM system, this power backup could be as large as 1.5 dB, which could result in a lower overall range for the system [11].

3.2.2 Blind channel estimation and blind symbol synchronization

Another important feature of ZP-OFDM is its blind channel estimation and blind symbol synchronization capability. When both transmitted symbols and noise are white, the autocorrelation matrix of the received symbol $\mathbf{y}_{zp,t}$ is $\mathbf{R}_y = \mathbf{H}_{ZN}\mathbf{H}_{ZN}^H + \sigma^2\mathbf{I}_Z$, where $\mathbf{H}_{ZN} = \mathbf{H}_Z\mathbf{T}_{ZP}$ is the tall Toeplitz channel matrix in ZP-OFDM, σ^2 is the variance of the Additive White Gaussian Noise (AWGN) term, $\mathbf{I}_Z$ is an $Z \times Z$ identity matrix (see

Section 2.4.2. for details). The first column of $\mathbf{R}_y$ is $\left[|h_1|^2+\sigma^2,\ \ h_1^* h_2,\ \ \cdots\ \ h_1^* h_L,\ \ 0,\ \ \cdots\ \ 0\right]^T$, which recovers all the channel coefficients (scaled by h_1^*) except the first one; in this expression, $(\cdot)^*$ denotes conjugate and $(\cdot)^T$ denotes transpose. If the noise variance is known, we can estimate all channel coefficients to within the scale factor h_1^*. However, the CP-based channel estimator is more complex, because the autocorrelation matrix used by the ZP subspace algorithm is half the size of the CP case. The sample autocorrelation matrix used by the ZP case reaches full rank with fewer samples than in the CP case, meaning a reduced accuracy of the CP-based channel estimator [60, 61].

For ZP systems, it has been shown that blind channel estimation can be done with fewer received blocks by a repeated use of each block [27]. This concept was later generalized in [26] using a parameter called *repetition index*. The feature of using much less received data in the aforementioned blind channel estimation algorithms can also be properly transferred to blind synchronization algorithms if we adopt the repetition index concept. Subspace methods, combined with the repetition index, are shown to significantly improve the symbol synchronization performance with sufficient amount of received data. Reference [26] shows that properly chosen repetition indices, guarantee correct symbol synchronization in absence of noise using only two receive symbols in ZP-OFDM while three are needed in the CP-OFDM case.

3.2.3 Equalization

The strongest point of CP-OFDM relies on its simplicity of equalization procedure, due to the circular structure of the channel matrix. Paper [10] proposed two fast equalizers for ZP-OFDM. One is called ZP-OFDM-FAST-MMSE, as shown at the bottom of Fig. 2.4 (C). Essentially, it adopts an expanded circulant matrix instead of $\mathbf{C}_N$ (**h**), to speed up equalization; that is why it is called FAST. MMSE stands for minimum mean square error. Although, it is still slightly more complex than CP-OFDM, it guarantees symbol recovery and has a better BER performance than the conventional CP-OFDM [10, 62]. The second equalizer (ZP-OFDM-OLA) is more mimicking CP-OFDM, see Fig. 2.4.(B); the linear convolution is transformed to a cyclic convolution like

CP-OFDM; this makes a trade-off possible between the BER performance and complexity of equalization, knowing the sensitivity of channel zeros close to subcarriers. This equalizer will give colors to the original white noise; this drawback can be overcome by using a Viterbi decoder with the consequence of extra system complexity. By virtue of that, ZP-OFDM-FAST-MMSE deserves more attention for future application in cooperative communication.

Circularity of the channel matrix $\mathbf{C}_N(\mathbf{h})$ in Eq. (2-9) is the key point for simplicity of the CP-OFDM equalizer. Therefore, in ZP-OFDM-FAST-MMSE an expanded circulant matrix $\mathbf{C}_Z(\mathbf{h}) = \mathrm{Circ}_Z\left(h_1 \quad 0\cdots 0 \quad h_L \cdots h_2\right)$ was created in paper [10] to obtain a circular convolution property. Thanks to the trailing zeros combating the ISI, Eq. (2-14) can be rewritten as:

$$\mathbf{y}_{zp,t} = \mathbf{C}_Z\left(\mathbf{h}\right)\mathbf{F}_{zp}\mathbf{x}_f + \mathbf{n}_{Z,t} \tag{3-1}$$

The channel matrix can be diagonalized using a $Z \times Z$ FFT matrix $\mathbf{F}_Z$ with entries $\exp(j2\pi mk/Z)/\sqrt{Z}$ as follows:

$$\begin{aligned}\mathbf{F}_Z\mathbf{y}_{zp,t} &= \mathbf{F}_Z\mathbf{C}_Z\left(\mathbf{h}\right)\mathbf{F}_{zp}\mathbf{x}_f + \mathbf{F}_Z\mathbf{n}_{Z,t} \\ &= \mathbf{F}_Z\mathbf{C}_Z\left(\mathbf{h}\right)\mathbf{F}_Z^H\mathbf{F}_Z\mathbf{F}_{zp}\mathbf{x}_f + \mathbf{n}_{Z,f} \\ &= \mathbf{D}_Z\left(\tilde{\mathbf{h}}_Z\right)\mathbf{F}_Z\mathbf{F}_{zp}x_f + \mathbf{n}_{Z,f}\end{aligned} \tag{3-2}$$

where

$$\tilde{\mathbf{h}}_Z := \left[H(0) \quad H(2\pi/Z) \quad \cdots \quad H\left(2\pi(Z-1)/Z\right)\right]^T = \sqrt{Z}\mathbf{F}_Z\mathbf{h} \tag{3-3}$$

$\mathbf{D}_Z\left(\tilde{\mathbf{h}}_Z\right)$ is a $Z \times Z$ diagonal matrix with diagonal $\tilde{\mathbf{h}}_Z$. By comparing Eq. (3-2) with Eq.(2-10), we find that the slightly increased complexity of the ZP-OFDM equalizer comes from the increased number of points of FFT to obtain $\tilde{\mathbf{h}}_Z$ and from calculating the channel irrespective structured matrix $\mathbf{F}_Z^H\mathbf{F}_{zp}^H$. By taking the advantage of using the FFT, this arithmetic complexity becomes a small burden.

3.2.4 Bit Error Rate (BER) performance

By virtue of zero padding, in the absence of equalization, the wireless multi-path channel using ZP-OFDM possesses an inherent better BER performance than when using CP-OFDM. This is because the zeros from other paths introduce less interference than CP, as shown in Fig. 3.2. In this example, we assume a 256-subcarrier BPSK OFDM with a 2-path Ricean plus AWGN channel, and a Ricean *K* factor of 10 dB. The CP length and the amount of ZP are both equal to the second path delay, i.e.: 100 bits, 200 bits and 250bits, and take care of the ISI. It is obvious that the ZP-OFDM has a better performance, and its BER improves as the ZP increases, since more zeros are inserted, which introduces less interference. Meanwhile, the curves of the CP-OFDM remain nearly the same, and represent a poorer BER performance as can be explained by the circular structure of CP.

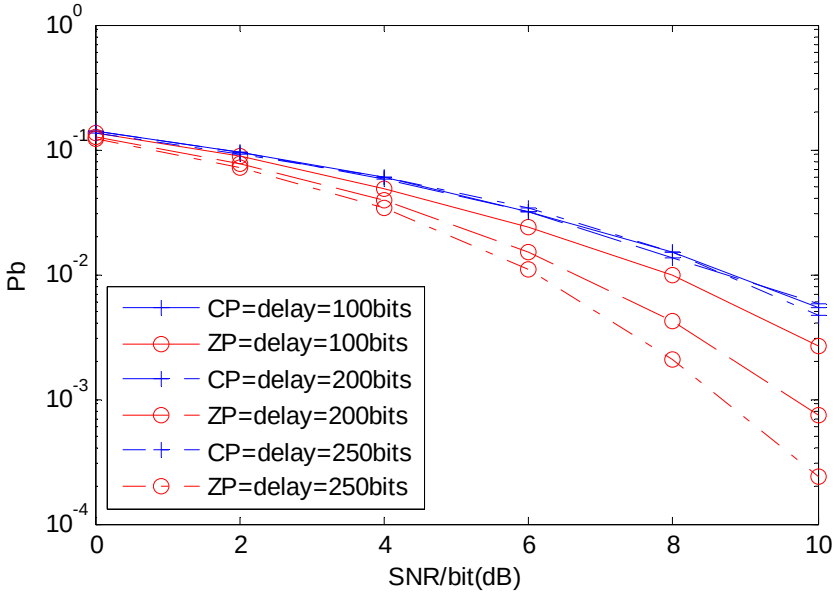

Fig. 3.2. BER performance without equalization of CP and ZP in a Ricean fading channel (Ricean *K* factor =10 dB).

If the second path delay is fixed at 120 bits and the SNR is 25dB, as shown in the Fig. 3.3, ZP-OFDM again always outperforms the CP-OFDM in BER performance; this can be justified by the fact that

ZP-OFDM always gains from less interference of the delayed path.

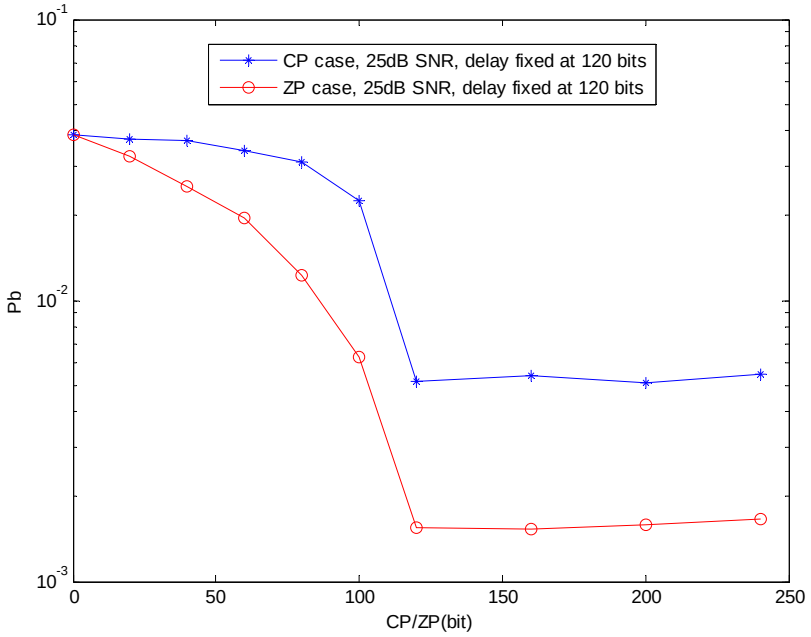

Fig. 3.3. BER performance without equalization of CP and ZP in the Ricean channel with fixed channel delay (Ricean K factor =10 dB).

After equalization, the linear structure of the channel matrix in ZP-OFDM will guarantee full symbol recovery and will further improve BER performance. If we define $\mathbf{H}_{ZN}$ as the first N columns of the $Z \times Z$ convolution matrix $\mathbf{H}_Z$, after ISI removing, Eq. (2-14) becomes

$$\mathbf{y}_{zp,i} = \mathbf{H}_{ZN}\mathbf{F}_N^H \mathbf{x}_f + \mathbf{n}_{Z,t} \qquad (3\text{-}4)$$

$\mathbf{H}_{ZN}$ is a Toeplitz and full column rank matrix, and is always guaranteed to be invertible, which assures symbol recovery (perfect detectability in the absence of noise) regardless of the channel zeros locations [60, 63]. This is a distinct advantage of ZP-OFDM to provide a better BER performance, while this is not the case for CP-OFDM. In fact, the channel-irrespective symbol detectable property of ZP-OFDM is equivalent to claiming that ZP-OFDM enjoys maximum diversity gain [62]. In other words, ZP-OFDM is capable of recovering the diversity

loss incurred by CP-OFDM. Intuitively, this can be understood as the ZP-OFDM retains the entire linear convolution of each transmitted symbol with the channel.

In ZP-OFDM, the tall Toeplitz structure of equivalent channel matrix always guarantees its full rank (it only becomes rank deficient when the channel impulse response is identically zero, which is impossible in practice). In other words, the full rank property guarantees the detection of transmitted symbols. Nevertheless, the zero-padding and linear structure of ZP-OFDM outperforms CP-OFDM in the lower frequency spikes, as zero-padding replaces cyclic prefix in the OFDM symbols, and so significantly reduces the ripples in the PSD. Compared to CP, tailing zeros save transmit power. In the blind channel estimation and blind symbol synchronization area, ZP-OFDM also has its advantage over CP-OFDM in reducing the system complexity, again due to its linear structure. Therefore, ZP-OFDM is a good candidate for future cooperative wideband communication. In the following sections, we investigate the diversity issue of cooperative ZP-OFDM communication with the unique nature of a tall Toeplitz structure. We show how the system takes advantage of this nature to achieve the full cooperative and multi-path diversity, and to combat the multiple CFOs from different cooperative relays, only with linear equalizers (such as the ZF or MMSE equalizer).

3.3 Cooperative ZP-OFDM system model and cooperative tall Toeplitz scheme

In this section, we consider a DF cooperative ZP-OFDM system as shown in Fig. 3.4. In case the relay can fully decode the signal, DF always outperforms AF in transmission performance. Fully decoding relay can be guaranteed by employing an error detection code, such as cyclic redundancy check, or easily pick up the relay with a SNR larger than the threshold[3]. Therefore, we assume the relays shown in Fig. 3.4 can fully decode the information, participate in the cooperation, and occupy different frequency bands to forward the data to the destination. We also assume that each relay-destination link undergoes uncorrelated

[3] The threshold is $\left(2^{B}-1\right)/h_{S,Q_r}$; where B is the target rate and h_{S,Q_r} denotes the power gain from source to relay Q_r .

multi-path Rayleigh fading. According to Eq. (2-14), for the relay r, $r \in [1,2,\cdots,R]$, R is the number of relays, the received signal of r-th relay can be formulated as

$$\mathbf{y}_{r,f} = \mathbf{F}_Z \mathbf{D}_{Z,r} \mathbf{H}_r \mathbf{T}_{ZP} \mathbf{F}_N^H \mathbf{x}_f + \mathbf{n}_{Z,f} . \tag{3-5}$$

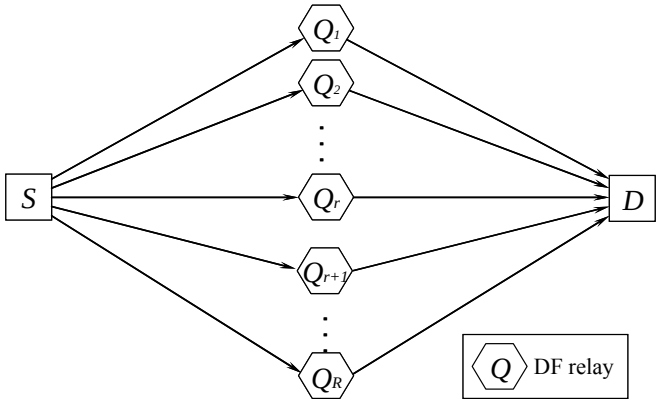

Fig. 3.4. DF cooperative ZP-OFDM system architecture, (*S*: Source, *D*: Destination, Q_r: *r*-th Relay).

The subscript r here indicates the index of the r-th relay. The matrix $\mathbf{H}_r$ is a $Z \times Z$ lower triangular matrix with first column vector $\left[h_{1,r},\cdots,h_{L,r},0\cdots 0\right]^T$, and first row vector $\left[h_{1,r},0\cdots 0\right]$; $h_{L,r}$ denotes the L-th path gain over the r-th relay and destination link. Without loss of generality, we assume that the channel lengths of different relay-destination links are all L. The matrix $\mathbf{D}_{Z,r}$ is a diagonal matrix representing the residual carrier frequency error over the r-th relay and destination link and is defined in terms of its diagonal elements as $\mathbf{D}_{Z,r} = \mathrm{diag}\left(1,\alpha_r,\cdots,\alpha_r^{Z-1}\right)$, with $\alpha_r = \exp\left(j2\pi q_r / N\right)$; q_r is the normalized carrier frequency offset of the r-th relay with a symbol duration of ZP-OFDM. $\mathbf{n}_{Z,f}$ is the FFT processed noise, which remains an additive white Gaussian term since $\mathbf{F}_Z$ is a unitary matrix [8, 64]. Here, we define $\mathbf{H}_{T,r} = \mathbf{H}_r \mathbf{T}_{ZP}$, which is a full column rank tall Toeplitz matrix, and whose correlation matrix is always guaranteed to be invertible. Consequently, Eq. (3-5) can be rewritten as:

$$\mathbf{y}_{r,f} = \mathbf{F}_Z \mathbf{D}_{Z,r} \mathbf{H}_{T,r} \mathbf{F}_N^H \mathbf{x}_f + \mathbf{n}_{Z,f} . \quad (3\text{-}6)$$

The DPS technique, based on insertion of the permutation matrix

$$\mathbf{P}_r = \begin{bmatrix} \mathbf{0} & \mathbf{I}_{(r-1)L} \\ \mathbf{I}_{Z-(r-1)L} & \mathbf{0} \end{bmatrix} \quad (3\text{-}7)$$

between the channel matrix $\mathbf{H}_r$ and tailing zero matrix $\mathbf{T}_{ZP}$, can be used to form a tight tall Toeplitz channel matrix, which is illustrated later (in Fig. 3.7). This procedure is regarded as applying a DPS coding on the time-domain signal. It does not change the original data rate, but guarantees the maximum possible spatial and multi-path diversity in the MIMO system, due to characteristics of the tight tall Toeplitz channel matrix [56, 57]. However, in the cooperative relay system, a CFOs problem due to the oscillator mismatching between different relays is inevitable. In this situation, DPS cannot obtain the cooperative and multi-path diversity with linear receivers. We will verify this observation by the theoretical analysis and simulation results later. In order to cope with the CFOs problem and achieve full cooperative and multi-path diversity with only linear equalizers, we design a cooperative tall Toeplitz scheme; we arrange transmitted symbols in different frequency bands according to the corresponding relay, as shown in the Fig. 3.5.

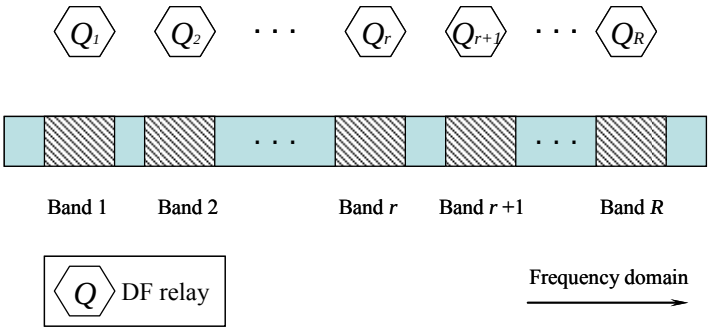

Fig. 3.5. Cooperative tall Toeplitz design for cooperative ZP-OFDM relays.

We take $\mathbf{x}_f$ as information symbols correctly received at the r-th relay nodes involved in the DF-cooperative scheme. After full decoding,

$\mathbf{x}_f$ is assigned to the corresponding *r*-th frequency band as shown in the Fig. 3.5, and forwarded to the destination. This design is also suitable for a cognitive radio system when several spectrum holes are available for the cooperative communication. The above design is equivalent to multiplying a matrix $\mathbf{G} = \left[\mathbf{I}_1, \mathbf{I}_2, \cdots, \mathbf{I}_R\right]^T$ with $\mathbf{F}_N^H \mathbf{x}_f$, where $\mathbf{I}_r$ is an $N \times N$ identity matrix, $r \in \left[1, 2, \cdots, R\right]$; the received signal at the destination from all *R* relay nodes yields

$$\mathbf{y}_f = \mathbf{FDHGF}_N^H \mathbf{x}_f + \mathbf{n}_{RZ,f}, \tag{3-8}$$

where $\mathbf{F} = \mathrm{diag}\left(\overbrace{\mathbf{F}_Z, \mathbf{F}_Z, \cdots, \mathbf{F}_Z}^{R \text{ times}}\right)$, $\mathbf{D} = \mathrm{diag}\left(\mathbf{D}_{Z,1}, \mathbf{D}_{Z,2}, \cdots, \mathbf{D}_{Z,R}\right)$, $\mathbf{H} = \mathrm{diag}\left(\mathbf{H}_{T,1}, \mathbf{H}_{T,2}, \cdots, \mathbf{H}_{T,R}\right)$, are all diagonal matrices with *R* relay's components on their diagonals. $\mathbf{n}_{RZ,f}$ denotes the AWGN vector with zero mean, variance N_o=1 and length *RZ*. For instance, when we consider a 2-relay cooperation system, i.e., *R* = 2, then the structures of $\mathbf{F}$, $\mathbf{D}$, and $\mathbf{H}$ can be illustrated as shown in Fig. 3.6.

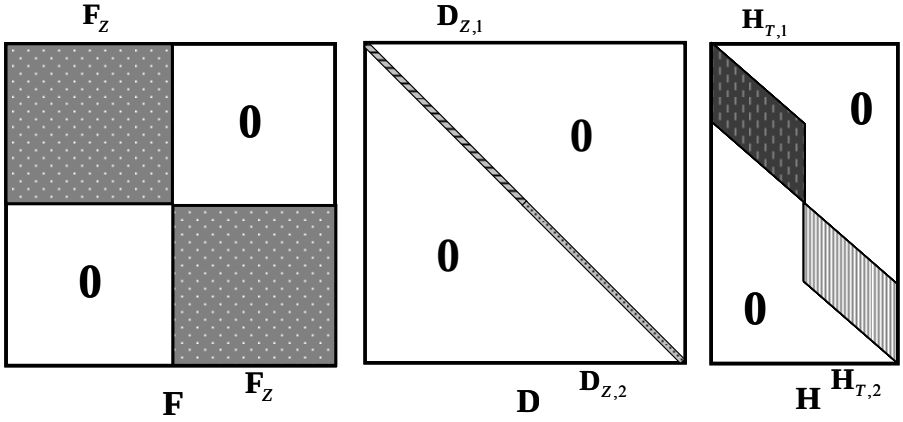

Fig. 3.6. Structures of the FFT matrix, CFOs matrix and channel matrix for a 2-relay cooperative system; left: FFT matrix $\mathbf{F}$, middle: CFOs matrix $\mathbf{D}$, right: channel matrix $\mathbf{H}$. Blank parts are all 0's, the shaded parts correspond to non-zero entries.

If we denote $\mathbf{HG}=\hat{\mathbf{H}}_T$, then, $\hat{\mathbf{H}}_T = \left[\mathbf{H}_{T,1}^T, \mathbf{H}_{T,2}^T, \cdots, \mathbf{H}_{T,R}^T\right]^T$ will be a linear

Toeplitz matrix, or tall Toeplitz matrix, with $\hat{\mathbf{h}}_1 = \left[\hat{h}_{1,1},\cdots,\hat{h}_{L,1},\mathbf{0},\hat{h}_{1,2},\cdots,\hat{h}_{L,2},\mathbf{0},\cdots,\hat{h}_{1,R},\cdots,\hat{h}_{L,R},\mathbf{0}\right]^T$ being $\hat{\mathbf{H}}_T$'s first column. $\hat{\mathbf{H}}_T$ can be regarded as a tall Toeplitz channel matrix, with the channel length $L_T = Z\times(R-1)+L$ as well. For the case $R = 2$, $\hat{\mathbf{H}}_T$ is shown at the left hand side of Fig. 3.7. The DPS technique proposed in [56] is used to convert the R transmit-antenna system, where each frequency-selective channel has L taps into a single transmit antenna system, where the equivalent channel has RL taps. $\mathbf{H}_D$, shown at the right-hand-side of Fig. 3.7, is the channel matrix adopting the DPS technique. Comparing $\hat{\mathbf{H}}_T$ with $\mathbf{H}_D$ learns that the tight tall Toeplitz structure of $\mathbf{H}_D$ enables the system to have a high bandwidth efficiency. However, when CFOs exist at different relays, the DPS technique cannot remove this deleterious effect and subsequently degrades the diversity gains. We will show this drawback later in our theoretical analysis and simulation results as well.

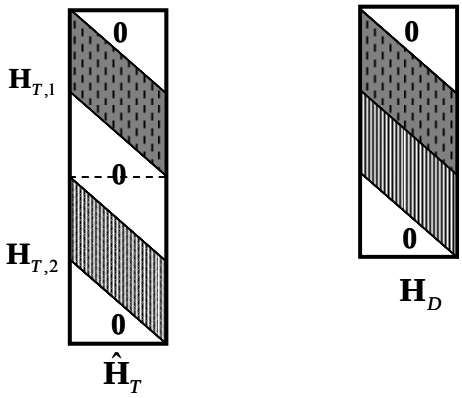

Fig. 3.7. Structures of the proposed tall Toeplitz channel matrix $\hat{\mathbf{H}}_T$ and channel matrix based on DPS $\mathbf{H}_D$. Blank parts are all 0's, the shaded parts correspond to non-zero entries.

We notice that since the relays perform the forwarding in different bands, matrix $\mathbf{G}$ spreads the R copies of the time-domain signal $\mathbf{x}_t = \mathbf{F}_N^H \mathbf{x}_f$, according to the corresponding R cooperative relays. Therefore, matrix $\mathbf{G}$ can be regarded as a coding on the time-domain signal, for different relays and different bands, and is called the Space-Time-Frequency Coding (STFC) [24, 25]. Then, Eq. (3-8)

becomes

$$\mathbf{y}_f = \mathbf{F}\mathbf{D}\hat{\mathbf{H}}_T\mathbf{F}_N^H\mathbf{x}_f + \mathbf{n}_{RZ,f}\,. \tag{3-9}$$

If we denote $\mathbb{H} = \mathbf{F}\mathbf{D}\hat{\mathbf{H}}_T\mathbf{F}_N^H$ as the *RZ*-row times *N*-column equivalent channel matrix, we get

$$\mathbf{y}_f = \mathbb{H}\mathbf{x}_f + \mathbf{n}_{RZ,f}\,. \tag{3-10}$$

$\mathbb{H}$ in Eq. (3-10) is called the overall equivalent channel. In Section 3.5, we will exploit $\mathbb{H}$ to show that our cooperative tall Toeplitz scheme can achieve the full cooperative and multi-path diversity and combat the CFOs, with only LEs. Beforehand, we review the two concepts: equalization and channel orthogonality deficiency.

3.4 Equalization and channel orthogonality deficiency

Given the equivalent channel model in Eq. (3-10), there are various ways to decode $\mathbf{x}$ from observation $\mathbf{y}$. We first provide the definitions of the equalizers that we consider in this chapter. On the one hand, an often used method, which is also optimal if there is no prior information on the symbols or when symbols are treated as deterministic parameters, is the MLE. The output of the MLE $\mathbf{x}_{ml}$ is then given as

$$\mathbf{x}_{ml} = \arg\min_{\tilde{\mathbf{x}}\in S^N} \left\|\mathbf{y} - \mathbb{H}\tilde{\mathbf{x}}\right\|, \tag{3-11}$$

where $\tilde{\mathbf{x}}$ is the transmitted symbol and *S* is the finite alphabet of the transmitted symbols.

On the other hand, LEs, such as the ZF equalizer and MMSE equalizer are favored for their low decoding complexity. The output of the ZF equalizer $\mathbf{x}_{zf}$ is defined as

$$\mathbf{x}_{zf} = \mathbb{H}^{\dagger}\mathbf{y}\,, \tag{3-12}$$

where $\mathbb{H}^{\dagger} = \left(\mathbb{H}^H \mathbb{H}\right)^{-1} \mathbb{H}^H$ denotes the pseudo-inverse of the channel matrix $\mathbb{H}$.

The output of the MMSE equalizer $\mathbf{x}_{mmse}$ is defined as

$$\mathbf{x}_{mmse} = \left(\mathbb{H}^H \mathbb{H} + N_0 \mathbf{I}_N\right)^{-1} \mathbb{H}^H \mathbf{y}, \tag{3-13}$$

We note that, with the definition of an extended system

$$\widehat{\mathbb{H}} = \begin{bmatrix} \mathbb{H} \\ \sqrt{N_0}\mathbf{I}_N \end{bmatrix} \text{ and } \widehat{\mathbf{y}} = \begin{bmatrix} \mathbf{y} \\ \mathbf{0}_{N\times 1} \end{bmatrix}, \tag{3-14}$$

the MMSE equalizer in Eq. (3-13) can be rewritten as $\mathbf{x}_{mmse} = \widehat{\mathbb{H}}^{\dagger}\widehat{\mathbf{y}}$; this indicates that the ZF equalizer and MMSE equalizer are both LEs, and share the linear properties. Therefore, some analysis based on the ZF equalizer can be extended to the MMSE equalizer, and vice versa.

The important reason that hinders LEs from getting more attention in theory and practice is that their performance loss, relative to MLEs, is not quantified in general. In the following, to critically quantify the performance gap between LEs and MLE, we adopt the parameter, orthogonality deficiency (*od*), of the channel matrix $\mathbb{H}$ as in [58].

Definition 1 (Orthogonality Deficiency): For an equivalent channel matrix $\underline{\underline{\mathbb{H}}} = [\underline{\mathbf{h}}_1, \underline{\mathbf{h}}_2, \cdots, \underline{\mathbf{h}}_N]$, with $\underline{\mathbf{h}}_n$ being the $\underline{\underline{\mathbb{H}}}$'s *n*-th column, its orthogonality deficiency $od\left(\underline{\underline{\mathbb{H}}}\right)$ is defined as

$$od\left(\underline{\underline{\mathbb{H}}}\right) = 1 - \frac{\det\left(\underline{\underline{\mathbb{H}}}^H \underline{\underline{\mathbb{H}}}\right)}{\prod_{n=1}^{N} \left\|\underline{\mathbf{h}}_n\right\|^2}. \tag{3-15}$$

If $\underline{\underline{\mathbb{H}}}$ is singular, $od\left(\underline{\underline{\mathbb{H}}}\right) = 1$. The closer $od\left(\underline{\underline{\mathbb{H}}}\right)$ to zero, the more orthogonal the $\underline{\underline{\mathbb{H}}}$. Given the model in Eq. (3-10), if $od\left(\underline{\underline{\mathbb{H}}}\right) = 0$, and thus $\underline{\underline{\mathbb{H}}}^H \underline{\underline{\mathbb{H}}}$ is diagonal, then LEs have the same performance as that of MLE.

3.5 Diversity analysis of the proposed cooperative ZP-OFDM scheme

3.5.1 Full cooperative and multi-path diversity with Carrier Frequency Offsets (CFOs) and Linear Equalizers (LEs)

For the proposed cooperative tall Toeplitz scheme, we first cite the following theorem from [58]:

Theorem 1: Consider the linear system as in Eq. (3-10). A LE achieves full diversity and collects the same diversity as MLE does, if there exists a constant $\varepsilon \in (0,1)$ such that $\forall\ \mathbb{H}$, $od(\mathbb{H}) \le \varepsilon$.

Then, we have the Lemma as follows:

Lemma 1: For the cooperative tall Toeplitz scheme, when CFOs appear, the LEs are the only equalizer requirement to achieve full cooperative and multi-path diversity order of *RL*. The proof of this lemma is shown in Appendix 3.1.

For the conventional DPS technique, it provides a compact tall Toeplitz structure channel matrix, as shown in Fig. 3.7, which results in CFO matrices overlapping each other accordingly. The overlapped CFO matrices cause that the unitary property is lost, and consequently the channel matrix of DPS with CFOs is not a tall Toeplitz any more, and loses frequency orthogonality, which means that $\det(\mathbb{H}^H\mathbb{H})$ of the DPS case cannot always guarantee to be larger than zero, and that $od(\mathbb{H})$ may be equal to 1. Therefore, according to *Theorem 1*, when CFOs from different relays appear, the DPS technique with LEs cannot achieve full diversity gains. We will verify this theoretical claim by simulations as shown in Section 3.8.

3.5.2 Upper bound of the channel orthogonality deficiency of the proposed scheme

In order to provide a further insight into the channel factors that affect the cooperative transmission performance, we consider the orthogonality deficiency of a pure channel, and denote $\bar{\mathbb{H}} = \mathbf{D}\hat{\mathbf{H}}_T$. The orthogonality

deficiency of the pure channel can be represented as

$$od\left(\bar{\bar{\mathbb{H}}}\right)=1-\frac{\det\left(\bar{\bar{\mathbb{H}}}^{H}\bar{\bar{\mathbb{H}}}\right)}{\prod_{n=1}^{N}\left\|\bar{\mathbf{h}}_{n}\right\|^{2}}=1-\frac{\det\left(\hat{\mathbf{H}}_{T}^{H}\hat{\mathbf{H}}_{T}\right)}{\prod_{n=1}^{N}\left\|\bar{\mathbf{h}}_{n}\right\|^{2}}, \qquad (3\text{-}16)$$

where $\bar{\mathbf{h}}_{n}$ is $\bar{\bar{\mathbb{H}}}$'s *n*-th column. For the *RZ*-row times *N*-column tall Toeplitz channel matrix $\hat{\mathbf{H}}_{T}$, suppose $m=\arg\max_{l_{rz}\in[1,\,RZ]}\left|\hat{h}_{l_{rz}}\right|^{2}$ and $\left|\hat{h}_{m}\right|^{2}>0$, the tall Toeplitz channel matrix $\hat{\mathbf{H}}_{T}$ can be split into three submatrices as $\hat{\mathbf{H}}_{T}=\left[\hat{\mathbf{H}}_{T,o1}^{T},\hat{\mathbf{H}}_{T,m}^{T},\hat{\mathbf{H}}_{T,o2}^{T}\right]^{T}$, where matrix $\hat{\mathbf{H}}_{T,o1}$ consists of the first $(m-1)$ rows of $\hat{\mathbf{H}}_{T}$, $\hat{\mathbf{H}}_{T,o2}$ has the last $(RZ-2m)$ rows of $\hat{\mathbf{H}}_{T}$, and $\hat{\mathbf{H}}_{T,m}$ is of the size $N \times N$ with $\hat{h}_{m}$ on the diagonal entries. Therefore, we have $\hat{\mathbf{H}}_{T}^{H}\hat{\mathbf{H}}_{T}=\hat{\mathbf{H}}_{T,o1}^{H}\hat{\mathbf{H}}_{T,o1}+\hat{\mathbf{H}}_{T,m}^{H}\hat{\mathbf{H}}_{T,m}+\hat{\mathbf{H}}_{T,o2}^{H}\hat{\mathbf{H}}_{T,o2}$. It is easy to show that $\det\left(\hat{\mathbf{H}}_{T,m}^{H}\hat{\mathbf{H}}_{T,m}\right)=\left(\left|\hat{h}_{m}\right|^{2}\right)^{N}$ when $N > RZ$. Thus, we bound $\det\left(\bar{\bar{\mathbb{H}}}^{H}\bar{\bar{\mathbb{H}}}\right)$ as

$$\det\left(\bar{\bar{\mathbb{H}}}^{H}\bar{\bar{\mathbb{H}}}\right)\geq\det\left(\hat{\mathbf{H}}_{T,m}^{H}\hat{\mathbf{H}}_{T,m}\right)=\left(\max_{l_{rz}\in[1,\,RZ]}\left(\left|\hat{h}_{l_{rz}}\right|^{2}\right)\right)^{N}. \qquad (3\text{-}17)$$

We note that, for the unitary CFO matrix, $\left|\alpha_{r}^{z}\right|^{2}=1$, $z\in[0,1,\cdots,Z-1]$, and

$$\prod_{n=1}^{N}\left\|\bar{\mathbf{h}}_{n}\right\|^{2}=\left(\sum_{l_{rz}=1}^{RZ}\left|\hat{h}_{l_{rz}}\right|^{2}\right)^{N}, \qquad (3\text{-}18)$$

We find for the upper bound of Eq. (3-16)

$$od\left(\bar{\bar{\mathbb{H}}}\right)\leq 1-\frac{\left(\max_{l_{rz}\in[1,\,RZ]}\left(\left|\hat{h}_{l_{rz}}\right|^{2}\right)\right)^{N}}{\left(\sum_{l_{rz}=1}^{RZ}\left|\hat{h}_{l_{rz}}\right|^{2}\right)^{N}}. \qquad (3\text{-}19)$$

Each column vector of the tall Toeplitz channel matrix $\hat{\mathbf{H}}_{T}$, includes at most *RL* non-zero values. Thus, we obtain

$$\left(\sum_{l_{rz}=1}^{RZ}\left|\hat{h}_{l_{rz}}\right|^2\right)^N \le \left(RL\left(\max_{l_{rz}\in[1,\,RZ]}\left(\left|\hat{h}_{l_{rz}}\right|^2\right)\right)\right)^N . \qquad (3\text{-}20)$$

Consequently, we can write for the upper bound of the $od\left(\bar{\mathbb{H}}\right)$

$$od\left(\bar{\mathbb{H}}\right) \le 1-\frac{\left(\max_{l_{rz}\in[1,\,RZ]}\left(\left|\hat{h}_{l_{rz}}\right|^2\right)\right)^N}{\left(RL\left(\max_{l_{rz}\in[1,\,RZ]}\left(\left|\hat{h}_{l_{rz}}\right|^2\right)\right)\right)^N} = 1-\frac{1}{(RL)^N} . \qquad (3\text{-}21)$$

Note that RL is the full diversity order. If we keep RL as a constant, and reduce the upper bound of $od\left(\bar{\mathbb{H}}\right)$ by decreasing N, i.e., the channel becomes more orthogonal, the upper bound of the BER also becomes smaller; this indicates that LEs may achieve a better BER performance with full diversity order. Later, we will verify this theoretical claim by simulations in Section 3.8.

3.6 Capacity analysis of the proposed cooperative ZP-OFDM scheme

Besides BER, mutual information is another important criterion when comparing the performance of different systems, since it measures how efficiently the transceivers utilize the channels. The concept "capacity" here denotes the maximum mutual information when a certain transceiver is adopted. Given a random channel, the instantaneous capacity is also random. In this case, to depict the capacity, one not only needs the capacity, but also the outage capacity, i.e. C^{th}, a capacity threshold which indicates the outage behavior [65]. In this section, we compare the outage capacity of the ZF equalizer with that of the MLE. The results can be easily extended to other LEs. We first consider the capacity when no channel state information is available at the transmitter, and the MLE is adopted at the receiver. Given the linear equivalent channel model in Eq. (3-10), the capacity achieved by MLE, i.e., C_{ml} is given by

$$C_{ml}\left(\mathbb{H}\right) = \log_2\left[\det\left(\mathbf{I}_N + \left(1/N_o\right)\mathbb{H}^H\mathbb{H}\right)\right]. \qquad (3\text{-}22)$$

When a ZF equalizer is adopted at the receiver, the capacity can be expressed as [66]

$$C_{zf}\left(\mathbb{H}\right)=\log_2\left[\det\left(\mathbf{I}_N+\left(1/N_o\right)\mathbb{N}^{-1}\right)\right], \qquad (3\text{-}23)$$

where $\sigma_n^2\mathbb{N}$ is called the covariance matrix of the equivalent noise vector with $\mathbb{N}=\mathrm{diag}\left[k_{1,1},k_{2,2},\cdots,k_{N,N}\right]$, and $k_{i,i}$ being the (i,i) -th entry of matrix $\mathbb{k}=\left(\mathbb{H}^H\mathbb{H}\right)^{-1}$. It is well known that $C_{zf}\left(\mathbb{H}\right)\le C_{ml}\left(\mathbb{H}\right)$ is always satisfied, and the difference between $C_{zf}\left(\mathbb{H}\right)$ and $C_{ml}\left(\mathbb{H}\right)$ for each realization of $\mathbb{H}$ can be as approximated by [58]

$$C_{ml}\left(\mathbb{H}\right)-C_{zf}\left(\mathbb{H}\right)\approx-\log_2\left(1-od\left(\left(\mathbb{H}^{\dagger}\right)^H\right)\right). \qquad (3\text{-}24)$$

This expression shows that the capacity difference between the ZF equalizer and MLE is also related to the *od* of the channel matrix. Similar to the discussion in the previous Section, we also consider the pure channel effect $\overline{\mathbb{H}}$ here. We observe that as $od\left(\left(\overline{\mathbb{H}}^{\dagger}\right)^H\right)$ decreases, i.e., the inverse of the channel matrix is more orthogonal, the capacity gap between the MLE and ZF equalizer decreases.

Next, we show that, with the ZF equalizer, the proposed cooperative ZP-OFDM scheme collects the same outage diversity as that of the MLE. The outage diversity order G_o is defined as

$$G_o=\lim_{\mathrm{SNR}\to\infty}-\frac{\log\left(\mathrm{Prob}\left(C<C^{th}\right)\right)}{\log\left(\mathrm{SNR}\right)}\quad. \qquad (3\text{-}25)$$

If two Cumulative Density Functions (CDFs) of channel capacities are in parallel, it can be shown that they have the same outage diversity [58]. In order to prove that the proposed cooperative ZP-OFDM scheme in this chapter employing the ZF equalizer achieves the same outage diversity as the MLE, we cite the results from [58] in the following theorem:

Theorem 2: Given the system model of Eq. (3-10) with channel state information at the receiver but not at the transmitter, and if $od\left(\overline{\mathbb{H}}\right) \le \varepsilon$, $\forall\ \overline{\mathbb{H}}$, and $\varepsilon \in (0,1)$, then at high-SNR regime, the ZF equalizer collects the same outage diversity as that of the MLE.

Note that the condition in *Theorem 2* is the same as the condition in *Theorem 1*. Similar to the verification for the full cooperative diversity, by taking the advantage of the linear tall Toeplitz structure of the proposed cooperative ZP-OFDM scheme, it means that by utilizing the proposed cooperative ZP-OFDM scheme with the tall Toeplitz equivalent channel matrix, the ZF equalizer has the same outage diversity as that of the MLE.

In summarizing this section, we showed that the mutual information loss between the ZF equalizer and MLE also depends on the *od* of the channel matrix. When the *od* of the channel matrix has an upper bound which is strictly less than one, (for example, derived from the proposed cooperative tall Toeplitz scheme), the performance diversity i.e., cooperative and multi-path diversity, and the outage diversity in Eq. (3-25) of the ZF equalizer are the same as those of MLE.

3.7 Low complexity design based on LEs

In modern wireless communication systems, the decoding complexity is usually given a significant concern, because a more complex decoding scheme always means a higher computational burden and consequently an increase in energy consumption. Thus, the decoding complexity is an important measure for the comparison of different equalizers. In this section, we discuss the complexity of the commonly used equalizers, and then show the importance of the LEs.

To quantify the complexity of different equalizers, we count the average number of arithmetic operations in terms of numbers of real multiplications and real additions, needed to estimate Eq. (3-10). Using the ZF equalizer in Eq. (3-12) as an example, the complexity results

from computing $\mathbb{H}^{\dagger} = \left(\mathbb{H}^{H}\mathbb{H}\right)^{-1}\mathbb{H}^{H}$ using the QR decomposition [4] and calculating $\mathbb{H}^{\dagger}\mathbf{y}$. As shown in paper [67], if we consider $\mathbb{H}$ as an $M \times N$ matrix, $M = R \times (N + L)$, the number of real multiplications for the ZF equalizer equals $O(N^3) + O(N^2 M) + O(NM^2)$ and the number of real additions is also $O(N^3) + O(N^2 M) + O(NM^2)$, where $O(\cdot)$ denotes the Landau notation[5]. The optimum equalizer, MLE in Eq. (3-11) enjoys the best performance; however, it requires the highest complexity as well. As shown in [67], the number of arithmetic operations for the MLE in Eq. (3-11) is $O\left(|\mathbf{x}|^N\right)MN$. We learn from the comparison that the major advantage of LEs is their low decoding complexity.

Although the MLE enjoys the maximum diversity performance, the complexity in MLE can be determined by the number of channels involved and the memory length of the channels. Therefore, MLE's exponential decoding complexity makes it infeasible for certain practical systems. Some near-ML schemes (e.g., Sphere Decoding (SD)) can be used to reduce the decoding complexity. However, at low SNR or when large decoding blocks are sent/or high signal constellations are employed, the complexity of near-ML schemes is still high. As shown in [51], the SD method generally requires an exponential worst case complexity, whereas the heuristic search methods require only $O(N^3)$ computations on the average. This complexity does even not include the complexity from any pre-processing (e.g., decomposition) and it is an average. Simulation results in [68] show that the SD method still has a high complexity compared with conventional LEs, since the SD method adopts linear equalizers as pre-processing steps. To further reduce the complexity, when the system model is linear, one may apply LEs.

3.8 Simulation results and analysis

In this section, we use simulation results to show the effect of the proposed cooperative ZP-OFDM scheme on the performance, and to

[4] A QR decomposition (also called a QR factorization) of a matrix is a decomposition of a matrix **A** into a product **A** = **QR** of an orthogonal matrix **Q** and an upper triangular matrix **R**.

[5] $O(\cdot)$, the Landau notation describes the limiting behavior of a function when the argument tends towards a particular value or infinity, usually in terms of simpler functions.

verify our theoretical claims on diversity and capacity issues. We consider the N sub-carriers ZP-OFDM system with ZP accounts for 25% of the OFDM symbol duration which undergoes Rayleigh channel fading. We consider the 1-relay and 2-relay cases; the normalized CFOs of relay 1 and relay 2 are $q_1 = 0.3$, and $q_2 = 0.5$, respectively. The details of simulation parameters are shown in Table 1.

Table 1. Simulation parameters for cooperative ZP-OFDM

Modulation scheme	BPSK
Multicarrier scheme	CP-OFDM, ZP-OFDM
Number of OFDM subcarriers	8, 16, 32, 64
Length of guard interval	25% of OFDM symbol duration
Number of multi-path	1, 2, 3, 4
Average channel gain of 1-4 path	1, 0.663, 0.487, 0.4255
Transmission bandwidth	500MHz
Number of random trial symbols	1000
Number of relays	1, 2
Normalized CFOs	$q_1 = 0.3$, $q_2 = 0.5$

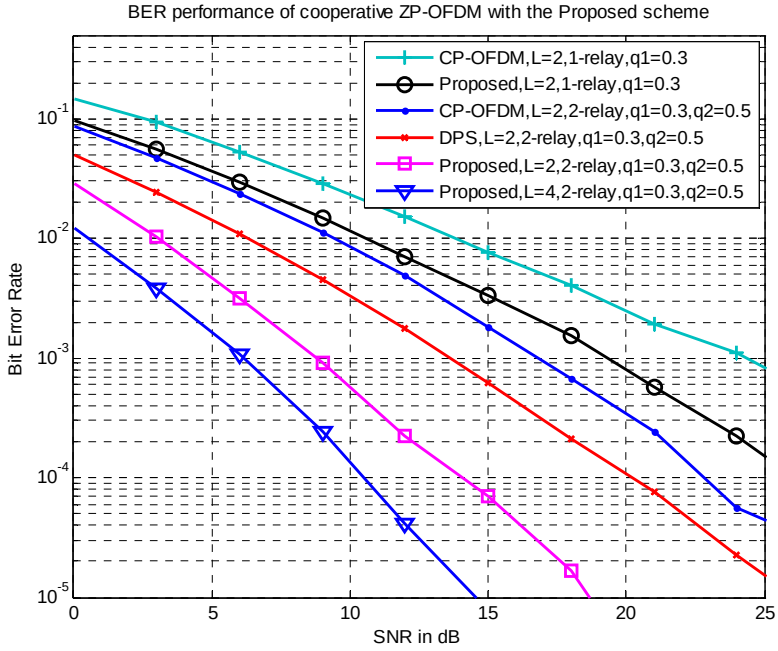

Fig. 3.8. Comparison of the proposed scheme to other conventional schemes for full diversity with LEs and CFOs.

Test Case 1 (Cooperative tall Toeplitz scheme for a full diversity design): In this example, we present simulation results to test the performance of the proposed cooperative tall Toeplitz scheme on ZP-OFDM system with 32 sub-carriers, i.e., $N = 32$, and compare the results with to the conventional DPS technique. Fig. 3.8 shows the BER performance vs. E_b/N_o with different cooperative and multi-path diversity orders, i.e., cooperative diversity order $R = 1, 2$, and multi-path diversity order $L = 2, 4$. Since the MMSE equalizer can be transformed into the ZF equalizer, in the following two cases, we adopted the MMSE equalizer to show the performance of the LEs. The diversity order can be shown as the asymptotic slope of the BER vs. E_b/N_0 curve. It describes how fast the error probability decays with SNR. We can see from Fig. 3.8 that, when CFOs appear at the different relays, the proposed cooperative tall Toeplitz scheme can achieve the full cooperative and multi-path diversity only with the linear equalization, as the asymptotic slope of the curve increases with the increase of the number of relays and multi-path length. However, with CFOs and LEs, the DPS technique loses diversity gains and shows a poor BER performance, which agrees with our theoretical approach in Section 3.5. A. Without DPS technique, the conventional CP-OFDM takes the advantage of easy equalization but a loss in multi-path diversity gain. Adopting the DPS technique, CP-OFDM and ZP-OFDM will achieve the same diversity gain, but still shows a worse performance than the proposed scheme.

Test Case 2 (Bounded channel orthogonality deficiency): In this example, we focus on the upper bound of channel orthogonality deficiency as derived in Eq. (3-21), and show how a change in N affects the channel orthogonality deficiency and BER performance. The frequency-selective channel order L is fixed to be 2, i.e., the multi-path diversity orders are the same. As shown in Fig. 3.9, after adopting the cooperative tall Toeplitz scheme, $od\left(\bar{\mathbb{H}}\right) \le \varepsilon < 1$, which means that the full cooperative diversity is achieved with the linear MMSE equalizer. We also notice that when ε gets smaller as N decreases, the BER performance gets better. This is consistent with the analysis, as shown in Eq. (3-21), i.e., $od\left(\bar{\mathbb{H}}\right)$ decreases with decreasing N. When ε is smaller, the channel is more orthogonal, and the upper bound of the BER performance also becomes smaller. In general, for LEs, a smaller

$od\left(\bar{\mathbb{H}}\right)$ bound indicates a higher coding gain while the diversity gain is the same. Again, because the DPS technique is unable to cope with the CFOs effect, it shows a worse BER performance than the proposed cooperative tall Toeplitz scheme. Conventional CP-OFDM cannot gain from the multi-path diversity, and shows the worst BER performance.

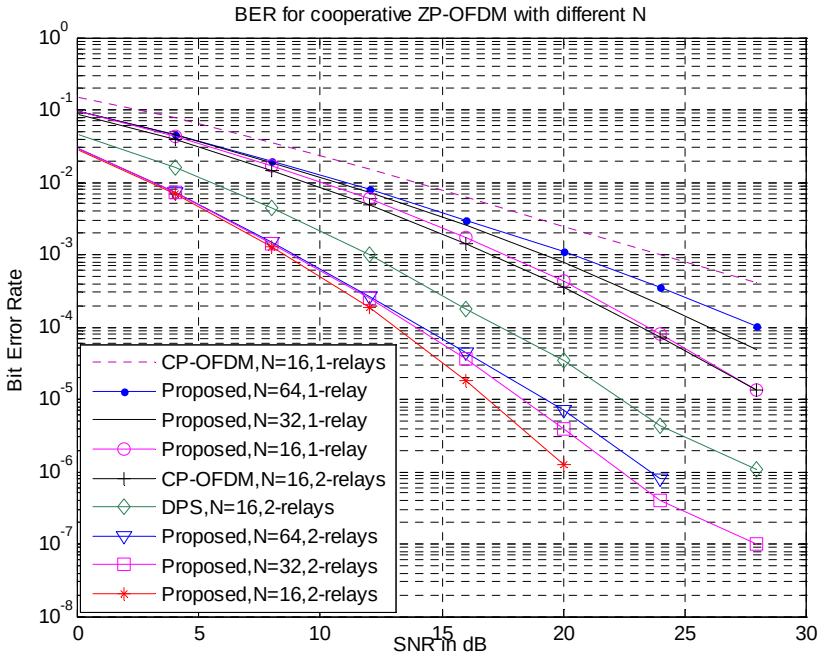

Fig. 3.9. Comparison of the proposed scheme with different numbers of sub-carriers and relays.

*Test Case 3 (Capacity of proposed cooperative tall Toeplitz scheme):*Fig. 3.10 shows the average capacity of a Rayleigh channel with the proposed cooperative tall Toeplitz scheme for the case of two relays cooperation, and without the proposed scheme, i.e., by direct combining of the 2-relays signals in the same frequency band at the destination, the 2-relay system only yields 3 dB power gain. For the low SNR region, average capacity curves are close to each other, and difficult to exhibit the comparison, so we chose to show the SNR region above 0 dB. As shown in the figure, the proposed cooperative tall Toeplitz scheme slightly improves the system capacity, because of exploiting the linear structure and frequency orthogonality of the channel. We notice that the $od\left(\bar{\mathbb{H}}\right)$ gets smaller as the channel length decreases,

and thus the capacity gaps between the ZF and ML equalizer shrink. We also show the average capacity of the CP-OFDM case, which achieves the smallest gap between the ZF and ML equalizer, since CP-OFDM has the pure orthogonal channel matrix. This confirms the observation in Eq. (3-24) that, the capacity gap between the ZF and ML equalizer not only depends on SNR but also on channel orthogonality. The CDFs of the capacity $\text{Prob}\left(C < C^{th}\right)$ with ZF and ML equalizer are depicted in Fig. 3.11, with SNR = 25 dB. We notice that, for the ZF equalizer (ZFE) case without the proposed scheme, the curve is not in parallel with the one of the MLE case, which means a loss of outage diversity. By adopting the proposed cooperative tall Toeplitz scheme, the curve of the ZFE becomes parallel with that of MLE, which indicates that the proposed cooperative tall Toeplitz scheme achieves the same outage diversity as MLE. This is consistent with *Theorem 2* and our analysis in Section 3.6.

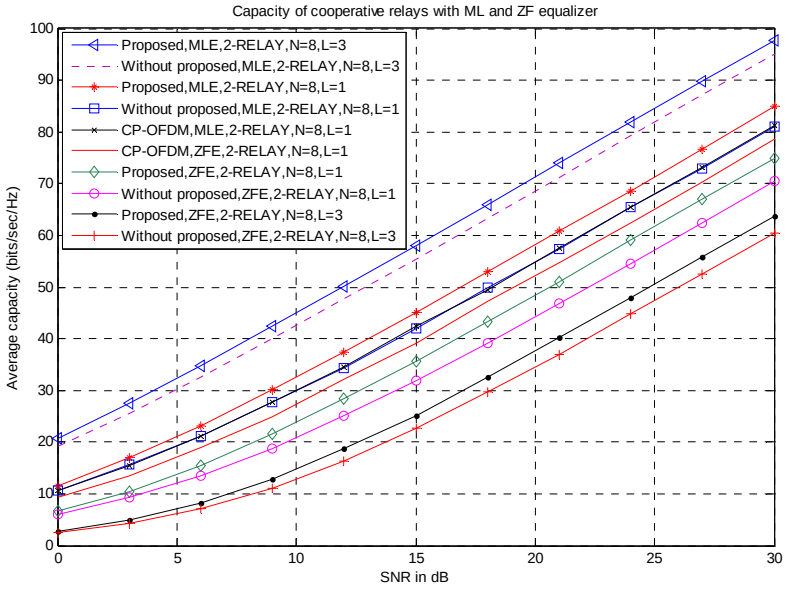

Fig. 3.10: Average capacity of cooperative ZP-OFDM with ML and ZF equalizer.

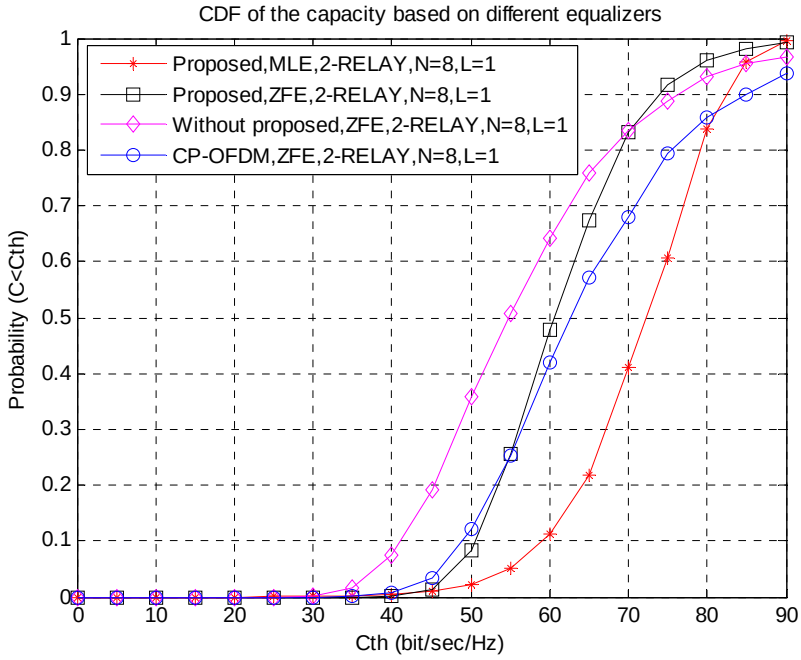

Fig. 3.11: CDF of the capacity of cooperative ZP-OFDM with ML and ZF equalizer.

3.9 Conclusions

In this chapter, we investigated diversity, capacity and complexity issues in cooperative ZP-OFDM communication. We first reviewed the main features of ZP-OFDM and explain why ZP-OFDM is suitable for cooperative wideband communication. Then, we designed a cooperative tall Toeplitz scheme for the cooperative ZF-OFDM communication system, with different CFOs at different relays and over a multi-path Rayleigh channel, i.e., a doubly time-frequency selective channel. In the proposed cooperative tall Toeplitz scheme, the tall Toeplitz structure together with the frequency orthogonality of the channel matrix has a unique feature, which guarantees full cooperative and multi-path diversity, and easily combats the CFOs, only with the LEs. We derived the upper bound of the channel orthogonality deficiency, which provides an insight into how the change of channel factors affects the system performance in terms of BER performance and capacity. According to the theoretical analysis and simulation results, only with linear equalizers,

the cooperative tall Toeplitz scheme achieves the same cooperative, multi-path and outage diversity as those of MLEs, while the system complexity is reduced significantly.

Appendix 3.1

In the following, we verify *Lemma 1* that for the cooperative tall Toeplitz scheme, when CFOs appear, the LEs are the only requirement of equalizer to achieve full cooperative and multi-path diversity order of *RL*.

Proof:

In the cooperative tall Toeplitz scheme, and quivalent channel matrix $\mathbb{H}=\left[\mathbf{h}_1,\mathbf{h}_2,\cdots,\mathbf{h}_N\right]$, with $\mathbf{h}_n$ being $\mathbb{H}$'s *n*-th column, we note that $\mathbf{F}_Z$, $\mathbf{D}_{Z,r}$, $\mathbf{F}_N^H$, $\mathbf{F}$ and $\mathbf{D}$ are all unitary matrices. Therefore, we have

$$\begin{aligned}\det\left(\mathbb{H}^H\mathbb{H}\right)&=\det\left(\mathbf{F}_N\hat{\mathbf{H}}_T^H\hat{\mathbf{H}}_T\mathbf{F}_N^H\right)\\&=\det\left(\mathbf{F}_N\right)\det\left(\mathbf{F}_N^H\right)\det\left(\hat{\mathbf{H}}_T^H\hat{\mathbf{H}}_T\right)\\&=\det\left(\hat{\mathbf{H}}_T^H\hat{\mathbf{H}}_T\right),\end{aligned}\qquad\text{(A3-1)}$$

where $\det\left(\mathbf{F}_N\right)\det\left(\mathbf{F}_N^H\right)=1$. Since $\hat{\mathbf{H}}_T$ is a tall Toeplitz matrix, then $\det\left(\hat{\mathbf{H}}_T^H\hat{\mathbf{H}}_T\right)>0$ for any nonzero channel response, i.e., when $\hat{h}_{l,r}$'s are not equal to zero simultaneously, where $l\in\left[1,2,\cdots,L\right]$, $r\in\left[1,2,\cdots,R\right]$, [69-71]. Consequently, we have $\det\left(\mathbb{H}^H\mathbb{H}\right)>0$.

Meanwhile, for any practical channel, since the components of vector $\mathbf{h}_n$ cannot be equal to zero simultaneously, $\prod_{n=1}^{N}\left\|\mathbf{h}_n\right\|^2>0$ is always satisfied. Therefore, $od\left(\mathbb{H}\right)$ is always smaller than 1, i.e., there exists a constant $\varepsilon\in\left(0,1\right)$ such that $\forall\ \mathbb{H}$, $od\left(\mathbb{H}\right)\le\varepsilon$.

According to *Theorem 1*, we can verify that the proposed cooperative tall Toeplitz scheme can achieve full cooperative and multi-path diversity, only with LEs, and can combat the CFOs at the different relays, simultaneously.

Chapter 4

Relay selection and resource allocation in cooperative relay OFDM communication

4.1 Introduction

As introduced in Chapter 2, cooperative communication has been receiving a lot of attention as promising techniques to increase the modern communication speed and transmission reliability.

In this chapter, we consider a hybrid cooperative Orthogonal Frequency Division Multiplexing (OFDM) wireless network with both Decode-and-Forward (DF) and Amplify-and-Forward (AF) relays and propose a thresholding scheme for the selection of DF and AF relays. Furthermore, a closed-form error probability expression for a hybrid cooperative OFDM network under Rayleigh fading channel is provided. Compared to the previous works by others, our analytical expression is compact, suitable for the proposed DF relay dominant hybrid networks, and also provides an insight into the factors that affect the cooperative transmission performance. Based on the analytical expression proposed in this chapter, a dynamic optimal combination strategy for the DF and AF relays is provided as well. After removing the unsuitable AF relays, the hybrid DF-AF cooperative system is able to further exploit the existing relays, to improve the communication performance and to enlarge the transmission coverage.

Most of the previous works in cooperative communication such as in paper [4] and paper [72] consider cooperative relay communication without relay selection. The work in paper [73] has shown that cooperative communication with relay selection provide better resource usage efficiency than without. Power allocation also plays an important role in boosting the cooperative communication performance. By allocating the optimal power, the optimal performance of the transmission can be achieved with the best energy efficiency [74].

The work in paper [37] is one of the earliest works in pricing for cooperative communication networks. Pricing is introduced to encourage

the relay nodes to forward information to the destination node. In paper [39], the Stackelberg game is used to solve relay selection and power allocation problem in a distributed manner.

For the relay selection and resource allocation based on game theory, this chapter is basically an extended work of paper [39]. In this paper, the system is considered interference free. In real life situation, interference may come from large number of nodes in neighboring wireless systems, and can have mean power even higher than the noise power. This can affect the performance of the relay selection and power allocation process. Then we show through simulation results that in the case when the number of available relay nodes is large, and each relay nodes have close initial prices relative to other nodes, the method proposed in paper [39] leads to underestimation in the performance. We therefore suggest an optimal relay selection process by limiting the number of usable nodes.

In this chapter, we investigate the relay selection issue in a wideband communication system as well. Wideband communication systems are defined as having a fractional bandwidth—the ratio of single-sided bandwidth relative to center frequency—that exceeds 0.2 [75].

Wideband channels are of interest in a variety of wireless communication scenarios including underwater acoustic systems and wideband terrestrial radio frequency systems such as spread-spectrum or ultra wideband radio. Due to the nature of wideband propagation, such channels exhibit some fundamental differences relative to so-called narrowband channels. In wideband systems, the effects of mobility in the multi-path mobile environment are not well described by frequency-domain spreading, but rather by time-domain scale spreading. More specifically, in narrowband channels, the transmitted signal experiences multiple propagation paths each with a possibly distinct Doppler frequency shift, and thus these channels are also known as multi-Doppler shift, multi-lag channels. For wideband channels, however, each propagation path experiences a distinct Doppler scale, hence the term here is, multi-scale, multi-lag channel. For both types of wideband and narrowband time-varying channels, so-called canonical channel models have been proposed [76-79], limiting the number of channel coefficients required to represent the channel.

In particular, there has been significant success in the application of canonical models to narrowband time-varying channels [76]. For wideband time-varying channels a canonical model has been proposed in [77-79], which we consider as the scale-lag canonical model. This model has been adopted for Direct Sequence Spread Spectrum (DSSS) communication systems [79] to develop a scale-lag RAKE receiver to collect the diversity inherent in the multi-scale multi-lag channel. In addition, this model has spurred the use of wavelet signaling due to the fact that when the wavelets are "matched" to the scale-lag model, the receiver structure is greatly simplified; i.e., the signals corresponding to different scale-lag branches of the model are orthogonal when a single wavelet pulse is transmitted. The single pulse case is examined in paper [78]. Multi-scale multi-lag wavelet signaling is possible as well [80, 81], although inter-scale and inter-delay interference results. In paper [80], multiple receiver designs to combat such interference are provided exploiting the banded nature of the resulting interference.

Note that scale-spreading arises from the same fundamental mechanism that causes Doppler spreading. This scale-lag diversity is better described by the wavelet transform than the conventional time-frequency representation for the narrowband Linear Time-Varying (LTV) system, and is then called wideband LTV representation [78, 79]. Wideband LTV representation has been proven and verified for many applications in terms of high data rate wireless communication [82-85], high-speed underwater acoustic communications [86-88], Vehicle-to-Vehicle (V2V) wideband communication systems [89, 90], and radar/sonar systems [91]. In general, the transmit waveform could be designed to optimally enable the scale-lag diversity in the wideband LTV system.

Doppler scaling and multi-path spread in the wideband system implementations are usually treated as distortions rather than potential diversity sources, and always compensated after estimation. In this chapter, Doppler scaling and multi-path spread are utilized to obtain a joint scale-lag diversity with the discrete multi-scale and multi-lag wireless channel model by properly designing signaling and reception schemes using the discrete wavelet transform. The wavelet technique used in the wideband system is well motivated since wideband processing is intimately related to the wavelet theory [92-94]. The

wideband LTV representation has proven useful in many applications as noted above. However, no cooperative wavelet implementations have been exploited to provide further increased performance for wideband systems.

In this chapter, we design a new cooperative wavelet communication scheme to exploit the joint scale-lag diversity in the wideband LTV system. Furthermore, we propose a not-yet-known analytical Bit Error Rate (BER) expression for the cooperative wideband system, and provide a dynamic optimal selection strategy for relay selection to gain from multi-relay, multi-scaling, and multi-lag diversity, and maximize the whole system transmission performance.

The rest of this chapter is organized as follows:

Section 4.2 investigates the on-BER-performance-based Relay selection for cooperative communication. In Sub-section 4.2.1, we construct the hybrid DF-AF cooperative OFDM wireless transmission strategy. Sub-section 4.2.2 formulates a new SNR threshold to divide between DF and AF relays; the lower and the upper bound of the SNR threshold are provided as well. Sub-section 4.2.3 derives the closed-form of BER expression for hybrid DF-AF OFDM cooperation in a Rayleigh fading channel, and represents the dynamic optimal combination strategy for the hybrid DF-AF cooperation.

Section 4.3 focuses on the Game theory based relay selection and resource allocation. In Sub-section 4.3.1, the system model and problem formulation is provided. In Sub-section 4.3.2, the proposed game theory model is analyzed for relay selection and resource allocation in cooperative communication.

Section 4.4 addresses the relay selection problem for cooperative communication over multi-scale and multi-lag wireless channels. In Sub-section 4.4.1, an overview of the multi-scale and multi-lag diversity in a wideband system is provided. In Sub-section 4.4.2, we construct the cooperative wavelet wideband transmission strategy, and derive the analytical BER expression for the cooperative wavelet communication in the multi-relay, multi-scale and multi-lag channel. In Sub-section 4.4.3, we represent the dynamic optimal selection strategy for the relay selection.

In Section 4.5, simulation results are provided and compared to the analytical formulas.

Finally, Section 4.6 concludes this chapter.

4.2 BER performance based relay selection for cooperative communication

4.2.1 Cooperative AF and DF relay communication system model

As reviewed in Section 2.3, we know that DF relaying performs better than AF relaying, due to reducing effects of noise and interference at the fully decoding relay. However, under some conditions, DF relaying entails the possibility of forwarding erroneously detected signals to the destination as well; such error propagation can diminish the performance of the system. The mutual information between the source and the destination is limited by the mutual information of the weakest link between the source–relay and the combined channel from the source-destination and relay-destination.

Reliable decoding is not always available; this also means that the DF protocol is not always suitable for all relaying situations. The trade-off between the time-consuming decoding, and a better cooperative transmission, finding the appropriate hybrid cooperative schemes which include both DF and AF for specific situations, is a critical issue for the cooperative relaying networks design.

In this Section, we consider a hybrid cooperative OFDM strategy as shown in Fig. 4.1, where we transmit data from source node S to destination node D through R relays, without the direct link between S and D. This relay structure is called 2-hop relay system, i.e., first hop from source node to relay, and second hop from relay to destination. The channel fading for different links is assumed to be identical and statistically independent (quasi-statistic) i.e., the channels are constant within several OFDM symbol durations. This is a reasonable assumption as the relays are usually spatially well separated and in a slow changing environment. We assume that the channels are well known at the corresponding receiver sides, and a one bit feedback channel from

destination to relay is used for removing the unsuitable AF relays. All the Additive White Gaussian Noise (AWGN) terms have equal variance N_0. Relays are re-ordered according to the descending order of the Signal-to-Noise Ratio (SNR) between S and Q, i.e., $\mathrm{SNR}_{SQ_1} > \cdots > \mathrm{SNR}_{SQ_R}$, where SNR_{SQ_r} denotes the r-th largest SNR between S and Q.

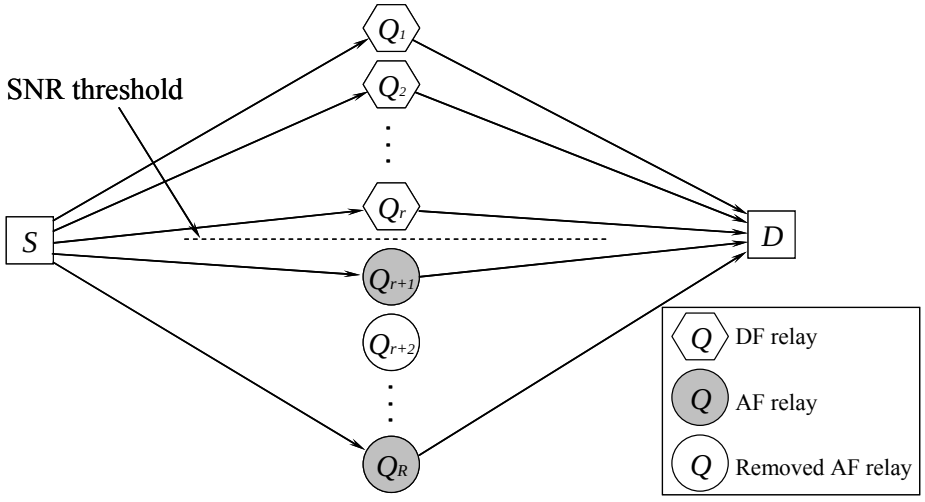

Fig. 4.1. Hybrid relay cooperation with dynamic optimal combination of DF-AF relays (S: Source, D: Destination, Q_r: r-th Relay).

In the model, relays can determine whether the received signals are decoded correctly or not, just simply by comparing the SNR to the threshold, which will be elaborated in Section 4.2.2. Therefore, the relays with a SNR above the threshold will be chosen to decode and forward the data to the destination, as shown with the white hexagons in Fig. 4.1. The white circle is the removed AF relay according to the dynamic optimal combination strategy as will be proposed in Section 4.2.3. The rest of the relays follow the AF protocol, as shown with the white hexagons in Fig. 4.1 [17].

The received SNR at the destination in the hybrid cooperative network can be denoted as

$$\gamma_h = \sum_{Q_i \in \mathrm{DF}} \frac{E_Q h_{Q_i,D}}{N_0} + \sum_{Q_j \in \mathrm{AF}} \frac{\dfrac{E_S h_{S,Q_j}}{N_0}\dfrac{E_Q h_{Q_j,D}}{N_0}}{\dfrac{E_S h_{S,Q_j}}{N_0} + \dfrac{E_Q h_{Q_j,D}}{N_0} + 1} \tag{4-1}$$

where $h_{Q_i,D}$, h_{S,Q_j} and $h_{Q_j,D}$ denote the power gains of the channel from the *i*-th relay to the destination in the DF protocol, source node to the *j*-th relay in AF protocol and *j*-th relay to the destination in AF protocol, respectively. E_S and E_Q in Eq. (4-1) are the average transmission energy at the source node and at the relays, respectively. By choosing the amplification factor A_{Q_j} in the AF protocol as

$$A_{Q_j}^2 = \frac{E_S}{E_S h_{S,Q_j} + N_0}, \tag{4-2}$$

and forcing E_Q in DF equal to E_S, it will be convenient to maintain constant average transmission energy at relays, equal to the original transmitted energy at the source node.

In this chapter, OFDM is used as modulation technique in the cooperative system to gain from its inherent advantages and combat frequency selective fading of each cooperative link, with W_r ($r = 1, 2, \cdots, R$) independent paths. As shown in the Fig. 4.2, the *r*-th relay first decides to adopt the DF or AF protocol according to the SNR threshold. For the DF-protocol, the symbols are decoded at the relays, and then an IFFT operation is applied on these blocks to produce the OFDM symbol. Before transmission, a prefix (Cyclic Prefix (CP) or Zero Padding (ZP)) is added to each OFDM symbol. For the AF-protocol, relays which undergo the deep fading will be removed by using the so called dynamic optimal combination strategy, discussed later in this section. Other AF relays are proper relays and amplify and forward the data to the destination. At the destination node, after the prefix removal, the received OFDM symbols are fast-Fourier-transformed, and the resulting symbols at the destination are used for the combination and detection.

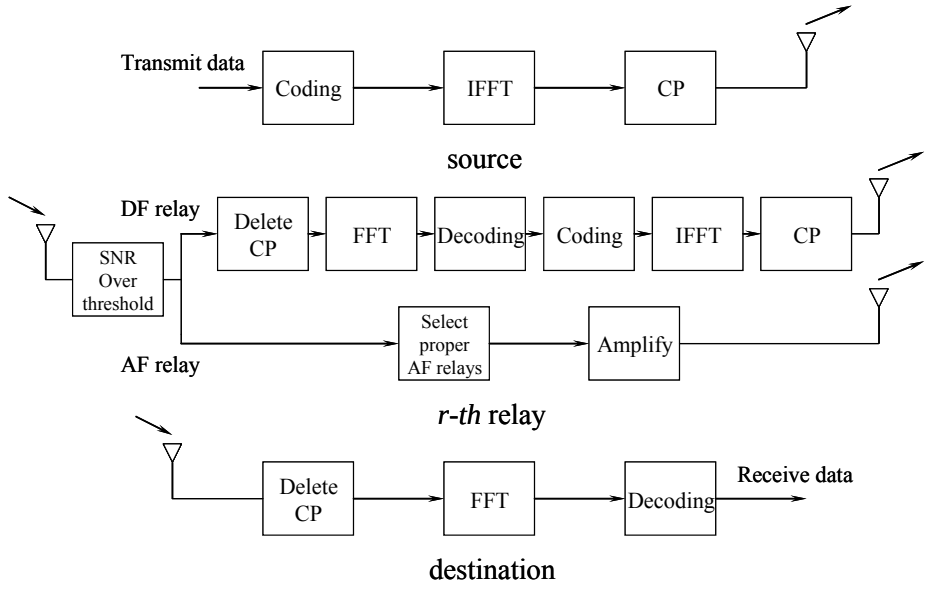

Fig. 4.2. Relay selection in the hybrid DF-AF cooperative OFDM wireless transmission strategy (top: source; middle: relay; bottom: destination).

The receiver at the destination collects the data from DF and AF relays and uses a Maximal Ratio Combiner (MRC). Because of the amplification in the intermediate stage in the AF protocol, the overall channel gain of the AF protocol should include the source to relay, relay to destination channel gains and amplification factors. The decision variable u at the MRC output is given by

$$u = \sum_{Q_i \in \mathrm{DF}} \frac{\left(H_{Q_i,D}\right)^* Y_{Q_i}}{\left(H_{Q_i,D}\right)^* H_{Q_i,D}} + \sum_{Q_j \in \mathrm{AF}} \frac{\left(H_{S,Q_j} A_{Q_j} H_{Q_j,D}\right)^* Y_{Q_j}}{\left(H_{S,Q_j} A_{Q_j} H_{Q_j,D}\right)^* \left(H_{S,Q_j} A_{Q_j} H_{Q_j,D}\right)}, \quad (4\text{-}3)$$

where Y_{Q_i} and Y_{Q_j} are the received signal from the DF i-th relay and AF j-th relays, respectively, and $(\cdot)^*$ denotes the conjugate operation. $H_{Q_i,D}$, H_{S,Q_j} and $H_{Q_j,D}$ are the frequency response of the channel power gains, respectively.

In the proposed hybrid DF-AF cooperative network, DF plays a dominant role in the whole system. However, switching to the AF

scheme for the relay nodes with a SNR below the threshold often improves the total transmission performance, and accordingly AF plays a positive compensating role.

4.2.2 SNR thresholding scheme for DF and AF relays

In general, mutual information I is the upper bound of the target rate B in bit/s/Hz, i.e., the spectral efficiency attempted by the transmitting terminal. Normally, $B \leq I$, while the case $B > I$ is known as the outage event. Meanwhile, the channel capacity C is also regarded as the maximum achievable spectral efficiency, i.e., $B \leq C$.

Conventionally, the maximum average mutual information I_D of the direct transmission between source and destination, achieved by independent and identically distributed (i.i.d) zero-mean, circularly symmetric complex Gaussian inputs, is given by

$$I_D = \log_2\left(1+\mathrm{SNR}\, h_{S,D}\right) \tag{4-4}$$

and is a function of the power gain $h_{S,D}$ from source to destination. According to the inequality $B \leq I$, we can derive the SNR threshold for full decoding as

$$\mathrm{SNR} \geq \frac{2^B-1}{h_{S,D}}. \tag{4-5}$$

Then, we suppose that all X relays adopt the DF cooperative transmission without direct transmission. The maximum average mutual information for DF cooperation I_{DF_co} becomes [72]

$$I_{DF\_co} = \frac{1}{X}\min\left\{\log_2\left(1+\sum_{r=1}^{R}\mathrm{SNR}\, h_{S,Q_r}\right), \log_2\left(1+\sum_{r=1}^{R}\mathrm{SNR}\, h_{Q_r,D}\right)\right\}, \tag{4-6}$$

which is a function of the channel power gains. Here, R denotes the number of relays.

For the r-th DF link, requiring both the relay and destination to decode perfectly, the maximum average mutual information I_{DF_li} yields

$$I_{DF\_li} = \min\left\{\log_2\left(1+\text{SNR}\, h_{S,Q_r}\right), \log_2\left(1+\text{SNR}\, h_{Q_r,D}\right)\right\}. \qquad (4\text{-}7)$$

The first term in Eq. (4-7) represents the maximum rate at which the relay can reliably decode the source message, while the second term in Eq. (4-7) represents the maximum rate at which the destination can reliably decode the message forwarded from relay. We note that such mutual information forms are typical for a relay channel with full decoding at the relay [14]. The SNR threshold of this DF link for target rate B is given by the condition $I_{DF\_li} \geq B$ and results into

$$\text{SNR} \geq \frac{2^B - 1}{\min\left(h_{S,Q_r}, h_{Q_r,D}\right)}. \qquad (4\text{-}8)$$

In the proposed hybrid DF-AF cooperative transmission, we only assumed that the relay can fully decode the signal transmitted over the source-relay link, and not over the whole DF link; thus, the SNR threshold for the full decoding at the r-th relay reaches its lower bound as

$$\gamma_{th} \geq \frac{2^B - 1}{h_{S,Q_r}}. \qquad (4\text{-}9)$$

For the DF protocol, let R denotes the number of total relays, and M denotes the set of participating relays, whose SNR_S are above the SNR threshold, meaning that for the M relays reliable decoding is possible. The achievable channel capacity, C_{DF}, with SNR threshold is calculated as

$$C_{DF} = \sum_M \frac{1}{R}\mathbf{E}\left(\log_2\left(1+y\middle|M\right)\right)\Pr\left(M\right), \qquad (4\text{-}10)$$

where $\mathbf{E}(\cdot)$ denotes the expectation operator. In Eq. (4-10), $y\middle|M = (R-K)\gamma_{S,D} + \sum_{Q\in M}\gamma_{Q,D}$, and represents the instantaneous received SNR at the destination for the given set M with K participating relays; $\gamma_{n,m}$ equals the instantaneous received SNR at node m, for the signal which is directly transmitted from n to m. $y\middle|M$ is the weighted sum of independent exponential random variables; as derived in paper [95] the Probability Density Function (PDF) of $y\middle|M$ can be obtained using its Moment Generating Function (MGF) and the partial fraction technique

for evaluation of the inverse Laplace transform. The probability of a particular set of *M* participating relays $\mathrm{Prob}(M)$ in Eq. (4-10) can be found from

$$\mathrm{Prob}(M)=\prod_{Q\in M}\exp\left(-\frac{R\gamma_{th}}{\Gamma_{S,Q\in M}}\right)\prod_{Q\notin M}\left(1\text{-}\exp\left(-\frac{R\gamma_{th}}{\Gamma_{S,Q\notin M}}\right)\right), \quad (4\text{-}11)$$

where $\Gamma_{u,v}$ denotes the average SNR over the link between nodes *u* and *v*.

By combining Eq. (4-6), Eq. (4-10) and Eq. (4-11) with the inequality $I_{DF\_co} \le C_{DF}$, and taking into consideration that the maximum average mutual information *I* is the upper bound by the achievable channel capacity *C*, we can calculate the upper bound of SNR threshold γ_{th} for fully decoding in the DF protocol.

We now can obtain the upper bound and the lower bound of the SNR threshold γ_{th} for hybrid DF-AF cooperation. Compared to the upper bound, the lower bound as shown in the Eq. (4-9) is more crucial for improving the transmission performance. This is because the DF protocol plays a dominant role in the hybrid cooperation strategy, and accordingly we want to find the lower bound which provides as much as possible DF relays, as introduced in *Theorem 2.1* (see page 23). A fully decoding check can also be guaranteed by employing the error detection code, such as cyclic redundancy check. However, the disadvantage is that it will increase the system complexity [96].

4.2.3 Dynamic optimal relay selection and combination strategy

In the maximum ratio combining the transmitted signal from *R* cooperative relays nodes, affected by independent identically distributed Rayleigh fading and forwarded to the destination node, are combined. In this case the SNR per bit per relay link γ_r has an exponential PDF with the average SNR per bit characterized by $\overline{\gamma}$:

$$p_{\gamma_r}(\gamma_r)=\frac{1}{\overline{\gamma}}e^{-\gamma_r/\overline{\gamma}}. \quad (4\text{-}12)$$

Since the fading on the R paths is identical and mutually statistically independent, the SNR per bit of the combined SNR γ_c will have a Chi-square distribution with $2R$ degrees of freedom. The PDF $p_{\gamma_c}(\gamma_c)$ becomes

$$p_{\gamma_c}(\gamma_c) = \frac{1}{(R-1)!\overline{\gamma_c}^{R}} \gamma_c^{R-1} e^{-\gamma_c/\overline{\gamma}_c}, \qquad (4\text{-}13)$$

where $\overline{\gamma}_c$ is the average SNR per channel, Then by integrating the conditional error probability over $\overline{\gamma}_c$, the average error probability P_e can be written as

$$P_e = \int_0^\infty \widehat{Q}\left(\sqrt{2g\gamma_c}\right) p_{\gamma_c}(\gamma_c)\, d\gamma_c, \qquad (4\text{-}14)$$

where $g = 1$ for coherent Binary Phase Shift Keying (BPSK), $g = ½$ for coherent orthogonal Binary Frequency Shift Keying (BFSK), $g = 0.715$ for coherent BFSK with minimum correlation; and $\widehat{Q}(\cdot)$ is the Gaussian Q-function, i.e., $\widehat{Q}(x) = 1/\sqrt{2\pi}\int_x^\infty \exp\left(-t^2/2\right) dt$. For the BPSK case, the average error probability can be found in closed form by successive integration by parts [97]:

$$P_e = \left(\frac{1-\mu}{2}\right)^R \sum_{k=0}^{R-1} \binom{R-1+k}{k} \left(\frac{1+\mu}{2}\right)^R, \qquad (4\text{-}15)$$

where

$$\mu = \sqrt{\frac{\overline{\gamma}_c}{1+\overline{\gamma}_c}}. \qquad (4\text{-}16)$$

In the hybrid DF-AF cooperative network with two hops in each AF relay, the average SNR per channel $\overline{\gamma}_c$ can be derived as

$$\overline{\gamma}_c = \frac{\gamma_h}{K + 2\times J}, \qquad (4\text{-}17)$$

where K and J are the numbers of the DF relays and AF relays, respectively. γ_h can be obtained from Eq. (4-1). In the DF protocol, due to the reliable detection, we can only consider the last hops, or the channels between the relay nodes and destination node.

As the average error probability P_e is a precise indication for the transmission performance, we consequently propose a dynamic optimal combination strategy for the hybrid DF-AF cooperative transmission. In this algorithm the proper AF relays are selected so that P_e may reach its maximum.

We note here that, like in the aforementioned procedure, all relays are reordered according to the descending order of the SNR between source and relays, as was shown in the Fig. 4.1. According to the proposed SNR threshold, we pick up the DF relays having a SNR greater than the threshold. Then, we proceed with the AF relay selection scheme, where the inappropriate AF relays are removed. The complete scheme describing the dynamic optimal combination strategy for the hybrid DF-AF cooperation is shown in the flow chart of Fig. 4.3.

Summarizing the novelties in this section, we proposed a hybrid OFDM cooperative strategy for multi-node wireless networks employing both DF and AF relaying. Fully decoding is guaranteed by simply comparing SNRs at relay nodes to a SNR threshold, which is more efficient than utilizing a conventional cyclic redundant checking code. The lower bound and the upper bound of the SNR threshold were provided as well. The closed-form BER expression of the hybrid OFDM cooperation in a Rayleigh fading channel was derived. The compact closed-form BER expression can easily provide good insight into results. It also may be a heuristic help for the design of future cooperative wireless systems.

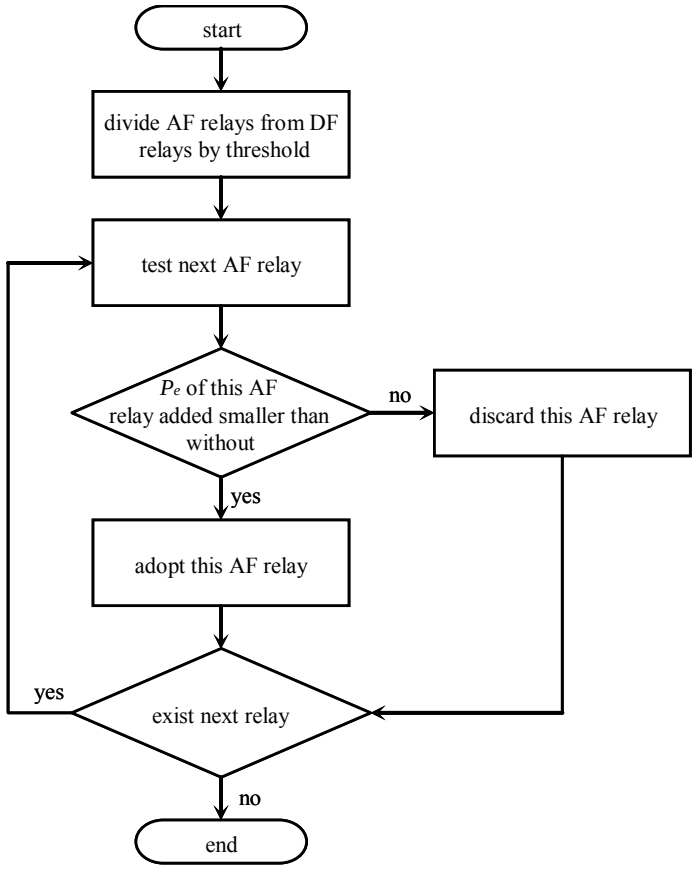

Fig. 4.3. Flow chart of the dynamic optimal combination strategy for the hybrid DF-AF cooperation.

4.3 Game theory based relay selection and resource allocation

In Section 2.5, some literature surveys on relay selection for cooperative communication have been provided. In this Section, we propose a novel resource allocation and optimization scheme based on the game theoretical approach. This Section includes contributions from my previous MSc. student W. A. Prasetyo [98]; he participated in my Ph.D. project and I was supervising on a daily basis his MSc. research. First, we illustrate the cooperative communication system with interference. Then, we formulate a pricing game model for the cooperative communication system with interference, and optimize the relay selection criterion. We show that interference from the neighboring

wireless systems can affect the game theoretical approach for relay selection and power allocation process in wireless cooperative communication networks. The proposed relay selection algorithm is able to maintain the source node utility function and reduce the total payment to relay nodes.

4.3.1 System model and problem formulation

The work of Wang *et al.* [39] provides the game theoretical approach in relay selection and resource allocation in cooperative communication. However, this system does not provide the effects of interference in the system to the relay selection and resource allocation process. In this Section, we will model the system with disturbance from interference and shows the effects of interference to the relay selection and resource allocation process.

The nodes we have in the system are configured as in Fig. 4.4. The nodes are divided into clusters as in paper [31], and each cluster consists of a source node, *N* relay nodes, and a destination node. The source node wants to transmit information to the destination node, through direct transmission and by using the relay nodes to forward the information. Due to the broadcasting nature of the wireless nodes, the relay nodes and the destination node at a cluster might receive interferences from other clusters. We first denote the received signal at the destination from direct transmission $y_{s,d}$ as

$$y_{s,d} = \sqrt{P_s G_{s,d}}\, x + \eta_{s,d} + \omega_d \,, \tag{4-18}$$

where P_s is the transmit power of the source node, $G_{s,d}$ represents the channel gain between the source node and the destination node, *x* is the unit power of information which the source node wants to transmit, $\eta_{s,d}$ is the independent Additive White Gaussian Noise (AWGN) with zero mean and variance σ^2 at the source-destination node link, and ω_d denotes the interference from the neighboring cooperative communication clusters to the destination node.

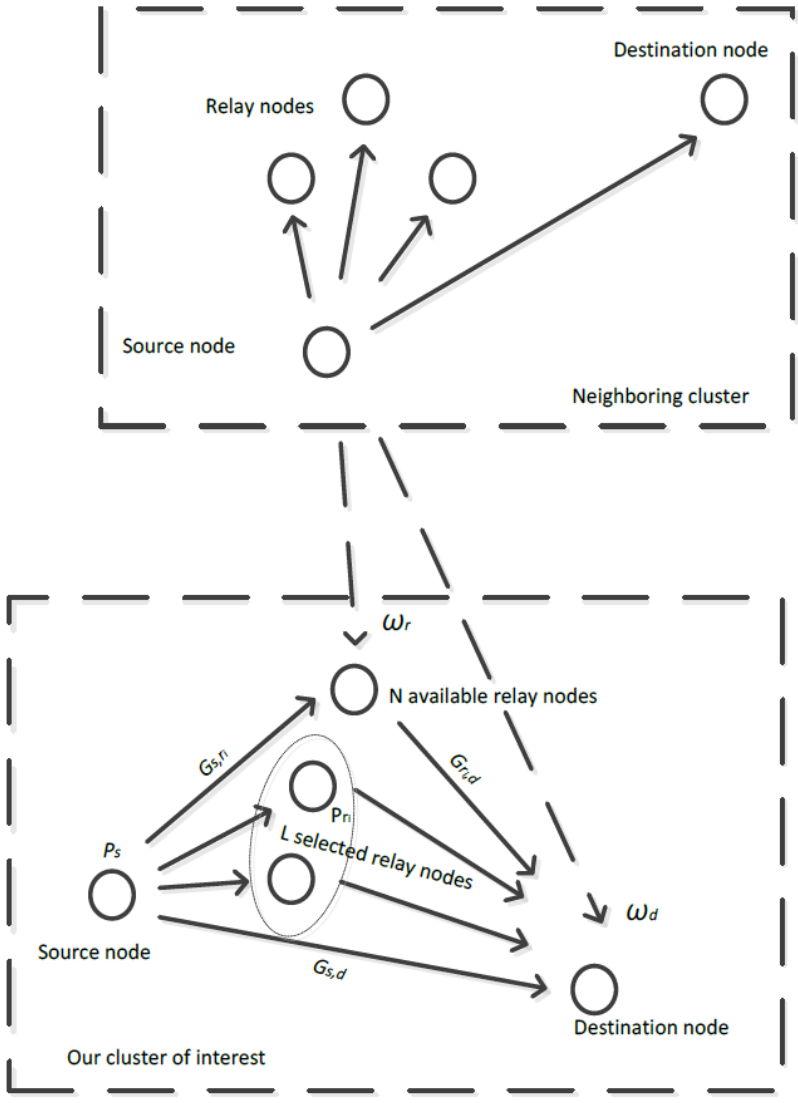

Fig. 4.4. Cooperative communication network with interference from a neighboring cluster.

Due to the broadcasting nature, the relay nodes also received the signal transmitted by source node. To increase the capacity of the transmission, the relay nodes help forward the received signals using the amplify–and–forward scenario. The received signal at relay node *i* is

$$y_{s,r_i} = \sqrt{P_s G_{s,r_i}}\, x + \eta_{s,r_i} + \omega_{r_i} \quad i \in N, \tag{4-19}$$

where N is the number of available relay nodes, G_{s,r_i} is the channel gain between the source node and relay node i, η_{s,r_i} is the independent AWGN with zero mean and variance σ^2 between the source node and relay node i, and ω_{r_i} denotes the interference from the neighboring cooperative communication clusters to the relay node i.

After receiving the signals from the source node, the relay nodes amplify the signals and then re-transmit the information to the destination node. The received signal from relay node i at the destination is denoted as

$$y_{r,d} = \sqrt{P_{r_i} G_{r_i,d}}\, x' + \eta_{r,d} + \omega_d \,, \tag{4-20}$$

where

$$x' = \frac{y_{s,r_i}}{\left| y_{s,r_i} \right|} \tag{4-21}$$

is the normalized transmitted information from relay node i to the destination node, P_{r_i} is the transmit power from relay node i , and $\eta_{r,d}$ is the independent AWGN with zero mean and variance σ^2 at the relay-destination node link.

If the interference is coming from a large number of nodes, according to the Central Limit Theorem, we can model it as a zero mean Gaussian distributed variable, with variance σ^2_{int} . Then, we can substitute Eq. (4-19) into Eq. (4-21) and find for Eq. (4-20)

$$y_{r_i,d} = \frac{\sqrt{P_{r_i} G_{r_i,d}} \left(\sqrt{P_s G_{s,r_i}}\, x + \eta_{s,r_i} + \omega_{r_i} \right)}{\sqrt{P_s G_{s,r_i} + \sigma^2_{\text{int}} + \sigma^2}} + \eta_{r_i,d} + \omega_d \tag{4-22}$$

We can calculate the Signal-to-Interference Noise Ratio (SINR) at the destination for the direct transmission as

$$\gamma_{s,d} = \frac{P_s G_{s,d}}{\sigma_{\text{int}}^2 + \sigma^2} \tag{4-23}$$

and the SINR at the destination for the relay node *i* transmission as

$$\gamma_{s,r_i,d} = \frac{P_{r_i} P_s G_{r_i,d} G_{s,r_i}}{\left(\sigma_{\text{int}}^2 + \sigma^2\right)\left(P_{r_i} G_{r_i,d} + P_s G_{s,r_i} + \sigma_{\text{int}}^2 + \sigma^2\right)} \tag{4-24}$$

According to the Shannon capacity theorem, the capacity of the direct transmission can be calculated as

$$R_{s,d} = W \log_2\left(1 + \gamma_{s,d}\right) \tag{4-25}$$

where W is the bandwidth of the transmission. Then, the total capacity of the transmission using maximal-ratio-combining where each relay occupies W bandwidth equals

$$R_{s,r,d} = W \log_2\left(1 + \gamma_{s,d} + \sum \gamma_{s,r_i,d}\right) \tag{4-26}$$

After we use the relay selection process, then if the number of selected nodes is L, where $L \in N$, we can re-calculate the total capacity of the transmission as

$$R_{s,r,d} = W \log_2\left(1 + \gamma_{s,d} + \sum_{i \in L} \gamma_{s,r_i,d}\right) \tag{4-27}$$

4.3.2 Relay selection and resource allocation using the Game theoretical approach in cooperative communication

After the system description mentioned above, we continue with the game theoretical model of the system. We define a pricing game model

based on the so called Stackelberg game similar to [39]. The Stackelberg game is a form of game where one player is chosen as leader and determines its strategy as first in the game. The other players are the followers, and choose the strategy according the strategy of the leader. We choose the Stackelberg game model because in this game model, the optimization process starts by assigning the optimal P_{r_i} for each relay connected with the source node, followed by assigning p_i for each relay connected with the relay nodes according to the P_{r_i}.

We define the utility function of the source node as the gain which the source node gets through the transmission, subtracted by the payment to the relay nodes. The utility function of the source node can be written as

$$U_s = aR_{s,r,d} - \sum_{i \in N} P_{r_i} p_i \tag{4-28}$$

where a is the gain per unit rate at the receiver. Then, we define the utility function of the relay node as the compensation which the relay node gets from the source node for forwarding the information subtracted by the fixed cost of relay nodes' power usage. We can write the utility function of relay node i as

$$U_{r_i} = \left(p_i - c_i \right) P_{r_i} \tag{4-29}$$

where c_i is the cost of relay node i for spending per unit power to forward the information to the receiver.

As mentioned before, the strategy of the source node is to assign the value of P_{r_i} to maximize the source node utility function

$$\max_{\{P_{r_i}\}} U_s = aR_{s,r,d} - \sum_{i \in N} P_{r_i} p_i, \quad P_{r_i} \geq 0 \tag{4-30}$$

and the strategy of the relay node i is to assign the value of p_i to maximize the utility function of relay node i

$$\max_{\{p_i\}} U_{r_i} = \left(p_i - c_i \right) P_{r_i} \tag{4-31}$$

Before deriving the solution for the pricing game between the source node and the relay nodes, we first define the relay selection criterion for the cooperative communication network. We use the price of the relay nodes as criterion for the selection. At the beginning of the game, the transmit power of the relay nodes have not been allocated and the initial p_i of the relay nodes are the same as its c_i. Then, we select relay nodes which has the following criterion

$$\frac{\partial U_s}{\partial P_{r_i}} = a \frac{\partial R_{s,r,d}}{\partial P_{r_i}} - p_i > 0, \quad i \in N \tag{4-32}$$

After substitution of Eq. (4-27), Eq. (4-32) becomes

$$\frac{\partial U_s}{\partial P_{r_i}} = a \frac{\partial}{\partial P_{r_i}} \left\{ W \log_2 \left(1 + \gamma_{s,d} + \sum_{i \in N} \gamma_{s,r_i,d} \right) \right\} - p_i > 0$$

$$= \frac{aW}{\ln 2} \frac{\partial}{\partial P_{r_i}} \left\{ \ln \left(1 + \frac{P_s G_{s,d}}{\sigma_{\text{int}}^2 + \sigma^2} + \sum_{i \in N} \frac{P_{r_i} P_s G_{r_i,d} G_{s,r_i}}{\left(\sigma_{\text{int}}^2 + \sigma^2 \right) \left(P_{r_i} G_{r_i,d} + P_s G_{s,r_i} + \sigma_{\text{int}}^2 + \sigma^2 \right)} \right) \right\} - p_i > 0 \tag{4-33}$$

If we define

$$A_i = \frac{P_s G_{s,r_i}}{\sigma_{\text{int}}^2 + \sigma^2 + P_s G_{s,d}}$$

and

$$B_i = \frac{P_s G_{s,r_i} + \sigma_{\text{int}}^2 + \sigma^2}{G_{r_i,d}},$$

Eq. (4-33) can be modified into

$$\frac{\partial U_s}{\partial P_{r_i}} = \frac{aW}{\ln 2}\frac{\partial}{\partial P_{r_i}}\left\{\ln\left(1+\frac{P_s G_{s,d}}{\sigma_{\text{int}}^2+\sigma^2}\right)\right\}$$
$$+\frac{aW}{\ln 2}\frac{\partial}{\partial P_{r_i}}\left\{\ln\left(1+\sum_{i\in N}\frac{P_{r_i}P_s G_{r_i,d}G_{s,r_i}}{\left(\sigma_{\text{int}}^2+\sigma^2\right)\left(P_{r_i}G_{r_i,d}+P_s G_{s,r_i}+\sigma_{\text{int}}^2+\sigma^2\right)}\frac{\sigma_{\text{int}}^2+\sigma^2}{P_s G_{s,r_i}+\sigma_{\text{int}}^2+\sigma^2}\right)\right\}$$
$$-p_i$$
$$=\frac{aW}{\ln 2}\frac{\partial}{\partial P_{r_i}}\left\{\ln\left(1+\frac{P_s G_{s,d}}{\sigma_{\text{int}}^2+\sigma^2}\right)\ln\left(1+\sum_{i\in N}\frac{A_i}{1+B_i/P_{r_i}}\right)\right\}-p_i \qquad (4\text{-}34)$$

After executing the differentiation, Eq. (4-35) becomes

$$\frac{\partial U_s}{\partial P_{r_i}} = \frac{aW}{\ln 2}\frac{A_i B_i}{\left(1+\sum_{i\in N}\frac{A_i P_{r_i}}{P_{r_i}+B_i}\right)\left(P_{r_i}+B_i\right)^2}-p_i>0. \qquad (4\text{-}35)$$

Since at the beginning of the game no power is allocated for each relay, i.e., $P_{r_i}=0$, we obtain

$$\frac{\partial U_s}{\partial P_{r_i}} = \frac{aW}{\ln 2}\left(\frac{A_i}{B_i}\right)-p_i>0 \qquad (4\text{-}36)$$

The rationalization of this criterion is that we choose relay nodes whose initial price p_i is low enough that by increasing P_{r_i}, U_s increases also, thus we use the first-order differential of U_s with P_{r_i}. Then, we compose all *L* selected relays into the selected relay set.

After this relay selection process, the pricing game is played between

the source node and the selected relay nodes. The source node assigns the value of P_{r_i} by using the first-order differential optimization as in

$$\frac{\partial U_s}{\partial P_{r_i}} = a\frac{\partial R_{s,r,d}}{\partial P_{r_i}} - p_i = 0, \quad i \in L \tag{4-37}$$

In Appendix 4-1 it will be shown that the extremum point at $\partial U_s / \partial P_{r_i} = 0$ is a global maximum. After relay selection and according to Eq. (4-35) and Eq. (4-37) we get

$$\frac{\frac{aW}{\ln 2}}{\left(1+\sum_{k\in L}\frac{A_k P_{r_k}}{P_{r_k}+B_k}\right)} = \frac{p_i}{A_i B_i}\left(P_{r_i}+B_i\right)^2 \tag{4-38}$$

Since the additive interference from neighboring clusters plus additive noise term can be taken into account as an additive noise term, similar to the derivation in paper [39], the left-hand side of Eq. (4-38) is the same for any relay node on the right-hand side; by equating the right-hand side of Eq. (4-38) for relay nodes r_i and r_j, we get

$$P_{r_j} = \sqrt{\frac{p_i A_j B_j}{p_j A_i B_i}}\left(P_{r_i}+B_i\right) - B_j \tag{4-39}$$

By using Eq. (4-23) we can modify $\frac{A_j}{1+B_j/P_{r_j}}$ in Eq. (4-34) for relay *j* into

$$\frac{A_j}{1+B_j/P_{r_j}} = A_j - \sqrt{\frac{p_j A_i B_i}{p_i A_j B_j}}\frac{A_j B_j}{\left(P_{r_i}+B_i\right)} \tag{4-40}$$

With $X = 1+\sum_{j\in L} A_j$ and $Y = \sum_{j\in L}\sqrt{p_j A_j B_j}$, we find the optimal power consumption

$$P_{r_i}^* = \sqrt{\frac{A_i B_i}{p_i}} \frac{Y + \sqrt{Y^2 + 4aXW/\ln 2}}{2X} - B_i \qquad (4\text{-}41)$$

which is the allocated power for relay node *i*. After the transmit power for each selected relay node has been allocated, the relay nodes assign the new prices which fulfill Eq. (4-22). We use the first-order differential maximization of the utility function of relay node *i*

$$\frac{\partial U_{r_i}}{\partial p_i} = P_{r_i}^* + \left(p_i - c_i\right)\frac{\partial P_{r_i}^*}{\partial p_i} = 0 \qquad (4\text{-}42)$$

Solving Eq. (4-42) for p_i, leads to the optimal price for relay node *i*

$$p_i^* = c_i - \frac{P_{r_i}^*}{\partial P_{r_i}^* / \partial p_i} \qquad (4\text{-}43)$$

where $\partial P_{r_i}^* / \partial p_i$ is the first-order differential of the optimal transmit power of relay node *i* to the price of relay node *i*; the differential becomes

$$\frac{\partial P_{r_i}^*}{\partial p_i} = \sqrt{\frac{A_i B_i}{p_i}} \frac{Y + \sqrt{Y^2 + 4aXW/\ln 2}}{2X} \left(-\frac{1}{2p_i} \left(1 - \frac{\sqrt{p_i A_i B_i}}{\sqrt{Y^2 + 4aXW/\ln 2}} \right) \right) \qquad (4\text{-}44)$$

The power and price updating function are the two strategies that each player plays in the pricing game. From Eq. (4-41) and Eq. (4-43) we can see that if P_{r_i} is changed, p_i will also change and vice versa. The game is played until we reach a convergence point for both P_{r_i} and p_i values. The convergence point is also the equilibrium in the game, which is the optimal solution for both Eq. (4-30) and Eq. (4-31), which are the objectives of the optimization process. More about the existence of the equilibrium and proof about the optimal solution will be provided in Appendix 4-1.

From Eq. (4-41) and Eq. (4-43) we can see that the updating function of the transmit power $P_{r_i}^*$ and the price p_i depend also on other selected relay nodes beside relay node i, $i \in L$. This shows that the pricing game is not played only between the source node and relay node i, but also with other selected nodes. Thus, the number of selected nodes affects the resource allocation process. Because of this property, in Section 4.5 we show in the simulation results that for some cases, the selected nodes might contribute to increase the source node utility function U_s at the beginning of the pricing game, but as the price increases through the updating function, the relay nodes will not contribute to increase the source node utility function U_s anymore.

We propose an algorithm to limit the number of selected relay nodes to mitigate the problem with the price updating function. First, we arrange the relay nodes based on their initial price by comparing each node price to all others. Next, we select the node with the lowest price, and perform the relay selection process and pricing at each iteration until the optimum is reached. Then, we add the next node with lowest initial price to the calculation and compare the current optimum to the previous optimum. If this is higher, we continue the process until the optimum stops increasing or starts decreasing. The maximum number of usable nodes is the number of the nodes when the maximum optimum is reached. The flowchart of the algorithm is shown in Fig. 4.5.

After we obtain the number of usable nodes, we sort the selected nodes according to its price, and select the nodes according to the maximum number of usable nodes. Afterwards, we perform the pricing game to allocate the optimum power and price for each relay node.

Summarizing the novelties in this Section, we proposed relay selection and resource allocation and optimization schemes for cooperative wireless communication networks with interference based on the Stackelberg game approach. We also proposed an algorithm to limit the number of selected relay nodes to mitigate this problem. Using this algorithm, we chose a number of relay nodes where the result of resource allocation and optimization is still beneficial for the value of the source node utility function.

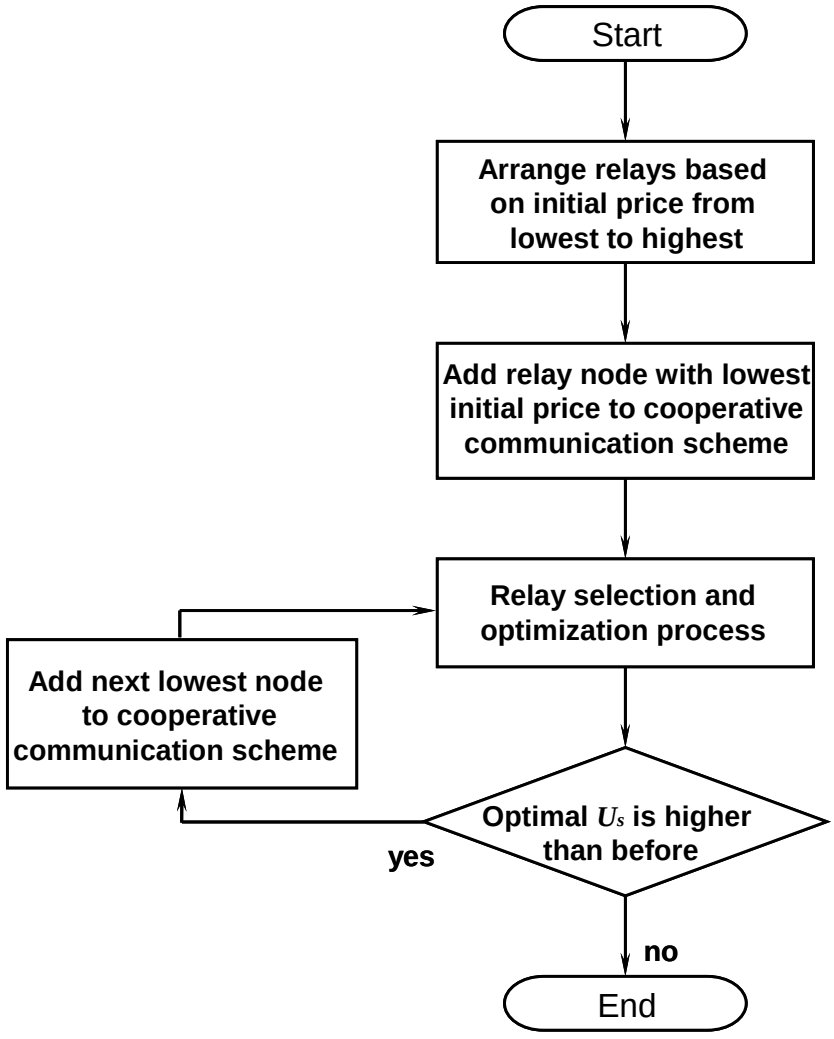

Fig. 4.5. Relay selection algorithm for limiting the number of nodes.

4.4 Relay selection for cooperative communication over multi-scale and multi-lag wireless channels

Wideband LTV channels are of interest in a variety of wireless communication scenarios including wideband terrestrial radio frequency systems such as spread-spectrum systems or UWB systems and underwater acoustic systems. Due to the nature of wideband propagation, such wideband LTV channels exhibit some fundamental differences

compared to the so-called narrowband channels. In particular, it has been shown that multi-scale, multi-lag channel descriptions offer improved modeling of LTV wideband channels over multi-Doppler-shift, multi-lag models [78-80]. OFDM technology has been introduced and examined for wideband LTV channels. Approaches include splitting the wideband LTV channel into parallel narrowband LTV channels [99] or assume a simplified model which reduces the wideband LTV channel to a narrowband LTV channel with a carrier frequency offset [100].

Receivers for single-scaled wavelet-based pulses for wideband multi-scale, multi-lag channels are presented in [78, 79], and a similar waveform is adopted in spread-spectrum systems [101] over wideband channels modeled by wavelet transforms; in [88] attention is paid to equalizers for block transmissions in wideband multi-scale, multi-lag channels. In order to achieve better realistic channel matching, single-scaled rational wavelet modulation was designed in [102]. The above mentioned schemes all employ single-scale modulation and thus do not maximize the spectral efficiency. In order to exploit the frequency diversity, a new form of Orthogonal Wavelet Division Multiplexing (OWDM) has been previously examined in [103] for additive white Gaussian noise channels.

However, no cooperative schemes for multi-scale, multi-lag channels have been exploited to provide further increased performance for wideband systems. In this section, we will design a cooperative wavelet communication scheme to exploit the joint scale-lag diversity in a wideband LTV system [104, 105]. Furthermore, we come forward with an analytical BER expression for the cooperative wideband system, and provide a dynamic optimal selection strategy for relay selection to gain from multi-relay, multi-scaling, and multi-lag diversity, and to maximize the whole system transmission performance.

4.4.1 Wideband multi-scale and multi-lag representation

Multi-scale and multi-lag representation is suitable for wideband systems to satisfy either an absolute condition or a relative condition. The absolute condition requires that the signal fractional bandwidth (ratio of bandwidth to center frequency) is larger than 0.2. For the relative condition, the motion velocity v, the propagation speed c and

the signal time bandwidth (TB) product should satisfy $2v/c \gg 1/(TW)$, where T stands for the transmitted signal duration and W denotes the transmitted signal bandwidth. Therefore, the multi-scale and multi-lag system can be defined as a system that operates high fractional bandwidths or large TB products with conditions on the v/c ratio.

An example can be, an ultra wideband (UWB) system transmits signals with high fractional bandwidths (> 0.2) or large TB products (10^5- 10^6) to improve resolution capacity and to increase noise immunity [106]. Another example concerns an underwater acoustic environment with fast moving objects; this could result in a large v/c ratio due to the relatively low speed of sound [87]. In these situations, multi-scale and multi-lag representation is needed to account for the Doppler scale effects, but not Doppler shift.

Assuming wideband conditions as just mentioned, we now consider a multi-scale and multi-lag system that is a signal $x(t)$, transmitted over a wideband propagation medium, is received as

$$y(t) = \int_{A_l}^{A_u} \int_0^{T_d} h(\tau, a)\sqrt{a}\, x\big(a(t-\tau)\big)\, d\tau da + n(t) \qquad (4\text{-}45)$$

where $a \approx 1 + 2v/c$ is the Doppler scale; the factor a results in a time compression or expansion of the waveform caused by a relative velocity v between transmitter and scatterer. When the Doppler scale is such that $a > 1$, then the scatterer is approaching the transmitter and the transmitted signal is compressed with respect to time; in contrast, when $0 < a < 1$, the received signal is dilated and the scatterer is moving away from the transmitter. τ is the propagation delay due to reflections of $x(t)$ by scatterers in the medium. Channel gain $h(\tau, a)$ can be modeled as a stochastic process, when the system is randomly varying [78]. Due to physical restrictions on the system, we can assume that $h(\tau, a)$ is effectively nonzero only when $0 < A_l \le a \le A_u$ and $0 \le \tau \le T_d$, where $A_u - A_l$ is the Doppler scale spread and T_d is the multi-path delay spread. The noise process, $n(t)$ is modeled as a white Gaussian random process.

Note that regardless the noise term, Eq. (4-45) is in the form of an inverse wavelet transform with $x(t)$ acting as wavelet. Therefore, according to the wavelet theory, we sample the multi-scale and multi-lag plane in a dyadic lattice as shown in Fig. 4.6 [78, 107].

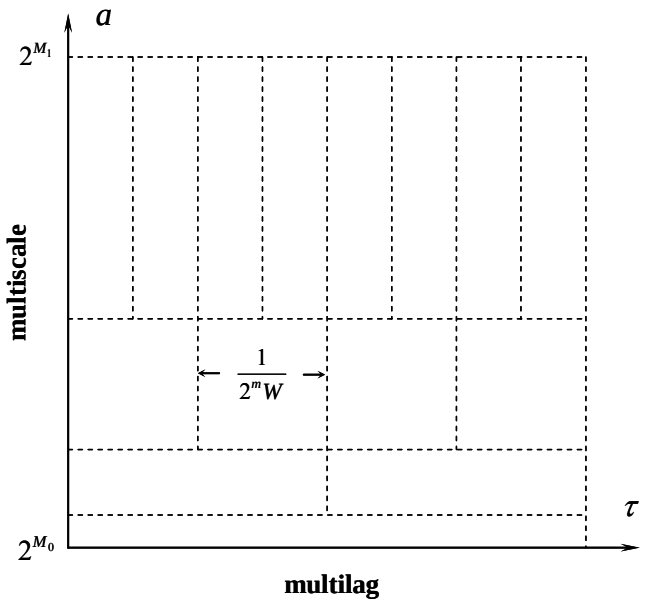

Fig. 4.6. Dyadic sampling in the multi-scale and multi-lag plane; the dyadic scale is $a = 2^m$; for the given $M_0 \le m \le M_1$, m, M_0, M_1 are all integer. The multi-lag resolution is $1/\left(2^m W\right)$, for a given signal bandwidth W.

Without loss of generality, we consider BPSK modulation, and the information-bearing symbol of the transmitted signal is $b_0 = \pm 1$. From the multi-scale and multi-lag channel defined in Fig. 4.6, the overall baseband signal at the receiver can be rewritten as:

$$y(t) = b_0 \sum_{m=M_0}^{M_1} \sum_{l=1}^{L(m)} h(m,l) \sqrt{2^m}\, x\left(2^m t - \frac{l}{W}\right) + n(t) \qquad (4\text{-}46)$$

where $L(m)$ denotes the number of the multi-lag for corresponding scaling index m, as shown to be the number of cross points on each row in Fig. 4.6. M_0 and M_1 are the lower and upper bounds of *m*, respectively. In fact, the multilag resolution in a wideband channel is $1/(aW)$ if the signal is scaled by a. When the number of scatterers contributing to the discrete channel gain $h(m,l)$ is exceedingly large, the random variables $h(m,l)$ can be assumed Gaussian and therefore independent.

Consequently, the inverse discrete wavelet transform description in Eq. (4-46) effectively decomposes the wideband channel into

$$M = \sum_{m=M_0}^{M_1} \left(L(m) \right) \tag{4-47}$$

orthogonal, flat-fading channels. This results in a potential joint scale-lag diversity order M that can be exploited to increase the system performance.

In order for a scale-lag RAKE receiver to collect the aforementioned diversity components, the transmitted signal should be designed as a wavelet-based waveform. A wideband multi-scale and multi-lag channel performs the inverse discrete wavelet transform on the transmitted signal $x_{m,l}(t)$. At the receiver side, for the diversity component corresponding to the *m*-th scale and *l*-th lag, the detection statistic

$$\lambda_{m,l} = \left\langle y(t), \sqrt{2^m} x\left(2^m t - \frac{l}{W} \right) \right\rangle = \int_{-\infty}^{\infty} y(t) \sqrt{2^m} x^* \left(2^m t - \frac{l}{W} \right) dt \tag{4-48}$$

is the correlator output of the received signal $y(t)$ and the basic waveform $\sqrt{2^m} x\left(2^m t - l/W\right)$. Therefore, the detection statistic $\lambda_{m,l}$ can be obtained by the dyadic scale-lag samples of the discrete wavelet transform of $y(t)$ associated with the wavelet function $x(t)$, which forms a scale-lag RAKE receiver. Then, the channel gain is combined

coherently to obtain the estimate of the transmitted information symbol b_0 as

$$\hat{b}_0 = \text{sign}\left\{ \text{Re}\left(\sum_{m=M_0}^{M_1} \sum_{l=1}^{L(m)} h^*(m,l)\lambda_{m,l} \right) \right\} \tag{4-49}$$

We note that this coherent detection of the scale-lag RAKE receiver corresponds to a Maximum Ratio Combining (MRC).

4.4.2 Cooperative wavelet communication scheme

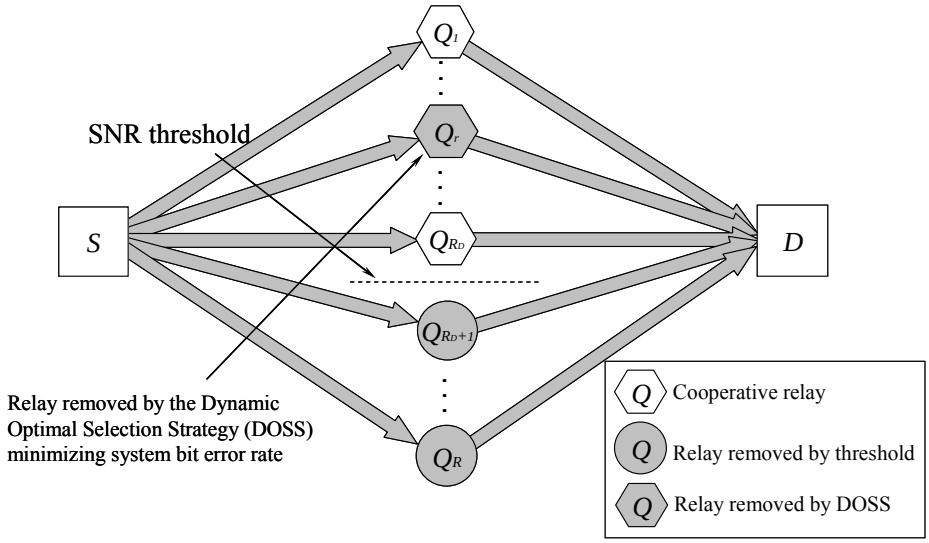

Fig. 4.7. Cooperative wavelet communication scheme with dynamic optimal selection of DF relays in wideband multi-scale and multi-lag channel (*S*: Source, *D*: Destination, Q_r: *r*-th Relay).

In this section, by taking advantage of the MRC property of the above mentioned multi-scale and multi-lag wideband channel and wavelet transceiver model, we consider a wideband cooperative wavelet communication scheme as shown in Fig. 4.7, where we transmit data from source node *S* to destination node *D* through *R* DF relays, without the direct link between *S* and *D*. This relay structure is called 2-hop relay

system, i.e., the first hop from source node to relay, and the second hop from relay to destination. Different relays operate at different frequency bands and all relay links undergo a multi-scale and multi-lag wideband channel. We assume that the channels are well known at the corresponding receiver sides. All AWGN terms have equal variance N_o. Relays are re-ordered according to the descending order of the SNR between *S* and *Q*, i.e., $\mathrm{SNR}_{SQ_1} > \cdots > \mathrm{SNR}_{SQ_R}$, where SNR_{SQ_r} denotes the *r*-th largest SNR between *S* and *Q*.

In this model, relays can determine whether the received signals are decoded correctly or not, by just simply comparing its received SNR to the threshold. The SNR threshold for the full decoding at the *r*-th relay reaches its lower bound as

$$\gamma_{th} \geq \frac{2^B - 1}{h_{S,Q_r}} \tag{4-50}$$

where B is the target rate of the link between source node and relay, and h_{S,Q_r} denotes the power gain of the channel from source node to the *r*-th relay[17]. Therefore, the relays with a SNR below the threshold will be removed first, as shown with the gray circles in Fig. 4.7. The other R_D relays shown with hexagons are DF relays. According to the dynamic optimal selection strategy, which will be proposed in the next section, we select proper DF relays for cooperation. A one bit feedback channel from destination to relay is used for removing the unsuitable DF relays.

Haar wavelet signaling is adopted in the cooperative wideband system to transfer the multi-scale and multi-lag channel into the total M_D flat-fading channels

$$M_D = \sum_{r=1}^{R_D} \sum_{m=M_{Q_r,0}}^{M_{Q_r,1}} \left(L(m) \right) \tag{4-51}$$

where $L(m)$ denotes the number of multi-lags for a corresponding scaling index m, and for the Doppler scale index *m* with spread

$M_{Q_{r,1}} - M_{Q_{r,0}}$, at the *r*-th cooperative link. For capturing the multi-scale and multi-lag diversity in the wideband channel, other wavelets, such as Daubechies wavelets, Symlets, etc., have the same capability, since they all possess orthogonality in both scale and lag domain. Rational orthogonal wavelets can be adopted for the scale factor of a_0^m, $1 \le a_0 \le 2$, which is more suitable for a practical scenario [102]. However, the wavelet selection problem is beyond the scope of this thesis. In this section, we focus on the multi-relay, multi-scale, and multi-lag diversity issue of a cooperative wideband system.

4.4.3 Dynamic optimal relay selection strategy

In maximum ratio combining, the transmitted signal from R_D cooperative relays nodes over all multi-scale and multi-lag channels, which underwent independent identically distributed (i.i.d.) complex Gaussian fading, are forwarded to the destination node and combined. In this case, the average error probability can be found in closed form as [17]

$$P_e = \left(\frac{1-\mu}{2}\right)^{M_D} \sum_{k=0}^{M_D-1} \binom{M_D - 1 + k}{k} \left(\frac{1+\mu}{2}\right)^{M_D} \qquad (4\text{-}52)$$

where

$$\mu = \sqrt{\frac{\overline{\gamma}_c}{1+\overline{\gamma}_c}} \qquad (4\text{-}53)$$

In the proposed DF cooperative wideband network, because of the fully decoding at the relays, we only consider the link between relays and destination. Therefore, the average SNR per channel $\overline{\gamma}_c$ can be derived as

$$\overline{\gamma}_c = \left(\prod_{Q_r \in \mathrm{DF}} \prod_{m=M_{Q_r,0}}^{M_{Q_r,1}} \prod_{l=0}^{L(m)} \frac{E_Q h_{Q_r,D}(m,l)}{N_o} \right)^{1/M_D} \tag{4-54}$$

where $h_{Q_r,D}(m,l)$ denotes the power gains (corresponding to the *m*-th scale and *l*-th lag), of the channel from the *r*-th relay to the destination in the DF protocol. By combining Eq. (4-52), (4-53) and (4-54), we derive the analytical expression of the BER performance for the proposed DF cooperative wideband network.

As the average error probability P_e gives precise information, we can use it to predict the comprehensive transmission performance, when only the channel gains and SNRs at the destination are known. Consequently, we propose a dynamic optimal selection strategy for the cooperative multi-scale and multi-lag communication. In this algorithm the proper relays are selected in order to reach a minimum P_e. First of all, relays are ordered according to the descending order of the SNR between source and relays, as shown in the Fig. 4.7. According to the proposed SNR threshold, we pick up the DF relays whose SNR is above the threshold.

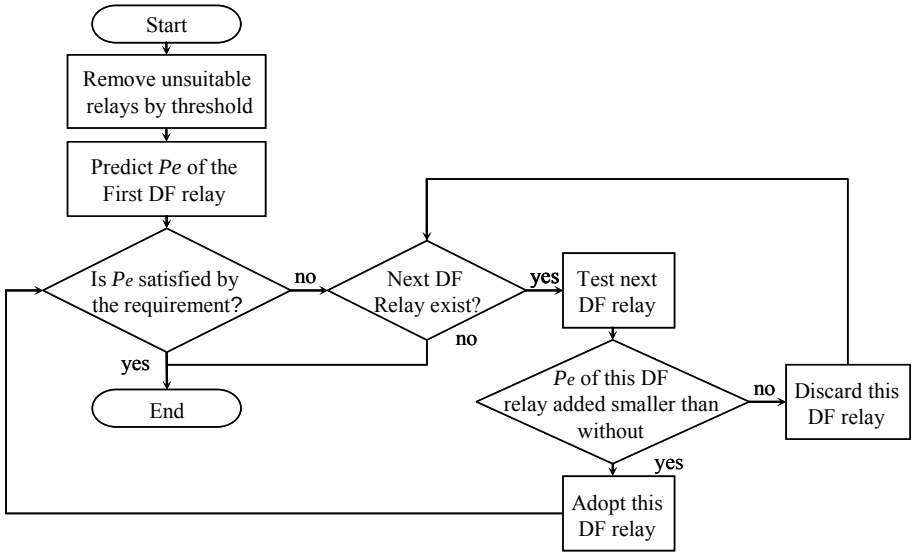

Fig. 4.8. Flow chart of the dynamic optimal selection strategy for cooperative wideband communication.

Then, we proceed with the relay selection to maximize the entire BER performance and try to satisfy the P_e requirement, where by the inappropriate DF relays are removed. The whole dynamic optimal selection strategy for the cooperative wideband communication is shown in the flow chart of Fig. 4.8.

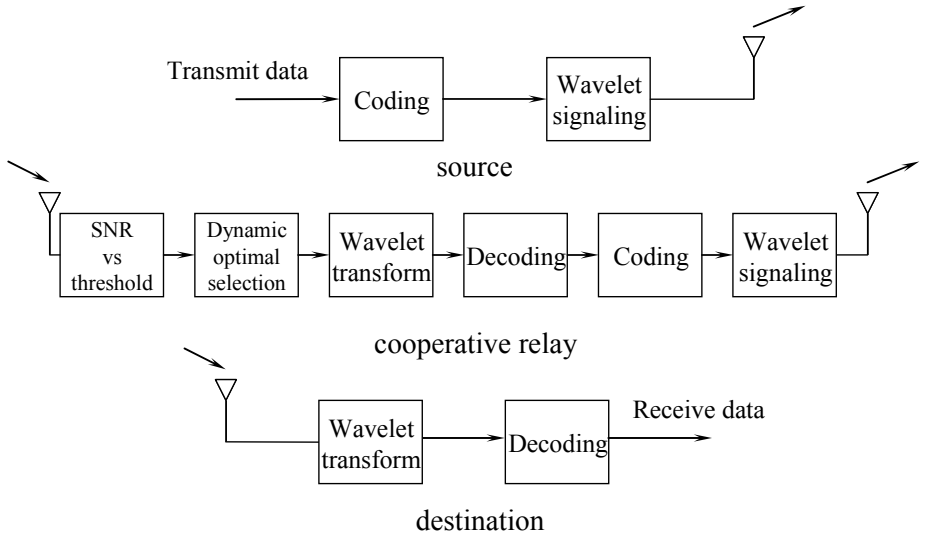

Fig. 4.9. Relay selection in the cooperative wavelet wideband wireless transmission strategy (top: source, middle: cooperative relay, bottom: destination).

The wavelet signaling and transceiver design are shown in Fig. 4 9. Before transmission, Haar wavelet signaling is adopted to capture the multi-scale and multi-lag diversity in the wideband channel. In the relaying section, we first remove un-decodable relays by using the SNR threshold. Then, those relays which undergo deep fading between relay-destination links will be removed by using the dynamic optimal selection strategy, in order to meet the P_e requirement. After recoding, Haar wavelet signaling is applied again on the signal. At the destination node, after inverse wavelet transformation, the resulting signals are used for the combination and detection.

Summarizing the novelties in this Section, cooperative relaying communication network has been set up for multi-scale and multi-lag wideband channels. We also provide a dynamic optimal selection strategy for relay selection to take advantage of the multi-relay, multi-scale and multi-lag diversity and maximize the system BER

performance.

4.5 Simulation results and analysis

Test Case 1 (BER performance based Relay selection for cooperative communication):

In this example, first, we simulated BPSK modulation, a Rayleigh channel, flat fading, without OFDM, and supposed a SNR threshold for correct decoding equal to $4E_b/N_0$; then we assumed $h_{Q_i,D} = h_{S,Q_j} = h_{Q_j,D} = 1$, for all branches, in order to verify the proposed analytical BER expression. The resulting average BER were plotted against the transmit SNR defined as SNR = E_b/N_0. As shown in Fig. 4.10, the theoretical curves of multi-DF cooperation derived from our analytical closed-form BER expression clearly agree with the Monte Carlo simulated curves, while the theoretical curves of 2-AF and 3-AF cooperation match the simulation result only at the low SNR region.

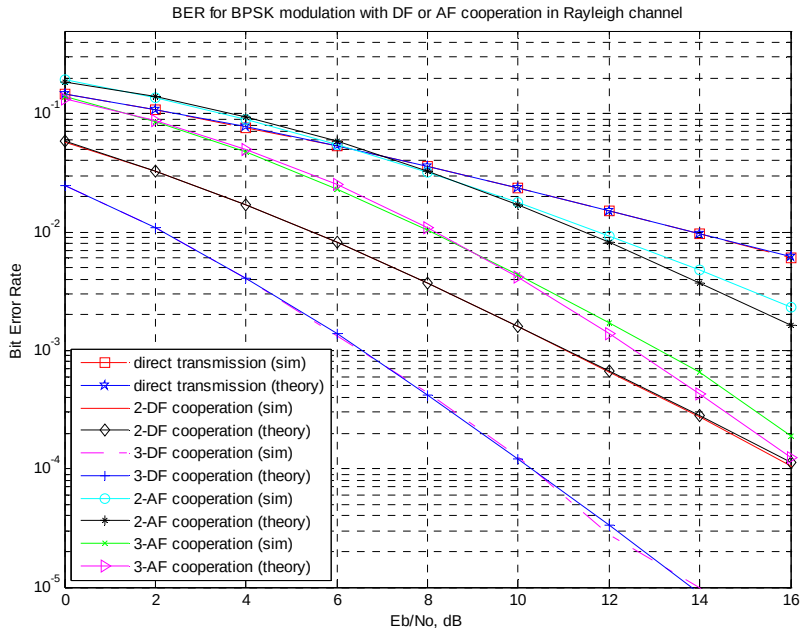

Fig. 4.10. BER performance for DF or AF cooperation.

Fig. 4.11 shows the BER performance for hybrid DF-AF cooperation.

For the DF-dominant hybrid cooperation, the theoretical curves exhibit a good match with the Monte Carlo simulation result curves. The slight gap between theoretical and simulation BER results for the hybrid case of 1-DF + multi-AF can be explained by the AF relay fading which was considered as a double Gaussian channel, a product of two complex Gaussian channels [108]. Obviously, the distribution of combined SNR (i.e., γ_c) will no longer follow the chi-square distribution giving rise to this slight difference.

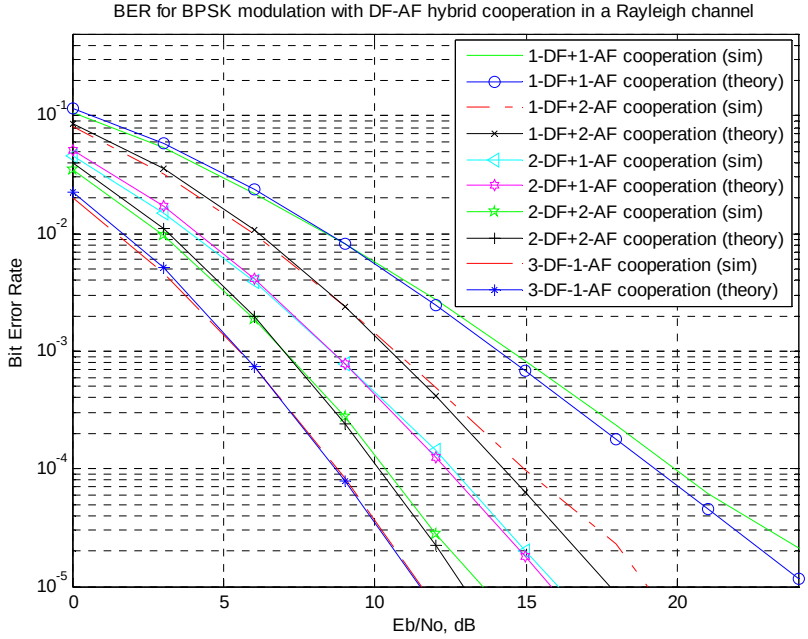

Fig. 4.11. BER performance for hybrid DF+AF cooperation.

As shown in *Theorem 2.1*, in the proposed hybrid cooperation protocol, DF is dominant. This DF dominant hybrid cooperative networks strategy can be verified by the above simulation results as well. Comparing 2-DF to 2-AF in Fig. 4.10, or 2-DF plus 1-AF to 1-DF plus 2-AF in Fig. 4.11, or other hybrid DF-AF protocols with the same *R*, we can see that the fully decoded DF protocols always show a better BER performance than AF protocols. Therefore, DF protocols with a reliable decoding play a more important role in hybrid cooperative networks than AF protocols. Meanwhile, we can see from the figure that changing to the AF scheme for the relay nodes with a SNR below the threshold also

improves the BER performance, as well as the diversity gain of the whole network. In fact, this is a better way than just discarding these relay nodes.

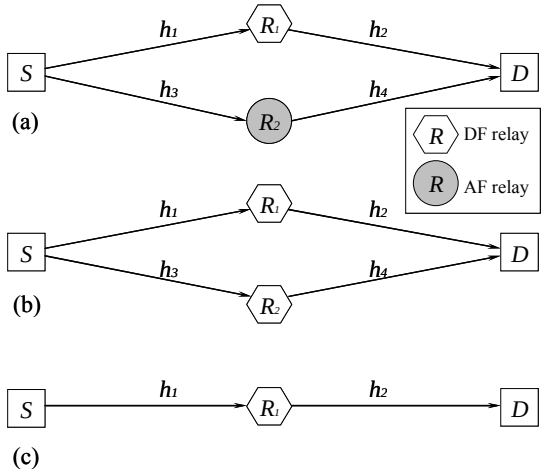

Fig. 4.12. hybrid DF-AF cooperation and DF cooperation architectures with different average power gains. (a) hybrid DF-AF cooperation, (b) dual DF cooperation, (c) single DF cooperation. (*S*: Source, *D*: Destination, *h*: average power gain between two nodes).

Paper [109] proposes a closed-form BER expression for the two-hop AF protocol, which includes Gauss' hypergeometric and Gamma functions. This closed-form BER expression needs more computational burden to derive the cooperative analytical expression. In paper [110], the analytical expression for multi-node DF protocol is provided with a complicated form as well. Instead, the compact closed-form BER expression for hybrid DF-AF cooperation proposed in this chapter allows us to achieve insight into the results with relatively low burden in computations. The simple expressions can also help in understanding the factors affecting the system performance. It can also be used for designing different network functions such as power allocation, scheduling, routing, and node selection.

In order to study the effect of the channel gains between source, relay and destination, we compare the hybrid DF-AF with the dual DF as well as the single DF cooperation in Fig. 4.12. In this figure, h_1, h_2, h_3 and h_4 stand for the average power gain between the corresponding two nodes. In this simulation, the SNR threshold for correct decoding is assumed to

be $4E_b/N_0$, and we set the first hop average power gain in the DF protocol, i.e., h_1 in Fig. 4.12 (a) and Fig. 4.12 (c), and h_1, h_3 in Fig. 4.12 (b) equal to 4, which means that the relay in DF protocol can fully decode the signal. The average power gains of the first hop in the AF protocol, i.e., h_3 in Fig. 4.12 (a) increases from 0.25 to 20. It can be seen from Fig. 4.13 that the dual DF cooperation with reliable decoding outperforms the hybrid DF-AF cooperation, when the corresponding average power gains are the same, i.e., the diamond marked curve is better than square marked curve in Fig. 4.13. Meanwhile, the comparison of the curves shows that, the AF relay which undergoes deep fading deteriorates the BER performance of hybrid DF-AF cooperation in the low SNR region. Thus, this AF relay should be removed according to the proposed dynamic optimal combination strategy to improve the transmission performance. Summarizing the above discussion leads to the observation that due to power control, long transmission range, serious attenuation, etc., a high SNR at the relay and full decoding for the DF protocol is not always feasible. In such case, relays can change to the AF protocol with enough SNR to gain from the cooperative diversity.

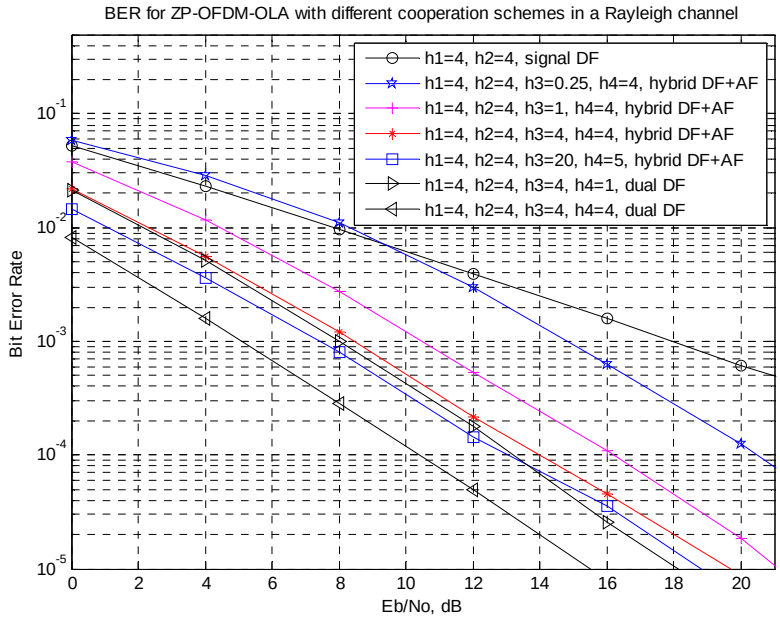

Fig. 4.13. BER performance for hybrid DF-AF cooperation and DF cooperation with different path gain.

Finally, we illustrate the validity of the theoretical results for the OFDM cooperation via simulations. An OFDM system with a 64-point FFT and a CP length of 16 samples (which accounts for 25% of the OFDM symbol) was considered. In the simulation, a more practical scenario was considered with a 3-path Rayleigh fading between each source node and relay node or relay node and destination node. The 3-path delays were assumed at 0, 1, 2 samples, respectively. As illustrated in Fig. 4.14, OFDM with CP can nicely cope with the multi-path, and the theoretical curves derived from Eq. (4-15) clearly agree with the Monte Carlo simulation curves. The simulation results indicate that under the condition of ISI resolved by OFDM and reliable decoding, the cooperative diversity gains from the increasing R, which is also shown by Eq. (4-1).

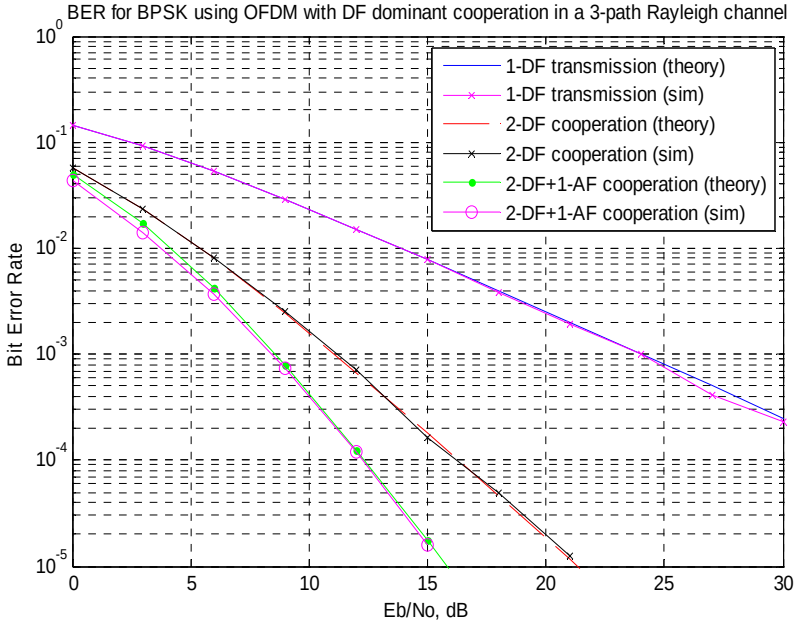

Fig. 4.14. BER performance for DF dominant OFDM cooperation.

Test Case 2 (Game theory based relay selection and resource allocation):

In Section 4.3, we have discussed the system model for relay selection and resource allocation and optimization. Based on the model considered

in Section 4.3, we have set up a simulation to justify our theoretical analysis for the system model and get more clear understanding of the system. In this test case we present results from our simulation model.

First, using the system and game models from Section 4.3, we simulate the relay selection and resource allocation for cooperative communication network with interference.

To see the effect of interference to the relay selection, we simulate the relay selection process for cooperative wireless communication networks with interference and without interference in relation to the different relay cost.

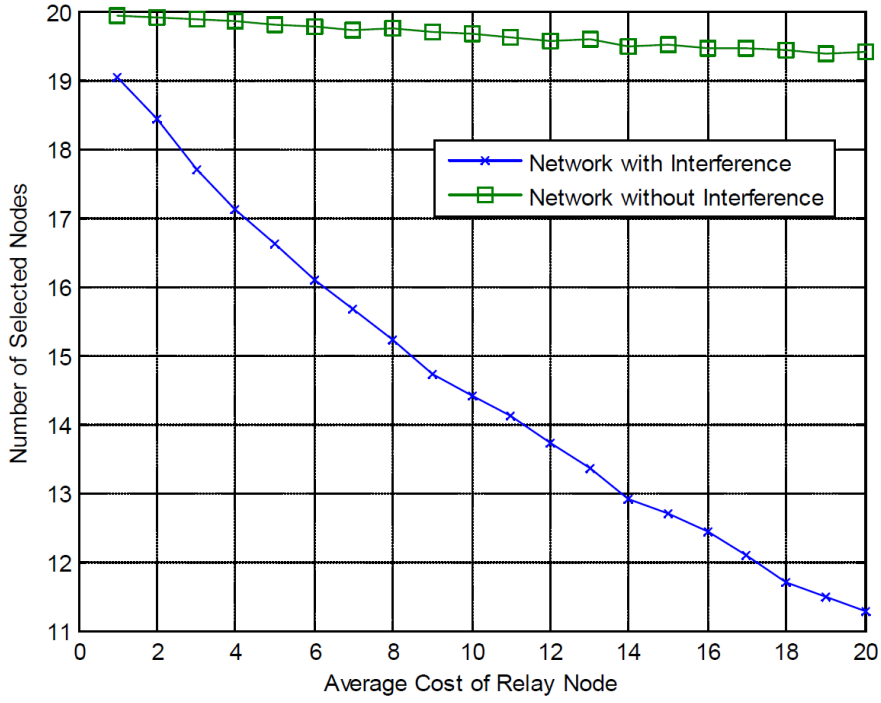

Fig. 4.15. Number of selected nodes from relay selection into a cooperative wireless communication network with and without interference for different relay cost.

From Fig. 4.15 we can see that the number of selected nodes when interference is included in the network is lower than when the interference is excluded. This result confirm our relay selection criterion

model according to Eq. (4-36)

$$\frac{\partial U_s}{\partial P_{r_i}} = \frac{aW}{\ln 2}\left(\frac{A_i}{B_i}\right) - p_i > 0$$

with

$$A_i = \frac{P_s G_{s,r_i}}{\sigma_{\text{int}}^2 + \sigma^2 + P_s G_{s,d}},$$

and

$$B_i = \frac{P_s G_{s,r_i} + \sigma_{\text{int}}^2 + \sigma^2}{G_{r_i,d}}.$$

We can see that the adding interference level will decrease the term

$$\frac{aW}{\ln 2}\left(\frac{A_i}{B_i}\right),$$

and then the relay node will be removed from the selection since $\partial U_s / \partial P_{r_i}$ will likely to be lower than zero.

We then apply the algorithm from Fig. 4.5 to our system model. We consider two different schemes when simulating the algorithm to limit the number of selected relay nodes. In Scheme #1, we have 18 different relay nodes with a price starting from 2 and increasing linearly to 40. In scheme #2, all relay nodes have an initial price distributed uniformly between 2 and 7. Then we consider two different scenarios. Our pricing game model provided in paper [39] is scenario #A; scenario #B stands for an algorithm where the relay selection criterion in our pricing game model is performed after every iteration in the game. In Fig. 4.16, we show that by using scenario #B, the number of relay nodes used decreases after a certain number of relays is available to the source node. This happens because the price of the relay nodes increases after each iteration according to the price updating function of the relay nodes

shown by Eq. 4.43. The price updating function depends on $P_{r_i}^*$ and $\partial P_{r_i}^* / \partial p_i$ which in turn depends on the number of selected relay nodes. When the number of selected relays is high, the optimal price will become too high and the relay nodes become not beneficial anymore to the source node. In scenario #B, these relays are removed by the relay selection process.

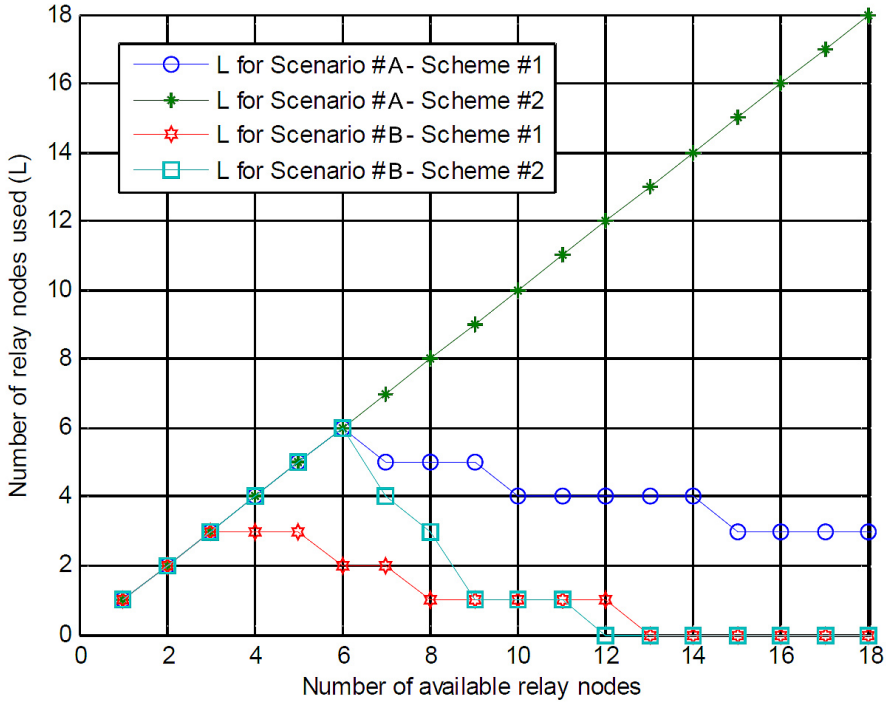

Fig. 4.16. Number of relay nodes used versus the number of available nodes.

Test Case 3 (Relay selection for cooperative communication over multi-scale and multi-lag wireless channels):

In this case, we use the simulation results to verify our theoretical claims on the analytical BER expression and illustrate the dynamic optimal selection strategy.

In the first example, simulation results justify the proposed analytical BER expression for cooperative wavelet communication over a multi-scale and multi-lag wireless channel, i.e., the combination of Eq. (4-52), (4-53) and (4-54), which can be used to predict the transmission

performance and enable the dynamic optimal selection strategy as shown in the Fig. 4.8. BPSK is adopted as modulation scheme. The 2-decomposition level Haar wavelet transform is adopted as a RAKE receiver to capture the multi-scale and multi-lag diversity components, and to transfer the multi-relay, multi-scale and multi-lag channel into the orthogonal flat-fading channels. Therefore, we consider 2-relay three orthogonal channels in this simulation. Relay 1 has 1-scale and 2-lag diversity components, the power gains are $h_1 = 4$ and $h_2 = 1$. Relay 2 has 1-scale and 1-lag diversity component, the power gain equals $h_3 = 1$. The resulting average BER are plotted against the transmit SNR defined as SNR = E_b/N_o. As shown in Fig. 4.17, the theoretical curves of different diversities derived from our analytical closed-form BER expression clearly agree with the Monte Carlo simulated curves.

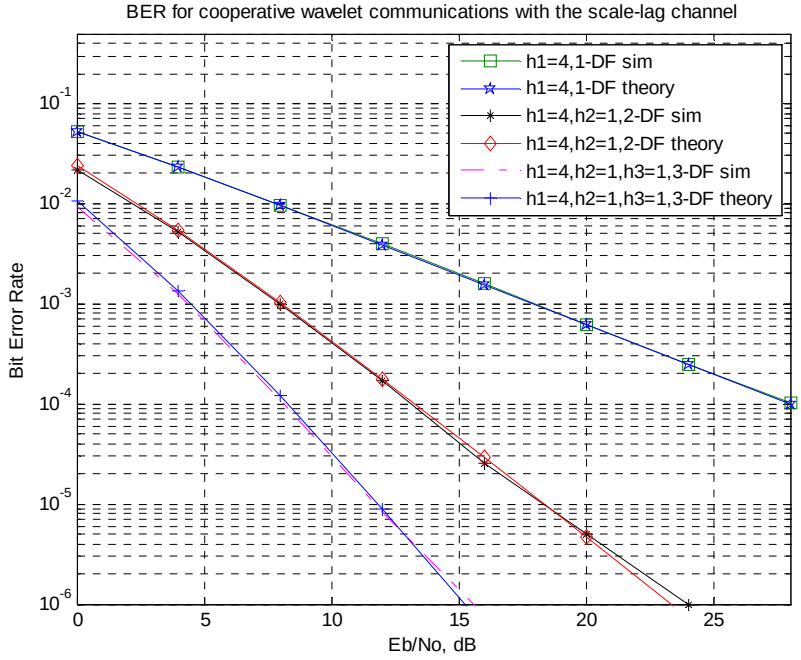

Fig. 4.17. BER performance for cooperative wavelet wideband communication.

In the second example, we illustrate how to exploit the proposed analytical BER expression together with dynamic optimal selection strategy to select relays for the cooperative wideband communication. We suppose the target P_e at SNR E_b/N_o = 10dB equals 10^{-4}. In the

original state, we suppose that we already have 1-Relay with 1-scale and 2-lag diversity components, with power gains $h_1 = 4$ and $h_2 = 1$. The BER performance is shown by the triangle marked curve in Fig. 4.18. The P_e requirement is not met by the original state, so we expect to cooperate with more relays, to gain from more diversity components. For the test 1, we test and combine with a deep fading relay having only one scale-lag diversity and power gain $h_3 = 0.04$. Analytical BER expression predicts that adding this deep fading relay deteriorates the BER performance. Therefore, we discard this relay. For the test 2, we test and combine with a relay with one scale-lag diversity, and power gain $h_3 = 4$, which improves the BER performance, and then satisfies the P_e requirement. Therefore, we adopt this relay.

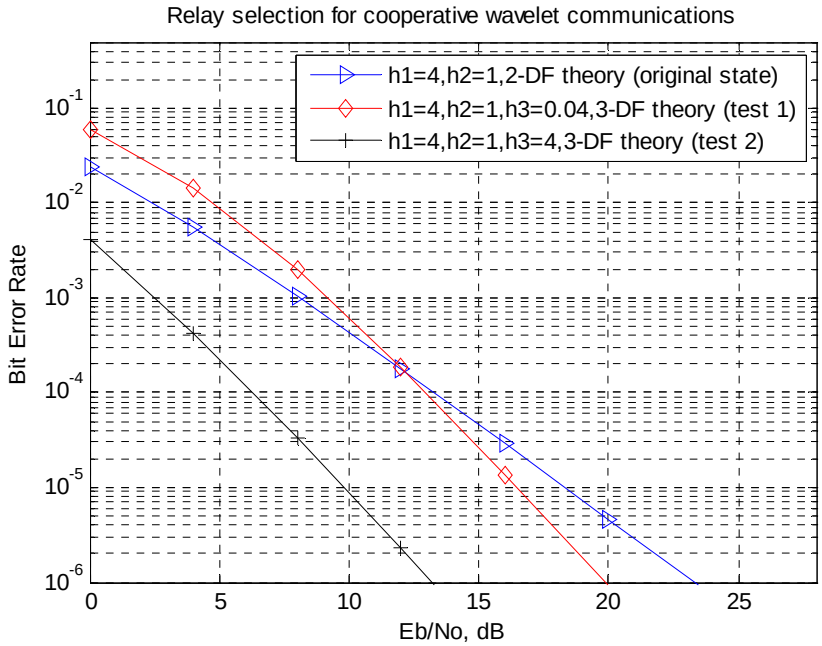

Fig. 4.18. Relay selection for cooperative 2-decomposition level wavelet wideband communication.

4.6 Conclusions

In this chapter, we investigated novel relay selection and resource allocation issues in cooperative communication.

First, we proposed a new hybrid OFDM cooperative strategy for multi-node wireless networks employing both DF and AF relaying. Fully decoding is guaranteed by simply comparing SNRs at relay nodes to the SNR threshold, which is more efficient than utilizing a conventional cyclic redundant checking code. The lower bound and the upper bound of the SNR threshold were provided as well. After correct decoding, the DF protocol outperforms AF protocol in terms of BER performance, which can be seen from Monte Carlo simulation as well as analytical results. These results justify that the DF protocol is dominant within the hybrid cooperation strategy. For the suggested hybrid DF-AF cooperation protocol, we also represented a dynamic optimal combination strategy for optimal AF selection. The closed-form BER expression of the hybrid OFDM cooperation in a Rayleigh fading channel was derived. The agreement between the analytical curves and numerical simulated results shows that the derived closed-form BER expression is suitable for the DF-dominant hybrid cooperation protocols. The compact and closed-form BER expression can easily provide an insight into the results as well as a heuristic help for the design of future cooperative wireless systems.

Subsequently, we proposed novel relay selection and resource allocation and optimization schemes for cooperative wireless communication networks with interference using the game theoretical approach. In this research, we proposed a pricing game based on the Stackelberg game for relay selection and resource allocation and optimization in cooperative communication networks with interference. Simulation results show that interference in the cooperative communication network can change the relay selection and resource allocation and optimization result. The calculations allow for predicting the behavior of the system in an environment closer to real world situation, compared to the case when only noise is considered in the system. Then we found out that the pricing game for resource allocation and optimization, when the number of available nodes is high, can result in a high payment to relay nodes which will highly reduce the source node utility function. Therefore, we proposed an algorithm to limit the number of selected relay nodes to mitigate this problem. Using this algorithm, we chose a number of relay nodes where the result of resource allocation and optimization is still beneficial for the value of the source node utility function.

Wideband scale-lag channels can be found in many applications, including ultra-wideband communication and underwater acoustic communication. Signaling and reception schemes using the wavelet theory enable the multi-scale and multi-lag diversity in the wideband system. In this chapter, we designed a cooperative wavelet system to capture the joint cooperative-scale-lag diversity. We proposed the analytical BER expression for the cooperative wavelet wideband communication. The agreement between the analytical curves and numerical simulated results shows that the derived analytical BER expression is suitable for the performance prediction of cooperative wavelet wideband communications. The compact and closed-form BER expression can easily provide an insight into the results as well as a heuristic help for the design of future cooperative wavelet wideband systems. For the suggested cooperative wavelet protocol, we also presented a dynamic optimal selection strategy for the optimal relay selection, which maximizes the whole system transmission performance.

Appendix 4-1.

In this Appendix, we provide derivations which support our hypothesis in Sub-section 4.3.2.

$P_{r_i}^*$ provided in Sub-section 4.3.2, is the optimal solution for the equation

$$\frac{\partial U_s}{\partial P_{r_i}} = a\frac{\partial R_{s,r,d}}{\partial P_{r_i}} - p_i = 0; \quad i \in L \tag{A4-1}$$

it requires U_s to be continuous and concave with P_{r_i}. Taking the second order derivatives of the source node utility function U_s, provided that

$$\frac{\partial U_s}{\partial P_{r_i}} = \frac{aW}{\ln 2}\frac{A_i B_i}{\left(1+\sum_{k\in L}\frac{A_k P_{r_k}}{P_{r_k}+B_k}\right)\left(P_{r_i}+B_i\right)^2} - p_i \tag{A4-2}$$

we can get

$$\frac{\partial^2 U_s}{\partial P_{r_i}^2} = -\frac{aW}{\ln 2}\frac{1}{\left(1+\sum_{k\in L}\frac{A_k P_{r_k}}{P_{r_k}+B_k}\right)^2}\left[\frac{A_i B_i}{\left(P_{r_i}+B_i\right)^2}\right]^2 - \frac{aW}{\ln 2}\frac{A_i B_i}{\left(1+\sum_{k\in L}\frac{A_k P_{r_k}}{P_{r_k}+B_k}\right)\left(P_{r_i}+B_i\right)^3} \quad , \tag{A4-3}$$

for each relay i, $W>0$, $a>0$, $A_i = P_s G_{s,r_i} \Big/ \left(\sigma_{\text{int}}^2 + \sigma^2 + P_s G_{s,d}\right) > 0$, $B_i = \left(P_s G_{s,r_i} + \sigma_{\text{int}}^2 + \sigma^2\right) \Big/ G_{r_i,d} > 0$ and $P_{r_i} \geq 0$. Therefore, we can always assume that $\partial^2 U_s \big/ \partial P_{r_i}^2 < 0$. By definition, since the second derivative of the utility function U_s is always negative,

$$\frac{\partial U_s}{\partial P_{r_i}} = \frac{aW}{\ln 2}\frac{A_i B_i}{\left(1+\sum_{k\in L}\frac{A_k P_{r_k}}{P_{r_k}+B_k}\right)\left(P_{r_i}+B_i\right)^2} - p_i = 0 , \tag{A4-4}$$

is the maximum point. Thus, we can verify that $P_{r_i}^*$ is the optimal solution for maximizing U_s.

Then, we proof that p_i^* is the optimal solution for the equation

$$\frac{\partial U_{r_i}}{\partial p_i} = P_{r_i}^* + \left(p_i - c_i\right)\frac{\partial P_{r_i}^*}{\partial p_i} = 0 . \tag{A4-5}$$

Since we have

$$\frac{\partial P_{r_i}^*}{\partial p_i} = \sqrt{\frac{A_i B_i}{p_i}}\,\frac{Y+\sqrt{Y^2+4aXW/\ln 2}}{2X}\left(-\frac{1}{2p_i}\left(1-\frac{\sqrt{p_i A_i B_i}}{\sqrt{Y^2+4aXW/\ln 2}}\right)\right), \tag{A4-6}$$

and

$$P_{r_i}^{*}=\sqrt{\frac{A_iB_i}{p_i}}\frac{Y+\sqrt{Y^2+4aXW/\ln 2}}{2X}-B_i, \qquad \text{(A4-7)}$$

the Eq. (A4-5) can be expanded as

$$\frac{\partial U_{r_i}}{\partial p_i}=-B_i+\sqrt{\frac{A_iB_i}{p_i}}\frac{Y+\sqrt{Y^2+4aXW/\ln 2}}{2X}\times\left(1-\frac{p_i-c_i}{2p_i}\left(1-\frac{\sqrt{p_iA_iB_i}}{\sqrt{Y^2+4aXW/\ln 2}}\right)\right) \qquad \text{(A4-8)}$$

Taking second order derivatives of Eq. (A4-8) we get

$$\frac{\partial^2 U_{r_i}}{\partial p_i^2}=\sqrt{\frac{A_iB_i}{p_i}}\frac{Y-\sqrt{p_iA_iB_i}}{2X}\left(1-\frac{\sqrt{p_iA_iB_i}}{\sqrt{Y^2+4aXW/\ln 2}}\right)\times\left(\frac{-p_i-3c_i}{4p_i^2}\right)$$

$$+\sqrt{\frac{A_iB_i}{p_i}}\frac{1}{8Xp_i^2\left(\sqrt{Y^2+4aXW/\ln 2}\right)^3}$$

$$\times\left\{\left[\left(Y-\sqrt{p_iA_iB_i}\right)^2+2\left(Y-\sqrt{p_iA_iB_i}\right)\sqrt{p_iA_iB_i}+4aXW/\ln 2\right]^2\left(-p_i-3c_i\right)\right\}$$

$$+p_iA_iB_i\left[\left(Y-\sqrt{p_iA_iB_i}\right)^2+2\left(Y-\sqrt{p_iA_iB_i}\right)\sqrt{p_iA_iB_i}\right]\left(-p_i-3c_i\right)$$

$$-16p_iA_iB_i\,ac_iXW/\ln 2 \qquad \text{(A4-9)}$$

Since $A_i>0$, $B_i>0$, $p_i>0$, $c_i>0$, $W>0$, $a>0$, $X=1+\sum_{j\in L}A_j>0$ and $Y=\sum_{j\in L}\sqrt{p_jA_jB_j}>0$, we always have $\partial^2U_s/\partial p_i^2<0$, which means the solution of

$$\frac{\partial U_{r_i}}{\partial p_i} = P_{r_i}^* + \left(p_i - c_i \right) \frac{\partial P_{r_i}^*}{\partial p_i} = 0 \qquad \text{(A4-10)}$$

is the maximum point.

After we have both solutions to maximize both U_s and U_{r_i}, we define the equilibrium of the game as $P_{r_i}^{eq}$ and p_i^{eq} which fullfill

$$U_s \left(P_{r_i}^{eq} \right) = \sup_{P_{r_i} \geq 0} U_s \left(P_{r_i} \right). \qquad \text{(A4-11)}$$

and

$$U_{r_i} \left(p_{r_i}^{eq} \right) = \sup_{p_{r_i} \geq 0} U_s \left(p_{r_i} \right). \qquad \text{(A4-12)}$$

The supremum $\sup(\cdot)$ of both utility functions mean that we have to find the value of P_{r_i} and p_i which is the least value for $P_{r_i}^*$ and p_i^* in the domain of an optimal solution. At the convergence point of the game, where $P_{r_i}^* (t+1) = P_{r_i}^* (t)$ and $p_i^* (t+1) = p_i^* (t)$, t is the iteration number in the game, the $P_{r_i}^*$ and p_i^* is a point where neither the source node or the relay nodes can increase their utility function without having other players change their strategies. Thus, $P_{r_i}^{eq}$ and p_i^{eq} are the equilibrium of the game.

Chapter 5

Wideband Localization with cooperative relays

5.1 Introduction

Wireless localization has gained considerable attention over the past decade, accurate position measurement is important for many wireless localization and navigation problems. Although the Global Positioning System (GPS) usually provides worldwide high-accuracy position measurements, it requires Line of Sight (LOS) to multiple satellites. For the GPS-denied scenarios [41, 47], such as indoor, in urban “canyons”, and under tree canopies, GPS is known to be ineffective due to the inability of the waves obstacle penetration. Moreover, in the presence of radio-frequency interference or jamming, GPS is unavailable. Thus, alternative methods of positioning and navigation are of interest, either as a backup or for use in areas unreachable by satellites. Beacon localization, on the other hand, relies on terrestrial anchors, such as WiFi access points or GSM base stations. However, in areas where network coverage is sparse, e.g., in emergency situations, localization errors can be unacceptably large [43].

Generally, in the LOS scenario, high-accuracy localization can be achieved using high-power base stations or a high-density base station deployment, both of which are cost prohibitive and impractical in realistic settings [43]. A practical way to address this need is through a combination of cooperative localization and wideband transmission, which is investigated in this chapter.

As reviewed in Chapter 2, cooperative localization is an emerging paradigm that offers additional localization accuracy by enabling the agents to help each other in estimating their positions [44]. There are mainly two relaying protocols in classical cooperative networks: Amplify-and-Forward (AF) and Decode-and-Forward (DF) [72], which have been clearly explained and analyzed in the above Chapters. In AF, the received signal is amplified and retransmitted to the destination. The advantage of this protocol is its simplicity and low-cost implementation. However, the noise is also amplified at the relay. In DF, the relay

attempts to decode the received signals. If successful, it re-encodes the information and retransmits it. If some relays cannot fully decode the signal, they should be discarded. In this chapter, we propose a new relaying technique for cooperative localization, called trigger relay, which combines the advantages of AF relay and DF relay, i.e., less complexity because of no decoding, while removing the noise and interference effect at the relay.

The fine delay resolution in time domain and robustness of wide bandwidth or Ultra-Wide Bandwidth (UWB) transmission enable accurate and reliable range measurements in harsh environments. Adopting a UWB signal, the cooperative network enables the high speed communication and refines the position estimation [42]. In the time measurement based localization, Time Difference of Arrival (TDOA) is a famous one, meaning the measurement of time difference of signal propagation between two transmission links received at one common receiver or two synchronized receivers. TDOA estimation is often determined from the cross correlation of the two received signals. TDOA possesses many advantages which rely on its immunity of the clock bias of the transmitters. Therefore, TDOA methods have been used for localization with asynchronous transmitters for decades; they find applications in GPS and cellular localization. It has been shown that Time of Arrival (TOA) with clock bias (treated as an unknown parameter) is equivalent to TDOA [111]. Therefore, in the following parts of this chapter, we focus on the cooperative wideband TDOA estimation based on ZP-OFDM. In order to obtain accurate TDOA estimations, we always collect as long received signal as possible, and then do the cross correlation. ZP-OFDM is a multi-carrier block transmission scheme, with a highly block-structured transmission format. This block structure enables us to calculate some statistical features (e.g., mean, variance, skewness, kurtosis, etc.) of each block. Then, we can only transmit or forward the block features values to calculate the TDOA of two transmission links, rather than transmitting the entire signal. This feature-based TDOA needs less transmission bandwidth and is called bandwidth efficient localization [112].

In this chapter, we analyze different features for feature-based TDOA and verify that the Peak to Average Power Ratio (PAPR) is the best feature for cooperative feature-based TDOA in terms of the TDOA estimation accuracy. Then, we propose a trigger relay for TDOA

estimation. Only a short pilot or preamble signal is sent to the primary receiver, which can achieve bandwidth efficient localization as well. Compared to the AF relay and DF relay with a block feature, the trigger relay reduces the system complexity and enhances the TDOA estimation accuracy.

The rest of the chapter is organized as follows. In Section 5.2, we explain why we investigate the cooperative wideband TDOA. The major sources of error in cooperative TDOA are reviewed in Section 5.3. In Section 5.4, we illustrate and analyze the relaying techniques in TDOA based cooperative localization.

Specifically, In Sub-section 5.4.1, the conventional cooperative TDOA estimations based on AF relay and DF relay are reviewed. Then, the cooperative feature-based localization with DF relay is described in Sub-section 5.4.2, where the PAPR is proposed as the best feature for cooperative feature-based localization. A 2-step TDOA computation process to meet the different accurate localization requirements is proposed in the same section. In order to combine the merits of AF relay and DF relay, the trigger relay TDOA estimation is proposed in Sub-section 5.4.3. In Sub-section 5.4.4, the TDOA estimation performances of different relaying schemes are shown and analyzed. Results illustrate that the trigger relay TDOA has advantages in bandwidth efficiency, system complexity and resolution. In section Sub-section 5.4.5, the cooperative-multi-path diversity design for cooperative TDOA with trigger relay is illustrated.

Simulation results are provided in Section 5.5 to verify the theoretical analysis. Finally, Section 5.6 concludes the chapter.

5.2 Why cooperative wideband Time Difference of Arrival (TDOA)

Wideband or UWB systems are inherently well suited for time measurement based cooperative localization because the use of extremely large transmission bandwidths results in desirable capabilities such as 1) accurate ranging due to fine delay resolution; 2) simple implementation for multiple-access communications; and 3) obstacle penetration capabilities [113].

In modern wideband wireless systems, Orthogonal Frequency Division Multiplexing (OFDM) technology is widely used. As reviewed in Chapter 2, Zero-Padding (ZP)-OFDM, with the advantages of low transmission power and low spikes in the Power Spectrum Density (PSD), has been recently adopted for various UWB Standards. Furthermore, ZP-OFDM provides advantages over its conventional counterpart Cyclic-Prefix (CP)-OFDM in terms of the accurate blind time synchronization, better blind channel estimation and better transmission performance. Thus, ZP-OFDM will play more and more a visible role in the wideband wireless systems.

In the time measurement based localization, TDOA possesses many advantages which rely on its immunity of the clock bias of the transmitters. Therefore, TDOA methods have been used for localization with asynchronous transmitters in the past. It has been shown that TOA with clock bias (treated as an unknown parameter) is equivalent to TDOA [111].

By utilizing cooperative wideband TDOA, we can combine this advantage. Therefore, in next section of this chapter, we will focus on the cooperative wideband TDOA estimation based on ZP-OFDM.

5.3 Major sources of error in cooperative TDOA

Multi-path propagation refers to a phenomenon that transmitted signals reach the receiver through multiple paths, arising from either object reflections or from scattering. This phenomenon is considered deleterious for the localization since the path-overlap in multi-path channels introduces interference in estimating the received data signals. Multi-path interference is a major source of the time-based range error. In the multi-path channel, the late-arriving multi-path components are self-interference that may dramatically decrease the Signal-to-Interference Noise Ratio (SINR) of the desired LOS signal. Especially, many multi-path signals can arrive just after the LOS signal and are then called early-arriving multi-path components. They contribute to their cross-correlations, and obscure the location of the peak related to the LOS signal. It is also noted that the LOS signal can be severely attenuated compared to the late-arriving multi-path

components, causing it to be “lost in the noise” and missed completely; this leads to large positive errors in the TOA estimate.

In multi-path and Non Line-of-Sight (NLOS) scenarios, rather than finding the highest peak of the cross-correlation, the receiver should extract the first-arriving peak because there is no guarantee that the direct transmission signal will be the strongest of the arriving signals. First-arriving peak detection can be done by measuring the time that the cross-correlation first crosses a threshold. Alternatively, in template-matching, the leading edge of the cross-correlation is matched in a Least-Squares (LS) sense to the leading edge of the auto-correlation (the correlation of the transmitted signal with itself) to achieve sub-sampling time resolutions [114].

However, scattering objects can be regarded as virtual cooperative mobile devices that can forward the copies of the transmitted signals to the base station, and introduce multi-path diversity. Thus, with the proper design of the transceiver, the signal detection at the receiver side can be improved by gaining from multi-path diversity. In this chapter, we will show how to achieve the full cooperative-multi-path diversity and contribute to the cooperative ZP-OFDM localization.

5.4 Relaying techniques in TDOA based cooperative localization

5.4.1 Conventional cooperative TDOA with AF or DF relay

In this chapter, we consider the cooperative localization for the wideband communication system in a LOS scenario. We assume the locations of the base station and relays are known by the primary receiver. Scatterers located between the base station, relays and primary receiver, are causing multi-path channels. ZP-OFDM is adopted as modulation scheme. In general, by using the $(q+1)$ TDOA estimates together with the classical hyperbolic intersection searching, the primary receiver can localize its position in q dimensions.

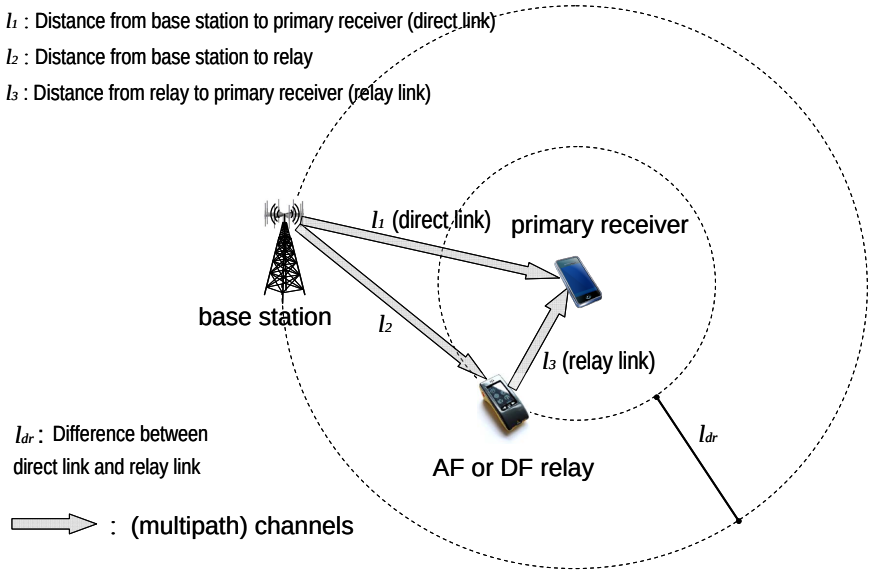

Fig. 5.1. Cooperative TDOA system model with classical AF relay or DF relay.

In this Subsection, we briefly review the conventional TDOA estimation based on AF relay or DF relay. As depicted in Fig. 5. 1, the base station first broadcasts the signal. The relay receives the signal, and then amplify-and-forwards or decode-and-forwards the signal to the primary receiver. In this figure the two circles are concentric, with the primary receiver as the centre of the circles. The radius of the inner circle represents the signal propagation time from relay to primary receiver, and the radius of the outer circle illustrates the signal propagation time from base station to primary receiver.

Signals from the base station and relay are transmitted on different subcarriers as a frequency division system. Therefore, the primary receiver can distinguish the signals from base station and relay. In order to obtain TDOA estimation, the primary receiver performs a correlation:

$$C_y(d_s) = \sum_{s=1}^{S} y_{ba}^*(s)\, y_{re}(s+d_s), \qquad (5\text{-}1)$$

where $y_{ba}(s)$ and $y_{re}(s)$ denote the s-th sample of the received signals at the primary receiver from the base station and the relay, respectively. $(\cdot)^*$ denotes the conjugate operation. The primary receiver needs to

compute Eq. (5-1) for all anticipated arrival time differences, i.e., $-D_s \le d_s \le D_s$; here D_s stands for the maximum anticipated arrival time difference relative to the sample time T_s, and d_s corresponds to delay time of samples normalized to sample time T_s. S refers to the number of received signal samples used for TDOA estimation. Then, the TDOA between the link from base station to relay to primary receiver and the link from base station directly to primary receiver TD_{brp} can be calculated from

$$\mathrm{TD}_{brp} = \delta T_s = \frac{l_2}{c} + T_r + \frac{l_3}{c} - \frac{l_1}{c}, \tag{5-2}$$

where

$$\delta = \arg\max_{-D_s \le d_s \le D_s} \left| C_y\left(d_s\right) \right|. \tag{5-3}$$

δ equals d_s when the absolute value of $C_y\left(d_s\right)$ reaches its maximum, c is the speed of light, T_r is the total data processing time at the relay, and $|\cdot|$ denotes the modulus. We suppose that the distance between base station and relay l_2 is known; the transmission time from base station to relay equals $T_{br} = l_2/c$. The TDOA between the link from base station to primary receiver and the link from relay to primary receiver TD_{br} can be expressed as

$$\mathrm{TD}_{br} = \frac{l_1}{c} - \frac{l_3}{c} = T_{br} + T_r - \mathrm{TD}_{brp}. \tag{5-4}$$

5.4.2 Feature based cooperative TDOA with DF relay

In the cooperative TDOA with DF relay, the boundary of the OFDM block can be determined. Therefore, block features of OFDM system can be exploited to achieve the bandwidth efficient TDOA [112]. The block features include the normalized central moments (mean, variance, skewness, and kurtosis) of the first Q samples of the k-th block effective OFDM symbol, i.e., the part of the OFDM symbol that includes

only the transmitted information and without the redundancy introduced by ZP. The features are calculated according:

the mean
$$\mu_{rx}(k) = \frac{1}{Q}\sum_{i=1}^{Q} y_{rx}(k)_i , \tag{5-5}$$

the variance
$$\sigma_{rx}^2(k) = \frac{1}{Q}\sum_{i=1}^{Q}\left(y_{rx}(k)_i - \mu_{rx}(k)\right)^2 , \tag{5-6}$$

the skewness
$$\lambda_{rx}(k) = \frac{1}{Q}\sum_{i=1}^{Q}\left(\frac{y_{rx}(k)_i - \mu_{rx}(k)}{\sigma_{rx}(k)}\right)^3 , \tag{5-7}$$

the kurtosis
$$\varepsilon_{rx}(k) = \frac{1}{Q}\sum_{i=1}^{Q}\left(\frac{y_{rx}(k)_i - \mu_{rx}(k)}{\sigma_{rx}(k)}\right)^4 , \tag{5-8}$$

where subscript "rx" denotes received signal either from the base station or relay, and $y_{rx}(k)_i$ refers to the i-th sample of the k-th block effective OFDM symbol.

Other additional block features, are the average symbol's phase

$$\Phi_{rx}(k) = \frac{1}{Q}\sum_{i=1}^{Q}\arctan\left(\frac{\mathrm{Im}\left(y_{rx}(k)_i\right)}{\mathrm{Re}\left(y_{rx}(k)_i\right)}\right), \tag{5-9}$$

the Peak Power (PP)

$$\mathrm{PP}_{rx} = \mathrm{Max}\left(\left|y_{rx}(k)_1\right|^2,\cdots,\left|y_{rx}(k)_Q\right|^2\right), \tag{5-10}$$

and the PAPR

$$\mathrm{PAPR}_{rx} = \frac{\mathrm{Max}\left(\left|y_{rx}(k)_1\right|^2,\cdots,\left|y_{rx}(k)_Q\right|^2\right)}{\frac{1}{Q}\sum_{i=1}^{Q}\left|y_{rx}(k)_i\right|^2}, \tag{5-11}$$

where $\mathrm{Im}(\cdot)$ and $\mathrm{Re}(\cdot)$ stand for the imaginary and real part of a complex value, respectively. $\mathrm{Max}(\cdot)$ denotes the maximum of a set of real values $(\cdot)$.

After receiving and decoding the signal from the base station, the DF relay calculates the above mentioned features for each OFDM block. Then, the block features are forwarded to the primary receiver. Meanwhile, the primary receiver calculates the features based on the signals transmitted from the base station. Subsequently, the primary receiver computes the cross correlation of the features from the base station and the relay to obtain the TDOA estimation. Generally, these features can be classified into 2 types. The first one is of a zero convergence type, which includes the mean, skewness, kurtosis and average symbol's phase, because for the random zero mean signals, their values converge to zero as Q increases. (see Appendix 5-1). The second one is of a power type, which includes the variance, PP and PAPR, since they are related to the power of the signals.

The zero convergence type features always have values close to zero. Thus, the noise can easily pollute these block features, which implies a bigger error in TDOA estimation. The power type features have larger values than the zero convergence type features; therefore, they are more robust against the noise. For constant modulus signals, such as Binary Phase Shift Keying (BPSK), Quadrature Phase Shift Keying (QPSK), 2-Quadrature Amplitude Modulation (QAM), 4-QAM, and after linear equalization, the variance of one block equalized signals always has a value between 0 and 1; the PAPR has the largest value among all the above mentioned features and is thus the best feature for TDOA estimation. For the non-constant modulus signal, such as 16-QAM, 64-QAM, etc., PP has the largest value among all the above mentioned features, and is then the best feature.

Given the features from the base station and relay, the primary receiver can compute the cross correlation of the features. Let us denote the k-th block feature values of the base station and relay as $f_{\mathrm{ba}}(k)$ and $f_{\mathrm{re}}(k)$, respectively. The primary receiver computes the cross correlation of the features as

$$C_f(d) = \sum_{k=1}^{K} f_{\text{ba}}(k)\left(f_{\text{re}}(k+d)\right)^*, \tag{5-12}$$

where K stands for the number of the OFDM blocks used for calculating the feature cross correlation. The primary receiver must compute Eq. (5-12) for all anticipated valid ranges of the block arrival time difference, say $-D \le d \le D$, where D stands for the maximum anticipated arrival time difference in the block. Thus, the TDOA between the link from base station to relay to primary receiver and the link from base station directly to primary receiver TD_{brpf} can be computed as

$$\text{TD}_{brpf} = T_s M \Delta, \tag{5-13}$$

where

$$\Delta = \arg \max_{-D \le d \le D} \left| C_f(d) \right|, \tag{5-14}$$

M stands for the number of the samples within each OFDM block, i.e., FFT size plus ZP samples. Then, similar to the conventional TDOA procedure, TD_{br} can be calculated.

Then, TD_{br} can be translated into distance difference between base station to primary receiver link and relay to primary receiver link by multiplying it with c. According to the hyperbolic theorem, the primary receiver should appear at the hyperbola with the locations of the base station and relay as its foci. Together with another two hyperbolas calculated from another base station and relay pairs, the primary receiver can locate its position in a 2-dimensional plane. Many location estimation algorithms were proposed to deal with the localization procedure, which have been reviewed in [114] and [46]. In this chapter, for the sake of simplicity, we only pay attention to the TDOA estimation and not localization.

5.4.3 Trigger relay for cooperative TDOA estimation

The advantage of AF is that it does not need the complicated signal decoding, while the strong point of DF relay relies on the fact that it can get rid of the noise effect and channel interferences. The DF relay with a block feature of an OFDM symbol can further reduce the transmitting

data and gains from the bandwidth efficiency. Therefore, we propose a trigger relay technique to take advantage of the above merits [115]. This scheme is shown in Fig. 5.2. Three circles are concentric circles, with the primary receiver as the centre of the circle. Three radii, from short to long, are the signal propagation times from relay 1, relay 2 and base station to the primary receiver, respectively.

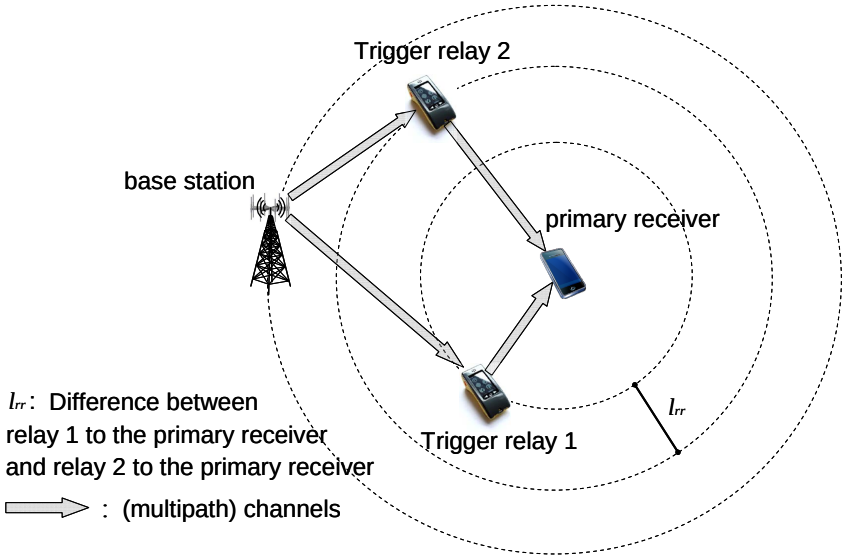

Fig. 5.2. Cooperative TDOA system model with trigger relays.

The diagram of signal transmissions in the trigger relay TDOA estimation is shown in Fig. 5.3. Immediately after relay 1 and relay 2 receiving the base station signals at t_1 and t_2, they transmit a predetermined signal to the primary receiver at known t_1' and t_2' time points, respectively. This predetermined signal can be a short pilot or preamble. We assume that the processing intervals at two relays are the same, i.e., $t_1' - t_1 = t_2' - t_2$. The primary receiver receives the signals from relay 1 and relay 2 at t_{r1} and t_{r2}, respectively. All the time points t_1, t_2, t_{r1} and t_{r2} are determined from the leading edges of the received signals.

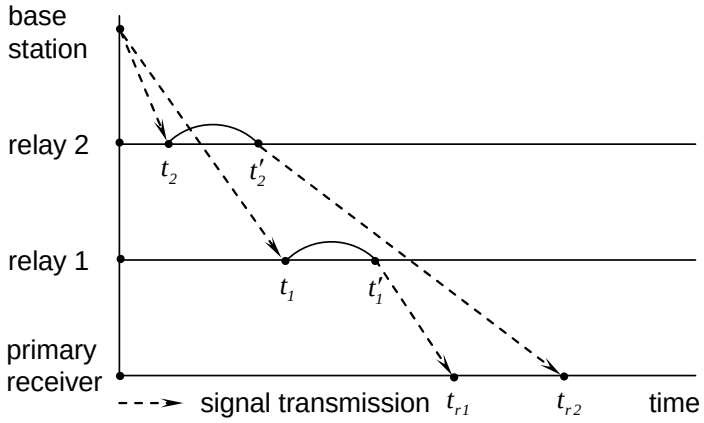

Fig. 5.3. Signal transmissions in trigger relay TDOA estimation scheme.

Subsequently, The TDOA between relay 1 to primary receiver link and the relay 2 to primary receiver link (TD_{rr}) can be calculated by primary receiver as:

$$\mathrm{TD}_{rr} = (t_{r2} - t_{r1}) + (t_1 - t_2), \tag{5-15}$$

where $(t_{r2} - t_{r1})$ can be achieved by correlation of signals from the two relays, similar to the AF and DF relay case, and $(t_1 - t_2)$ can be calculated from the known positions of base station and relays, which are already known by the primary receiver.

5.4.4 Comparison of different relay schemes in cooperative TDOA

In this Sub-section, we compare the AF relay, DF relay with block feature (DF feature) and trigger relay in the context of cooperative ZP-OFDM TDOA; their performances are summarized in Table 1.

TABLE I. COMPARISON OF TDOA PERFORMANCE FOR DIFFERENT RELAYING SCHEMES

	bandwidth efficiency	**system complexity**	**TDOA estimation error**
AF relay	**no**	**medium**	**reasonable**
DF feature	**yes**	**high**	**large**
Trigger relay	**yes**	**low**	**good**

In conventional cooperative TDOA with AF relay, the relay needs to forward the whole received data to the primary receiver, which requires large bandwidth to transmit the data. The DF relay with block feature was designed to extract one statistical feature from each OFDM symbol, and only forwards the feature data. This scheme significantly reduces (by about 160 times according to the MB-OFDM standards, see Appendix 5-2) the transmitting data compared to the conventional TDOA based on cross correlation of the whole received signal, and achieves a bandwidth efficient transmission. In this chapter, we propose a trigger relay sending a short pilot or preamble for TDOA estimation; this reduces the amount of data transmission compared to the conventional AF and DF relays. Thus, trigger relay possesses the merit of bandwidth efficiency similar to DF relay with a block feature.

As the name suggests, the AF relay requires a proper power amplifier to compensate the signal attenuation suffered in the base station to the relay link. The DF relay with block feature not only decodes the received signal, but also computes the feature from each OFDM symbol. Therefore, both AF and DF relays introduce extra complexity into the system [72]. Compared to the AF and DF relays, the proposed trigger relay enjoys the lowest system complexity. Trigger relay does not need to process the received data, i.e., neither decoding nor amplifying the received data. It only needs to be switched on by the incoming signal, and send a simple pilot to the primary receiver.

For estimating the TDOA, the DF relay with block feature can only reach block level resolution, not at sample level as the conventional TDOA does. When adopted the MB-OFDM standards [22, 23], the feature-based TDOA estimation resolution is lower bounded by its block interval, i.e., 312.5 ns. This resolution can be enhanced by utilizing smaller FFT size multi-carrier modulation and the block interval can be reduced accordingly. If more accurate localization is required, we need to compute TDOA involving a cross correlation of the signals at sample level, i.e. 1.894 ns in the MB-OFDM system. Sample signal correlation with AF relay and trigger relay can achieve resolution up to sample level. It is worth mentioning that, AF relay TDOA estimation suffers more from noise and multi-path interference in the base station to relay link than the trigger relay TDOA estimation. Thus, trigger relay obtains the highest TDOA resolution among the above mentioned three relaying

schemes.

5.4.5 Cooperative multi-path diversity for cooperative TDOA with trigger relay

In the cooperative ZP-OFDM transmission with multi-path channels, by adopting proper relay clustering scheme and transceiver design, trigger relay TDOA estimation can further gain from the cooperative multi-path diversity, and improve the TDOA accuracy.

In order to gain from the cooperative diversity due to the help of other relays, we propose a relay clustering scheme as shown in the Fig. 5.4. We consider each relay cluster has one core relay, shown as the black devices in the figure; we assume that the position of the core relay is known by the primary receiver. The neighboring cooperative relays, which are shown as gray devices, are temporally synchronized with the core relay, and grouped into one cluster. The cooperative relays transmit the same signal as core relay does, and help the core relay to gain from the spatial diversity, i.e., cooperative diversity.

Furthermore, the trigger relay based cooperative TDOA system can exploit multi-path diversity from multi-path propagation. Multi-path propagation refers to a phenomenon that transmitted signals reach the receiver through multiple paths, arising from either reflections or from scattering. This phenomenon is considered deleterious for the localization since the path-overlap in multi-path channels introduces interference in estimating the received data signals. In the cross-correlation based time measurement localization, because of the multi-path and Non Line of Sight (NLOS), the delayed peaks are usually detected to be stronger than the first detected peak, which introduces ambiguity into the position information. However, the scattering objects within the multi-path propagation can be regarded as virtual cooperative agents who can forward the copies of the transmitted signals to the corresponding receiver sides. The virtual cooperative agents resemble the amplify-and-forward (AF) relays in the cooperative system, and the multi-path diversity can be considered as the cooperative diversity among the virtual cooperative agents as well.

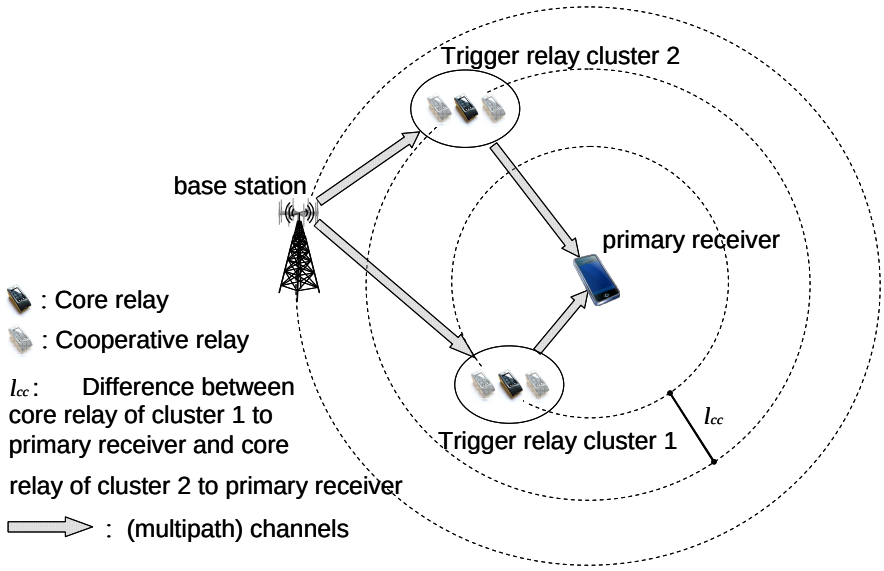

Fig. 5.4. Relay clustering scheme for a trigger relay based Cooperative TDOA system.

In order to achieve the above mentioned cooperative multi-path diversity in the trigger relay based cooperative TDOA system, we adopt the linear transceiver proposed in [20], which holds a linear structure or tall Toeplitz structure of the ZP-OFDM channel. Its full column rank property always guarantees matrix invertibility and signal detection. Furthermore, the tall Toeplitz matrix guarantees the full cooperative multi-path diversity gain of ZP-OFDM system, only with the linear equalizers, such as Zero-Forcing (ZF) and Minimum Mean Square Error (MMSE) equalizers [56, 24]. By gaining from the full cooperative multi-path diversity, the proposed system combats the noise effect, improves the transmission performance, and enhances the pilot signal detection. Utilizing the well detected pilot signal to process the TDOA estimation, it will consequently enhance the TDOA estimation accuracy. Meanwhile, this ZP-OFDM transceiver possesses lower system complexity, compared to those systems with non-linear maximum-likelihood equalizers.

Summarizing the novelties in this chapter, we proposed a trigger relay based cooperative localization technique with high resolution, low complexity and bandwidth efficiency. Compared to its counterparts (AF and DF relays), trigger relay achieves a better performance in terms of system complexity and TDOA accuracy.

5.5 Simulation results and analysis

In this section, we present a selection of our simulation results to show the performance of different block features, different relay schemes, cooperative multi-path diversity gains for TDOA estimation, and verify the above analysis. BPSK is adopted as modulation scheme. We consider the ZP-OFDM system with ZP accounts for 25% of the effective OFDM symbol duration, and with sample period $T_s = 1.894$ ns. The channels: from base station to relay, from base station to primary receiver and from relay to primary receiver are characterized by the identical independent Rayleigh distributed channels. We simulate different situations with subcarriers number *N = 8*, *16*, *32*, and multi-path channel length *L = 1*, *2*, *3*, *4*. In these simulations, the absolute error of TDOA estimation is shown in order to compare the performances of different schemes. The absolute error is defined as the absolute difference between the estimated TDOA and the true TDOA in ns.

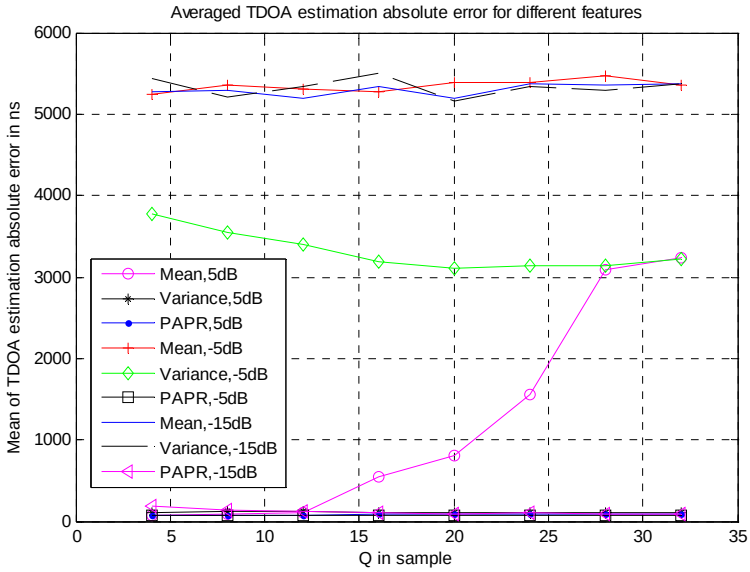

Fig. 5.5. Absolute errors of different features in TDOA estimation.

Test Case 1 (Feature selection): In this example, we compare the performance of different features in the TDOA estimation. Fig. 5.5 shows the averaged absolute error in feature-based TDOA estimation vs.

Q samples of the effective OFDM symbol with DF relay. We consider N = 32 and flat fading channel with Signal-to-Noise Ratio (SNR) = -15 dB, -5 dB and 5 dB in this case. Because the mean, skewness, kurtosis and average symbol's phase all belong to the zero convergence type, we only show the mean as an example, together with the variance and PAPR. We can see from Fig. 5.5 that the PAPR shows the smallest absolute error among the three features in the ZP-OFDM TDOA estimation, and accordingly is the best feature for the feature-based TDOA estimation. This simulation result verifies our theoretical analysis in Sub-section 5.4.2.

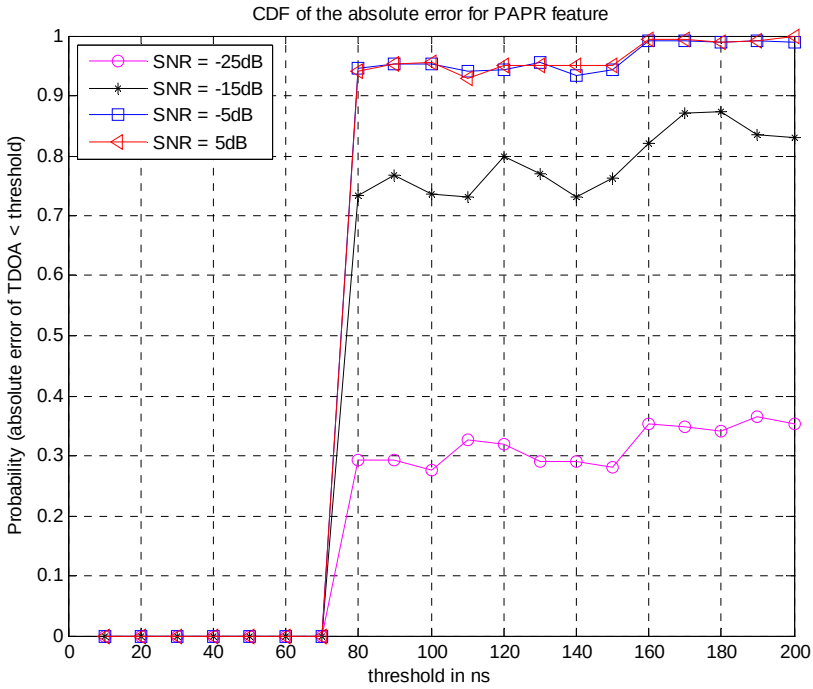

Fig. 5.6. CDF of the absolute error for the PAPR feature with different SNR.

In order to exhibit more details of the PAPR performance in TDOA estimation, we show the Cumulative Distribution Functions (CDFs) of $\mathrm{Prob}(\text{absolute error of TDOA} < \text{threshold})$ with different SNR scenarios in Fig. 5.6. We consider N = 32, and the PAPR is calculated from the first Q = 8 samples of the OFDM symbol. In this case, the feature-based TDOA estimation with DF relay can only achieve the symbol level resolution, i.e., 75.76 ns. When the threshold is longer than 75.76 ns, the

CDF curve becomes lower as the SNR decreases.

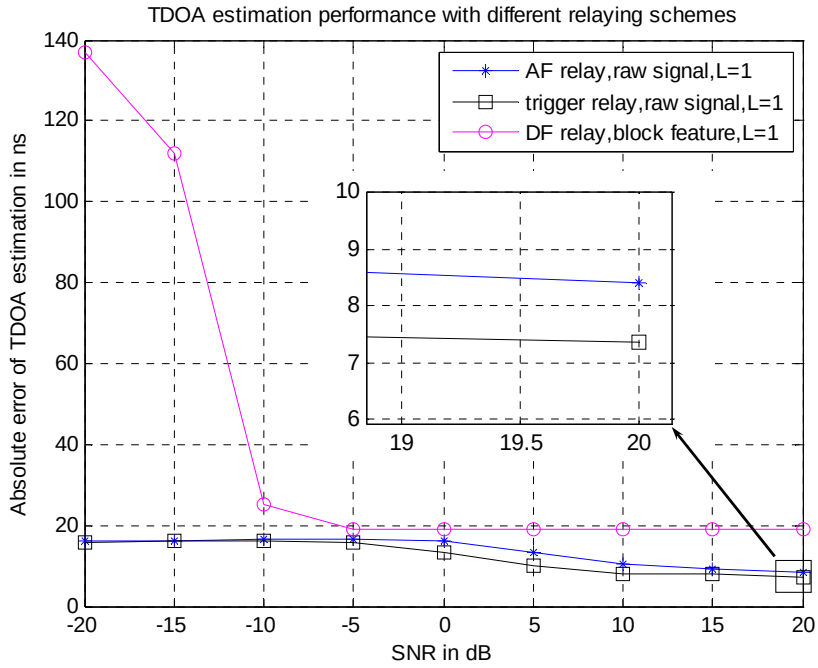

Fig. 5.7. Different relaying schemes for TDOA estimation in a flat fading channel.

Test Case 2 (Different relaying schemes): In this example, we compare different relaying schemes for TDOA estimation and consider a number of subcarriers $N = 8$. For the DF relay with block feature, we adopt the first 7 samples of the OFDM symbol for the PAPR feature calculation. For the AF relay and trigger relay cases, the primary receiver correlates the raw received signals, i.e., no channel equalization or decoding at primary receiver is assumed.

As shown in Fig. 5.7, a flat fading channel is considered, i.e., $L = 1$. The DF relay with block feature can only reach the block level resolution, i.e., 18.94 ns. Since the AF relay amplifies the noise before relaying, while the trigger relay does not, we can see from the figure that, the trigger relay slightly outperforms the AF relay in the middle region of the Single-to-Noise Ratios (SNR), and provides a better TDOA estimation error. The error gap between AF relay and trigger relay decreases as the SNR increases.

In Fig. 5.8, we consider a 3-path channel scenario, i.e., $L = 3$. Compared to Fig. 5.7, due to multi-path channel equalization, DF relay with block feature gains from multi-path diversity, and the TDOA resolution in low SNR region is improved accordingly. However, for the AF relay and trigger relay cases, as they do not use channel equalization, they cannot gain from multi-path diversity. In the high SNR region, multi-path interference becomes the dominant effect on TDOA estimation, which degrades the TDOA resolution for both AF relay and trigger relay cases. The error gap between AF relay and trigger relay in Fig. 5.8 is larger than the gap in Fig. 5.7, which comes from the multi-path interference in the base station to relay link of the AF case.

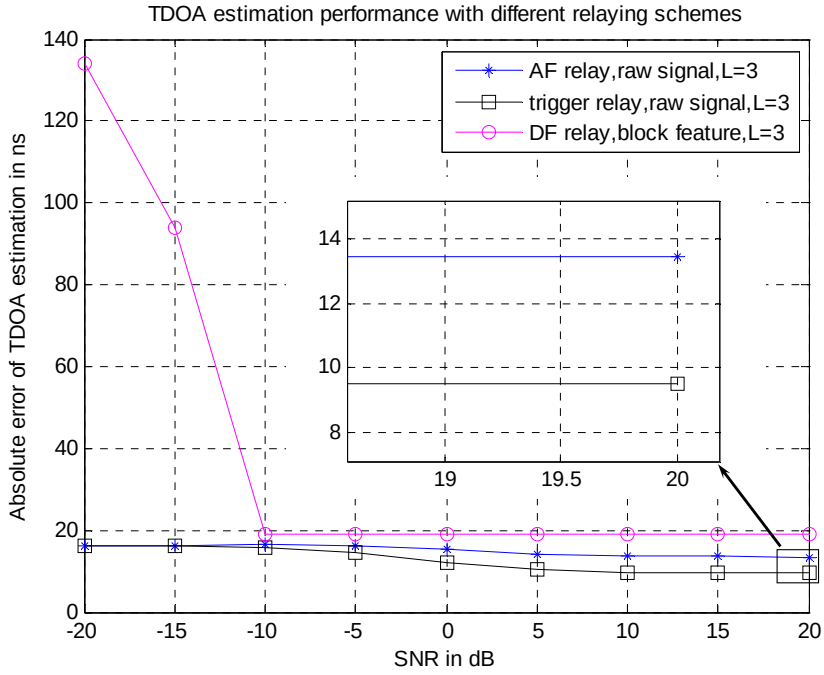

Fig. 5.8. Different relaying schemes for TDOA estimation in a multi-path channel.

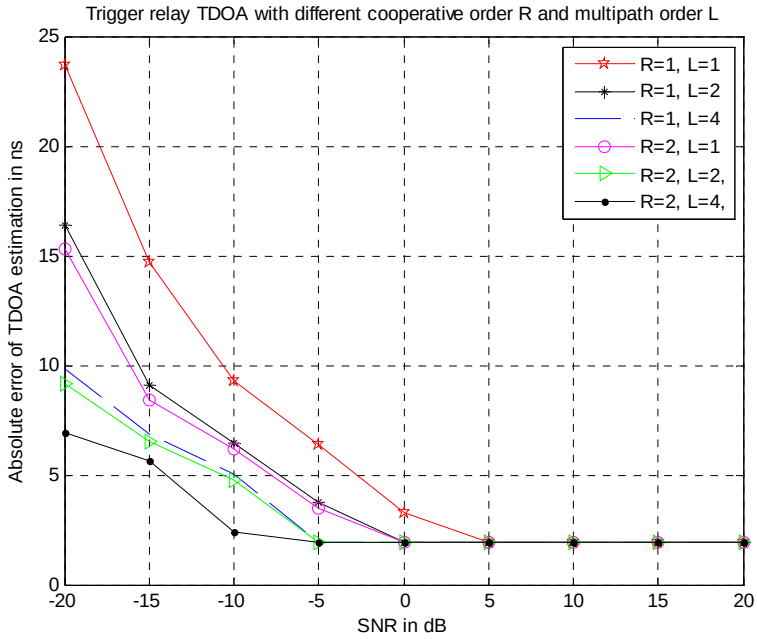

Fig. 5.9. Cooperative multi-path diversity for TDOA estimation with trigger relay.

Test Case 3 (Cooperative multi-path diversity for trigger relay): In this example, we show how the trigger relay TDOA estimation benefits from cooperative multi-path diversity. We consider the number of relays in one cluster as shown in Fig. 5.4, i.e., cooperative diversity order $R = 1, 2$, and assume that all relays undergo a similar multi-path channel. We consider different multi-path diversity order scenarios, i.e., $L = 1, 2,$ and 4. In order to achieve the cooperative multi-path diversity, the primary receiver should equalize the channel, detect the frequency domain signal, and then transfer it into the time domain by FFT, with zero-padding in order to restore the original time domain transmitted signal. Fig. 5.9 shows that, the signal detection improves the TDOA estimation error performance, and the absolute error of TDOA estimation reaches its lower bound at 1.894 ns. We can see from the figure that, in the low SNR region, cooperative multi-path diversity helps reducing the absolute TDOA estimation error, and the more cooperative multi-path diversity orders, the smaller the TDOA estimation error.

5.6 Conclusions

In this chapter, we investigated cooperative relaying schemes for ZP-OFDM TDOA estimation and a feature-based cooperative TDOA estimation to achieve bandwidth efficient transmission is analyzed. A trigger relay technique is proposed to gain from easy processing together with noise and interference immunity on the base station to relay link. According to the authors acknowledge, there is no similar idea has been proposed for the localization based on the cooperative relaying. Compared to AF relay and DF relay TDOA estimation cases, the trigger relay reduces the system complexity. Meanwhile, the trigger relay enables the bandwidth efficient TDOA, since it significantly reduces the amount of data for transmission. In terms of TDOA estimation error, among the AF relay, trigger relay and DF relay with a block feature, the trigger relay achieves the best accuracy. Furthermore, by exploiting cooperative multi-path diversity, the improved signal detection at the primary receiver further contributes to a better TDOA estimation error from the trigger relay approach.

Appendix 5-1

According to the central limit theorem, a large number of random zero mean signals follow the Gaussian distribution. Therefore, the Gaussian distributed nature is more obvious as the signal length Q increases. We consider the random zero mean signal vector $\mathbf{y}_{rx}(k)=\left[y_{rx}(k)_1 \cdots y_{rx}(k)_i \cdots y_{rx}(k)_Q \right]$ for a very large signal length Q, and use $y_{rx}(k)$ to indicate any signal element; its probability density function follows the Gaussian distribution as

$$\begin{aligned} f\left(y_{rx}(k)\right) &= \frac{1}{\sqrt{2\pi\sigma_{rx}^2(k)}} e^{-\frac{\left(y_{rx}(k)-\mu_{rx}(k)\right)^2}{2\sigma_{rx}^2(k)}} \\ &= \frac{1}{\sqrt{2\pi\sigma_{rx}^2(k)}} e^{-\frac{y_{rx}^2(k)}{2\sigma_{rx}^2(k)}} \end{aligned} \qquad \text{(A5-1)}$$

For the skewness,

$$\lambda_{rx}(k)=\frac{1}{Q}\sum_{i=1}^{Q}\left(\frac{y_{rx}(k)_i-\mu_{rx}(k)}{\sigma_{rx}(k)}\right)^3$$
$$=\mathrm{E}\left(\left(\frac{y_{rx}(k)-\mu_{rx}(k)}{\sigma_{rx}(k)}\right)^3\right)$$
$$=\frac{\mathrm{E}\left(y_{rx}^3(k)\right)-3\mu_{rx}(k)\mathrm{E}\left(y_{rx}^2(k)\right)+2\mu_{rx}^3(k)}{\mathrm{E}\left(\sigma_{rx}^3(k)\right)}$$
$$=\frac{\mathrm{E}\left(y_{rx}^3(k)\right)}{\sigma_{rx}^3(k)} \qquad \text{(A5-2)}$$

and

$$\mathrm{E}\left(y_{rx}^3(k)\right)=\int_{-\infty}^{\infty}y_{rx}^3(k)\,f\left(y_{rx}(k)\right)dy_{rx}(k)$$
$$=\int_{-\infty}^{\infty}y_{rx}^3(k)1\Big/\left(\sqrt{2\pi\sigma_{rx}^2(k)}\right)\exp\left(-y_{rx}^2(k)/2\sigma_{rx}^2(k)\right)dy_{rx}(k) \qquad \text{(A5-3)}$$

Because $y_{rx}^3(k)1\Big/\left(\sqrt{2\pi\sigma_{rx}^2(k)}\right)\exp\left(-y_{rx}^2(k)/2\sigma_{rx}^2(k)\right)$ is the odd function with respect to $y_{rx}(k)$, the integral as shown in Eq. (A5-3) equals to 0, and consequently the skewness $\lambda_{rx}(k)=0$.

For the kurtosis,

$$\varepsilon_{rx}(k)=\frac{1}{Q}\sum_{i=1}^{Q}\left(\frac{y_{rx}(k)_i-\mu_{rx}(k)}{\sigma_{rx}(k)}\right)^4$$
$$=\frac{\mathrm{E}\left(y_{rx}^4(k)\right)-4\mu_{rx}(k)\mathrm{E}\left(y_{rx}^3(k)\right)+6\mu_{rx}^2(k)\mathrm{E}\left(y_{rx}^2(k)\right)-3\mu_{rx}^4(k)}{\mathrm{E}\left(\sigma_{rx}^4(k)\right)}$$
$$=\frac{\mathrm{E}\left(y_{rx}^4(k)\right)}{\sigma_{rx}^4(k)}, \qquad \text{(A5-4)}$$

and

$$\mathrm{E}\left(y_{rx}^4(k)\right)=\int_{-\infty}^{\infty} y_{rx}^4(k)\, f\left(y_{rx}(k)\right)dy_{rx}(k)$$

$$=2\int_0^{\infty} y_{rx}^4(k)\left(1/\sqrt{2\pi\sigma_{rx}^2(k)}\right)\exp\left(-y_{rx}^2(k)/2\sigma_{rx}^2(k)\right)dy_{rx}(k)$$

$$=-6\sigma_{rx}^3(k)/\sqrt{2\pi}\left[\int_0^{\infty}\exp\left(-y_{rx}^2(k)/2\sigma_{rx}^2(k)\right)dy_{rx}(k)\right] \qquad \text{(A5-5)}$$

According to the definition of the Gaussian integral, $\int_0^{\infty}\exp\left(-y_{rx}^2(k)/2\sigma_{rx}^2(k)\right)dy_{rx}(k)=\sqrt{2\pi}\sigma_{rx}(k)/2$. Therefore, $\mathrm{E}\left(y_{rx}^4(k)\right)=3\sigma_{rx}^4(k)$, and $\varepsilon_{rx}(k)=3$. This result means that for the Gaussian distributed zero mean signal, its kurtosis equals to 3. Thus, we can simply process $\varepsilon_{rx}(k)-3$, and classify the kurtosis as a zero convergence type features.

For the average symbol's phase, it can be regarded as the zero mean random value in the range of $(-\pi,\pi)$. Therefore, the average symbol's phase equals to zero.

Appendix 5-2

According to the MB-OFDM standard [23], the sampling frequency equals 528 MHz meaning a sample duration of 1.894 ns. The total number of samples per symbol equals 165, which includes a total number of subcarriers (FFT size) of 128 and a number of samples in zero-padded suffix of 37. Therefore, the symbol duration or block duration becomes 312.5 ns.

Chapter 6

Conclusions and recommendations

6.1 Conclusions

In this thesis, we studied cooperative wideband Orthogonal Frequency Division Multiplexing (OFDM) communication, and how to select relays and to allocate resources for improving the communication performance, while localization capabilities are considered as important research aspects in cooperative communication networks as well.

First, we focused on the performance of cooperative wideband communication based on the Zero-Padding (ZP)-OFDM. We investigated diversity, capacity and complexity scenarios in cooperative ZP-OFDM communication. In this research, we first reviewed the main features of ZP-OFDM and explain why ZP-OFDM is suitable for cooperative wideband communication. Then, we designed a cooperative tall Toeplitz scheme for the cooperative ZF-OFDM communication system, with different Carrier Frequency Offsets (CFOs) at different relays having multipath Rayleigh channel characteristics, i.e., we assume a doubly time-frequency selective channel. In the proposed cooperative tall Toeplitz scheme, the tall Toeplitz structure together with the frequency orthogonality of the channel matrix has a unique feature, which guarantees full cooperative and multipath diversity, and easily combats the CFOs only with Linear Equalizers (LEs). We derived the upper bound of the channel orthogonality deficiency, which provides an insight into how the change of channel factors affects the system performance in terms of Average Bit Error Rate (BER) performance and capacity. According to theoretical analysis and simulation results, only with linear equalizers, the cooperative tall Toeplitz scheme achieves the same cooperative, multipath and outage diversity as with Maximum-Likelihood Equalizers (MLEs), while the system complexity is reduced significantly.

Next, we investigated relay selection and resource allocation issues in cooperative communication. We therefore proposed a hybrid OFDM cooperative strategy for multi-node wireless networks employing both Decode-and-Forward (DF) and Amplify-and-Forward (AF) relaying.

Fully decoding is guaranteed by simply comparing Signal-to-Noise Ratio (SNR) at relay nodes to a SNR threshold, which is more efficient than utilizing a conventional cyclic redundant checking code. The lower bound and the upper bound of the SNR threshold were provided as well. After correct decoding, the DF protocol outperforms the AF protocol in terms of BER performance, which can be seen from Monte Carlo simulations as well as from analytical results. These results justify that the DF protocol is dominant in this hybrid cooperation strategy. For the suggested hybrid DF-AF cooperation protocol, we presented a dynamic optimal combination strategy for optimal AF selection. The closed-form BER expression of the hybrid OFDM cooperation in a Rayleigh fading channel was derived. The agreement between the analytical curves and numerical simulated results shows that the derived closed-form BER expression is suitable for the DF-dominant hybrid cooperation protocols.

Subsequently, we proposed relay selection and resource allocation and optimization schemes for cooperative wireless communication networks with interference using a game theoretical approach. We assumed a pricing game based on the so called Stackelberg game. Simulation results show that interference in a cooperative communication network can change the relay selection and resource allocation and optimization result. This should not be neglected from calculations in order to allow us for predicting the system behavior in an actual environment better than the case in which only noise is considered in the system. We found out that the pricing game for resource allocation and optimization, assuming the number of available nodes is high, can result in a high payment to relay nodes meaning that the source node utility function will be highly reduced. Therefore, we proposed an algorithm to limit the number of selected relay nodes to mitigate this problem. Using this algorithm, we chose a number of relay nodes where the result of resource allocation and optimization is still beneficial for the source node utility function.

Wideband scale-lag channels can be found in many applications, including ultra-wideband communications and underwater acoustic communications. Signaling and reception schemes using the wavelet theory enable multi-scale and multi-lag diversity in the wideband system. In our research, we designed a cooperative wavelet system to capture joint cooperative-scale-lag diversity. We proposed to use an analytical BER expression for the cooperative wavelet wideband communication.

The agreement between the analytical curves and numerical simulated results shows that the derived analytical BER expression is suitable for performance prediction of cooperative wavelet wideband communication. The compact and closed-form BER expression can easily provide an insight into the results as well as a heuristic help for the design of future cooperative wavelet wideband systems. For the suggested cooperative wavelet protocol, we also presented a dynamic optimal relay selection strategy, which maximizes the whole system transmission performance.

In this thesis, we also investigated cooperative relaying schemes for ZP-OFDM Time Difference of Arrival (TDOA) estimation; a feature-based cooperative TDOA estimation to achieve bandwidth efficient transmission is analyzed. A trigger relay technique is proposed to gain from easy processing together with noise and interference immunity of the base station to the relay link. Compared to AF relay and DF relay TDOA estimation cases, the trigger relay reduces the system complexity. Meanwhile, the trigger relay enables a bandwidth efficient TDOA, since it significantly reduces the amount of data for transmission. In terms of TDOA estimation error, among AF relay, trigger relay and DF relay with a block feature, the trigger relay achieves the best accuracy. Furthermore, by exploiting cooperative-multipath diversity, the improved signal detection at the primary receiver further contributes to a better TDOA estimation error, when using the trigger relay approach.

6.2 Recommendations for future works

In this thesis research, the tall Toeplitz structured channel is a strong merit for the ZP-OFDM based cooperative wideband communication system design, which brings various diversity gains in cooperative ZP-OFDM systems. It is recommended to keep the tall Toeplitz in future cooperative wideband system designs.

BER performance based relay selection schemes are intuitive. In our design, the compact and closed-form BER expression can easily provide good insight into results. It also may be a heuristic help for the design of future cooperative wireless systems. It is expected that the closed-form BER performance based relay selection schemes can be a good direction for future relay selection and resource allocation design.

We studied trigger relay issues within TDOA estimation scenarios for cooperative localization. Since its lower complexity and lower estimation error than when using conventional DF and AF relay, the trigger relay has potentials in other time measurement based cooperative localization applications.

References

[1] S. Barbarossa, *Multiantenna Wireless Communication Systems*, Norwood, MA: Artech House, 2005.

[2] G. J. Foschini, and M. Gans, "On the limits of wireless communication in a fading environment when using multiple antennas," *Wireless Personal Commun.*, vol. 6, pp. 311-335, Mar. 1998.

[3] J. N. Laneman, "Cooperative diversity in wireless networks: algorithm and architectures," Ph.D. dissertation, MIT. Cambridge, MA, Sep. 2002.

[4] A. Sendonaris, E. Erkip, and B. Aazhang, "User cooperation diversity—Part I: System description," *IEEE Transaction on Commun.*, vol. 51, no. 11, pp. 1927-1938, Nov. 2003.

[5] A. Sendonaris, E. Erkip, and B. Aazhang, "User cooperation diversity—Part II: Implementation aspects and performance analysis," *IEEE Trans. Commun.*, vol. 51, no. 11, pp. 1939-1948, Nov. 2003.

[6] K. J. R. Liu, A. K. Sadek, W. Su and A. Kwasinski, *Cooperative Communications and Networks*, Cambridge University Press, 2009.

[7] http://www.ict-codiv.eu/

[8] http://www.newcom-project.eu/

[9] R. van Nee and R. Prasad, *OFDM for Wireless Multimedia Communications*. Norwell, MA: Artech House, 2000.

[10] B. Muquet, Z. Wang, G. B. Giannakis, M. Courville and P. Duhamel, "Cyclic prefixing or zero padding for wireless multicarrier transmissions," *IEEE Transaction on Communications*, vol. 50, no. 12, pp. 2136-2148, Dec. 2002.

[11] A. Batra, J. Balakrishnan, G. R. Aiello and A. Dabak, "Design of a multiband OFDM system for realistic UWB channel environments," *IEEE Transaction on Microwave and Techniques*, vol. 52, no. 9, pp. 2123-2138, Sep. 2004.

[12] http://dret.net/lectures/web-fall09/img/internet-of-things.jpg

[13] A. Nosratinia, T. E. Hunter, and A. Hedayat, "Cooperative communciation in wireless networks," *IEEE Commun. Mag.*, vol. 42, pp. 74-80, Oct. 2004.

[14] T. M. Cover and A. A. El Gamal, "Capacity theorems for the relay channel," *IEEE Transaction on Inf. Theory*, vol. IT-25, pp. 572-584, Sep. 1979.

[15] G. Kramer, M. Gastpar, and P. Gupta, "Cooperative strategies and capacity theorems for relay networks," *IEEE Transaction on Inf. Theory*, vol. 51, pp. 3037-3063, Sep. 2005.

[16] H. Lu and H. Nikookar, "A thresholding strategy for DF-AF hybrid cooperative wireless networks and its performance", *Proc. IEEE Symposium on Communications and Vehicular Technology, (SCVT '09),* UCL, Louvain, Nov. 2009.

[17] H. Lu, H. Nikookar, and T. Xu, Chapter "OFDM communications with Cooperative relays", book chapter in "*Communications and Networking*", Sciyo publisher, ISBN/ISSN 978-953-307-114-5. Sep. 2010

[18] Z. Wang and G. B. Giannakis, "A simple and general parameterization quantifying performance in fading channels," *IEEE Trans. Wireless*

Communications, vol. 51, no. 3, pp. 1389-1298, Aug. 2003.
[19] A. Riberiro, X. Cai and G. B. Giannakis, "Symbol Error Probabilities for General Cooperative Links," *IEEE Transaction on Wireless Communications*, vol. 4, no. 3, pp. 1264-1273, May 2005.
[20] B. Muquet, Z. Wang, G. B. Giannakis, M. Courville and P. Duhamel, "Cyclic prefixing or zero padding for wireless multi-carrier transmissions," *IEEE Transaction on Communications*, vol. 50, no. 12, pp. 2136-2148, Dec. 2002.
[21] H. Lu, H. Nikookar, and H. Chen, "On the potential of ZP-OFDM for cognitive radio", *Proc. The 12th International Symposium on Wireless Personal Multimedia communications, (WPMC'09),* Sendai, Japan, 7-10, Sep. 2009.
[22] A. Batra, et al, "Multi-band OFDM physical layer proposal for IEEE 802.15Task Group 3a," IEEE P802.15-04/0493r1, Sep. 2004.
http://www.ieee802.org/15/pub/2003/Jul03/03268r2P802-15_TG3a-Multi-band-CFP-Document.pdf
[23] Standard ECMA-368 High Rate Ultra Wideband PHY and MAC Standard, 3rd edition, Dec. 2008.
http://www.ecma-international.org/publications/files/ECMA-ST/ECMA-368.pdf.
[24] H. Lu, T. Xu and H. Nikookar, "A Cooperative Scheme for ZP-OFDM with Multiple Carrier Frequency Offsets over Multipath Channel," *Proc. IEEE Vehicular Technology Conference (VTC)*, Budapest, Hungary, pp. 1-5, 15-18, May 2011.
[25] H. Lu, T. Xu, H. Nikookar and L. P. Ligthart, "Performance Analysis of the Cooperative ZP-OFDM: Diversity, Capacity and Complexity", *Springer International Journal on Wireless Personal Communications*, DOI: 10.1007/s11277-011-0470-9, 2011.
[26] B. Su and P.P. Vaidyanathan, "New blind block synchronization for transceivers using redundant precoders," *IEEE Transaction on Signal Processing*, vol. 56, no. 12, pp. 5987-6002, Dec. 2008.
[27] J. H. Manton and W. D. Neumann, "Totally blind channel identification by exploiting guard intervals," *Syst. Control Lett.*, vol. 48, no. 2, pp. 113-119, 2003.
[28] B. Zhao and M. C. Valenti, "Practical relay networks: a generalization of hybrid-ARQ," *IEEE Journal on Selected Areas in Communications,* vol. 23, pp. 7-18, 2005.
[29] H. Zhao and W. Su, "Cooperative wireless multicast: performance analysis and power/location optimization," *IEEE Transactions on Wireless Communications,* vol. 9, pp. 2088-2100, 2010.
[30] M. Kaneko, K. Hayashi, P. Popovski, K. Ikeda, H. Sakai, and R. Prasad, "Amplify-and-Forward Cooperative Diversity Schemes for Multi-Carrier Systems," *IEEE Transactions on Wireless Communications* vol. 7, pp. 1845-1850, May 2008.
[31] I. Krikidis, J. Thompson, S. Mclaughlin, and N. Goertz, "Max-min relay selection for legacy amplify-and-forward systems with interference," *IEEE Transactions on Wireless Communications,* vol. 8, pp. 3016-3027, 2009.
[32] E. Borel, *Applications aux jeux de hazard*, Gauthier-Villars, Paris, 1938.
[33] J. von Neumann and O. Morgenstern, *The Theory of Games and Economic Behavior*, Princeton University Press, 1947.

[34] J. Nash, “Equilibrium points in n-person games,” *Proceedings of the National Academy of Sciences*, vol. 36, no. 1, pp. 48-49, 1950.
[35] J. Nash, “Non-Cooperative Games,” *The Annals of Mathematics*, vol. 54, no. 2, pp. 286-295, 1951.
[36] W.A. Prasetyo, H. Lu and H. Nikookar, “Optimal relay selection and power allocation using game theory for cooperative networks with interference”, *Proc. European Microwave Conference (EuMC 2011),* Manchester, UK, pp. 37-40, 10-13, Oct. 2011.
[37] O. Ileri, M. Siun-Chuon, and N. B. Mandayam, “Pricing for enabling forwarding in self-configuring ad hoc networks,” in *Wireless Communications and Networking Conference, 2004. WCNC. 2004*, vol.2, pp. 1034-1039, 2004.
[38] N. Shastry and R. S. Adve, “Stimulating Cooperative Diversity in Wireless Ad Hoc Networks through Pricing,” in *IEEE International Conference on Communications, 2006. ICC '06.* vol. 8, pp. 3747-3752, 2006.
[39] B. Wang, Z. Han, and K. J. R. Liu, “Distributed Relay Selection and Power Control for Multiuser Cooperative Communication Networks Using Stackelberg Game,” *IEEE Transactions on Mobile Computing*, vol. 8, pp. 975-990, 2009.
[40] Y. Shi, J. Wang, K. Letaief, and R. Mallik, “A game-theoretic approach for distributed power control in interference relay channels,” *IEEE Transactions on Wireless Communications,* vol. 8, pp. 3151-3161, 2009.
[41] E. Kaplan, Ed., *Understanding GPS: Principles and Applications*. Reading, MA: Artech House, 1996.
[42] S. Gezici, Z. Tian, G. B. Giannakis, H. Kobayashi, A. F. Molisch, H. V. Poor and Z. Sahinoglu, “Localization via Ultra-Wideband radios: A look at positioning aspects for future sensor networks,” *IEEE Signal Process. Mag.*, vol. 22, no. 4, pp. 70–84, Jul. 2005.
[43] M. Z. Win, A. Conti, S. Mazuelas, Y. Shen, W. M. Gifford, D. Dardari and M. Chiani “Network localization and navigation via cooperation,” *IEEE Comm. Mag.*, vol. 49, no. 5, pp. 56-62, May 2011.
[44] Y. Shen, H. Wymeersch and M. Z. Win, “Fundamental limits of wideband localization—Part II: cooperative Networks,” *IEEE Transactions on Inform. Theory*, vol. 56, no. 10, pp. 4981-5000, Oct. 2010.
[45] F. Gustafsson and F. Gunnarsson, “Mobile positioning using wireless networks: Possibilities and fundamental limitations based on available wireless network measurements,” *IEEE Signal Process. Mag.*, vol. 22, pp. 41-53, Jul. 2005.
[46] G. Sun, J. Chen, W. Guo, and K. J. R. Liu, “Signal processing technique in network-aided positioning,” *IEEE Signal Process. Mag*., vol. 22, pp. 12-23, Jul. 2005.
[47] H. Wymeersch, J. Lien, and M. Z. Win, “Cooperative localization in wireless networks,” *Proc. IEEE*, vol. 97, no. 2, pp. 427-450, Feb. 2009.
[48] M. O. Hasna and M. –S. Alouini, “Performance analysis of two-hop relayed transmissions over Rayleigh-fading channels,” *Proc. Vehicular Technology Conf.*, Birmingham, AL, pp. 1992-1996, 2002.
[49] K. B. Letaief and W. Zhang, “Cooperative communications for cognitive radio networks,” *Proceedings of IEEE*, vol. 97, pp. 878-893, 2009.

[50] O. Oyman, J. N. Laneman, and S. Sandhu, "Multihop relaying for broadband wireless mesh networks: From theory to practice," *IEEE Commun. Mag.,* vol. 45, pp. 116-122, Nov. 2007.
[51] B. Hassibi and H. Vikalo, "On the sphere-decoding algorithm I. Expected complexity," *IEEE Transactions on Signal Process.*, vol. 53, no. 8, pp. 2806-2818, Aug. 2005.
[52] X. Ma, and G. B. Giannakis, "Full-diversity full-rate complex-field space-time coding," *IEEE Transactions on Signal Processing,* vol. 51, no. 11, pp. 2917-2930, Nov. 2003.
[53] W. Su, Z. Safar, and K. J. R. Liu, "Towards maximum achieveable diversity in space, time, and frequency: peraformance analysis and code design," *IEEE Transactions on Wireless Communications*, vol. 4, no. 4, pp.1847-1857, Jul. 2005.
[54] W. Su, Z. Safar, and K. J. R. Liu, "Maximum achieveable diversity in space, time advantage," *IEEE Transactions on Information Theory*, vol. 51, no. 1, pp.229-249, Jan. 2005.
[55] W. Zhang and K. B. Letaief, "Space-time/frequency coding for MIMO-OFDM in next generation broadband wireless systems," *IEEE Wireless Communications Magazine*, vol. 14, no. 3, pp. 32-43, Jun. 2007.
[56] X. Ma, and G. B. Giannakis, "Space-time-multi-path coding using digital phase sweeping or block circular delay diversity," *IEEE Transactions on Signal Processing,* vol. 53, no. 3, pp. 1121-1131, Mar. 2005.
[57] K. Fang and G. Leus, "Space-Time Block Coding for Doubly-Selective Channels," *IEEE Transaction on Signal Processing*, vol. 58, no. 3, pp. 1934-1940, Mar. 2010.
[58] X. Ma and W. Zhang, "Fundamental limits of linear equalizers: diversity, capacity, and complexity," *IEEE Transactions on Inform. Theory*, vol. 54, no. 8, pp. 3442-3456, Aug. 2008.
[59] W. Zhang, X. Ma, B. Gestner, and D. V. Anderson, "Designing low-complexity equalizers for wireless systems," *IEEE Communications Magazine*, vol. 47, no. 1, pp. 56-64, Jan. 2009.
[60] A. Scaglione, G. B. Giannakis, and S. Barbarossa, "Redundant filterbank precoders and equalizers—Part I: Unification and optimal designs and Part II: Blind channel estimation, synchronization and direct equalization," *IEEE Transactions on Signal Processing*, vol. 47, pp. 1988-2022, July 1999.
[61] B. Muquet, M. de Courville, P. Duhamel and V. Buzenae, "A subspace based blind and semi-blind channel identification method for OFDM systems," *proc. IEEE Workshop Signal Proc. Advances in Wireless Comm.,* Annapolis, MD, pp. 243-246, May 1999.
[62] Z. Wang and G. B. Giannakis, "Wireless multicarrier communications: Where Fourier meets Shannon," *IEEE Signal Processing Mag.*, vol. 17, pp. 29-48, May 2000.
[63] G. B. Giannakis, "Filterbanks for blind channel identification and equalization," *IEEE Signal Processing Lett.*, vol. 4, pp. 184-187, June 1997.
[64] G. B. Giannakis, Z. Liu, X. Ma and S. Zhou, *Space-Time Coding for Broadband Wireless Communications*, Wiley Publication, 2007.
[65] A. S.Avestimehr and D. N. C. Tse, "Outage capacity of the fading relay

channel in the low-SNR regime," *IEEE Transactions on Inf. Theory*, vol. 53, no. 4, pp. 1401-1415, Apr. 2007.
[66] I. E. Telatar, "Capacity of multi-antenna Gaussian channels," *Europ. Trans. Telecommun.*, vol. 10, no. 6, pp. 585-595, Nov.-Dec. 1999.
[67] V. Pammer, Y. Delignon, W. Sawaya, and D. Boulinguez, "A low complexity suboptimal MIMO receiver: The combined ZF-MLD algorithm," *Proc. Personal, Indoor and Mobile Radio Communications*, Beijing, China, vol. 3, pp. 2271-2275, Sep. 2003.
[68] C. Windpassinger, L. Lampe, R. F. H. Fischer, and T. Hehn, "A performance study of MIMO detectors," *IEEE Transactions on Wireless Commun.*, vol. 5, no. 8, pp. 2004-2008, Aug. 2006.
[69] J. K. Zhang, J. Liu, and K. M. Wong, "Linear Toeplitz space time block codes," *Proc. IEEE ISIT'05*, Adelaide, Australia, Sept. 2005.
[70] Y. Shang and X. G. Xia, "On space-time block codes achieving full diversity with linear receivers," *IEEE Transactions on Inform. Theory*, vol. 54, pp. 4528-4547, Oct. 2008.
[71] H. Wang, X. G. Xia and Q. Yin "Distributed space-frequency codes for cooperative communication system with multiple carrier frequency offsets," *IEEE Transactions on Wireless Communication*, vol. 8, pp. 1045-1055, Feb. 2009.
[72] J. N. Laneman, D. N. C. Tse, and G. W. Wornell, "Cooperative diversity in wireless networks: Efficient protocols and outage behavior," *IEEE Transactions on Information Theory,* vol. 50, pp. 3062-3080, 2004.
[73] A. S. Ibrahim, A. K. Sadek, W. Su, and K. J. R. Liu, "Cooperative communications with relay-selection: when to cooperate and whom to cooperate with?" *IEEE Transactions on Wireless Communications,* vol. 7, pp. 2814-2827, 2008.
[74] Z. Han, T. Himsoon, W. P. Siriwongpairat, and K. J. R. Liu, "Resource allocation for multiuser cooperative OFDM networks: Who helps whom and how to cooperate," *IEEE Transactions on Vehicular Technology,* vol. 58, pp. 2378-2391, June 2009.
[75] Federal Communications Commission, "Revision of part 15 of the commission's rules regarding ultra-wideband transmission systems, First report and order," ET Docket 98-153, FCC 02-48, pp. 1–118, Feb. 14, 2002.
[76] A. M. Sayeed and B. Aazhang, "Joint multipath-Doppler diversity in mobile wireless communications," *IEEE Transactions on Commun.*, vol. 47, pp.123-132, 1999.
[77] S. Rickard, R. Balan, V. Poor, and S. Verdu, "Canonical time-frequency, time-scale, and frequency-scale representations of time-varying channels," *J. Comm. Infor. Syst.*, vol. 5, pp.1-30, 2005.
[78] Y. Jiang and A. Papandreou-Suppappola, "Discrete time-scale characterization of wideband time-varying systems," *IEEE Transactions on Signal. Proces.*, vol. 54, pp.1364-1375, 2006.
[79] A. R. Margetts, P. Schniter, and A. Swami, "Joint scale-lag diversity in wideband mobile direct sequence spread spectrum systems," *IEEE Transactions on Wirel. Commun.*, vol. 6, pp. 4308-4319, 2007.
[80] T. Xu, G. Leus, and U. Mitra. "Othogonal wavelet division multiplexing for

wideband time-varying channels." *Proc. IEEE ICASSP*, Prague (Czech Republic), pp. 3556-3559, May 2011.
[81] G. Leus, T. Xu, and U. Mitra. "Block Transmission over Multi-Scale Multi-Lag Wireless Channels." *Proc. of the Asilomar Conference on Signals, Systems, and Computers*, Pacific Grove, California, USA, Nov. 2010.
[82] S. Rickard, "Time-frequency and time-scale representations of doubly spread channels," Ph.D. dissertation, Applied and Computational Mathematics Dept., Princeton Univ., Princeton, NJ, Nov. 2003.
[83] A. Bircan, S. Tekinay, and A. Akansu, "Time-frequency and time-scale representation of wireless communication channels," *Proc. IEEE Int. Symp. Time-Frequency/Time-Scale Analysis*, Pittsburgh, PA, pp. 373-376, Oct. 1998.
[84] I. R. Capoglu, Y. Li, and A. Swami, "Effect of doppler spread in OFDM based UWB systems," *IEEE Transactions on Wireless Communictations*, vol. 4, no. 5, pp. 2559-2567, Sep. 2005.
[85] H. Zhang, H. H. Fan, and A. Lindsey, "A wavelet packet based model for time-varying wireless communication channels," *Proc. IEEE Workshop Signal Processing Advances Wireless Communications*, pp. 50-53, Mar. 2001.
[86] M. Johnson, L. Freitag, and M. Stojanovic, "Improved Doppler tracking and correction for underwater acoustic communications," *Proc. IEEE Int. Conf. Acoustic, Speech, Signal Processing*, vol. 1, Germany, pp. 575-578, Apr. 1997.
[87] B. S. Sharif, J. Neasham, O. R. Hinton, and A. E. Adams, "A computationally efficient Doppler compensation system for underwater acoustic communications," *IEEE J. Oceanic Eng.*, vol. 25, no. 1, pp. 52-61, Jan. 2000.
[88] U. Mitra and G. Leus, "Equalizers for multi-scale / multi-lag wireless channels," *Proc. IEEE Global Telecommunications Conference,* pp. 1-5, 2010.
[89] G. Acosta, K. Tokuda, and M. A. Ingram, "Measured joint Doppler-delay power profiles for vehicle-to-vehicle communications at 2.4 GHz," *Proc. IEEE Global Telecommunications Conference,* pp. 3813-3817, 2004.
[90] G. Acosta and M. A. Ingram, "Six time- and frequency-selective empirical channel models for vehicular wireless LANs," *1st IEEE International Symposium on Wireless Vehicular Communications*, Sep. 2007.
[91] R. E. Blahut, W. Miller Jr., and C. H. Wilcox, Eds., *Radar and Sonar, Part I, IMA Volumes in Mathematics and its Applications*. New York: Springer-Verlag, 1991.
[92] L. G. Weiss, "Wavelets and wideband correlation processing," *IEEE Signal Process. Mag.*, vol. 11, no. 1, pp. 13-32, Jan. 1994.
[93] R. K. Young, *Wavelet Theory and Its Applications*. Norwell, MA: Kluwer, 1993.
[94] M. K. Tsatsanis and G. B. Giannakis, "Time-varying system identification and model validation using wavelets," *IEEE Transactions on Signal Process.*, vol. 41, no. 12, pp. 3512-3523, Dec. 1993.
[95] G. Farhadi and N. C. Beaulieu, "On the Ergodic Capacity of Wireless Relaying System over Rayleigh Fading Channels," *IEEE Transactions on Wireless Communications*, vol. 7, no. 11, pp. 4462-4467, Nov. 2008.
[96] S. Lin and D. J. Constello, Jr., *Error Control Coding: Fundamentals and Applications*. Englewood Cliffs, NJ: Prentice–Hall, 1983.

[97] J. G. Proakis, *Digital Communications*, 4th ed., McGraw Hill, New York, 2001.
[98] W. A. Prasetyo, "Relay Selection and Resource Allocation in Cooperative Wireless Communication Networks," Msc. Thesis, Delft University of Technology, Aug. 2011.
http://repository.tudelft.nl/view/ir/uuid%3Afb1f77a5-7c2e-4f7a-b0cc-640db7b6df9b/
[99] G. Leus and P. van Walree, "Multiband OFDM for covert acoustic communications, " *IEEE J. Sel. Area. Comm.*, vol. 26, pp. 1662-1673, 2008.
[100] B. Li, S. Zhou, M. Stojanovic, L. Freitag, and P. Willett, "Multicarrier communication over underwater acoustic channels with nonuniform doppler shifts," *IEEE J. Oceanic. Eng.*, vol. 33, pp. 198-209, 2008.
[101] M. Martone. "Wavelet-based separating kernels for array processing of cellular ds/cdma signals in fast fading," *IEEE Transactions on Commun.*, vol. 48, pp. 979-995, 2000.
[102] L. Yu and L. B. White. "Optimum receiver design for broadband Doppler compensation in multipath/doppler channels with rational orthogonal wavelet signaling," *IEEE Transactions on Signal. Proces.*, vol. 55, pp. 4091-4103, 2007.
[103] S. L. Linfoot, M. K. Ibrahim, and M. M. Al-Akaidi, "Orthogonal wavelet division multiplex: An alternative to ofdm," *IEEE Transactions on Consum. Electr.*, vol. 53, pp. 278-284, 2007.
[104] H. Lu, T. Xu, M. Lakshmanan, and H. Nikookar, "Cooperative wavelet communication for multi-relay, multi-scale and multi-lag wireless channels", *Proc. IEEE Vehicular Technology Conference (VTC)*, Budapest, Hungary, pp. 1-5, 15-18, May 2011.
[105] H. Lu, T. Xu and H. Nikookar, "Cooperative Communication over Multi-scale and Multi-lag Wireless Channels", to appear in book chapter in "*Ultra Wideband*", InTech publisher, ISBN 979-953-307-809-9
[106] D. E. Iverson, "Coherent processing of ultra-wide-band radar signals," *Proc. Inst. Elect. Eng. Radar, Sonar, Navigation*, vol. 141, pp. 171-179, Jun. 1994.
[107] G.W. Wornell, "Emerging applications of multirate signal processing and wavelets in digital communications,'' *Proc. IEEE*, vol. 84, pp. 586-603, Apr. 1996.
[108] C. Patel, G. Stüber and T. Pratt, "Statistical properties of amplify and forward relay fading channels," *IEEE Transactions on Veh. Technol.*, vol. 55, no. 1, pp. 1-9, Jan. 2006.
[109] R. Louie, Y. Li, H. A. Suraweera and B. Vucetic, "Performance analysis of beamforming in two hop amplify and forward relay network with antenna correlation," *IEEE Transactions on Wireless Communications*, vol. 8, no. 6, pp. 3132-3141, Jun. 2009.
[110] A. K. Sadek, W. Su and K. J. R. Liu, "Multi-node cooperative communications in wireless networks," *IEEE Transactions on Signal Processing*, vol. 55, no. 1, pp. 341-355, Jan. 2007.
[111] D.H. Shin and T.K. Sung, "Comparisons of error characteristics between TOA and TDOA positioning," *IEEE Transactions on Aerosp. Electron. Syst.*, vol. 38, no. 1, pp. 307-311, Jan. 2002.
[112] R. K. Martin, J. S. Velotta, and J. F. Raquet, "Bandwidth Efficient

Cooperative TDOA Computation for Multi-carrier Signals of Opportunity," *IEEE Transactions on Signal Processing*, vol. 57, no. 6, pp. 2311-2322, Jun. 2009.
[113] [9] M. Z. Win and R. A. Scholtz, "Characterization of ultra-wide bandwidth wireless indoor communications channel: A communication theoretic view," *IEEE J. Sel. Areas Commun.*, vol. 20, pp. 1613-1627, Dec. 2002.
[114] N. Patwari, J. N. Ash, S. Kyperountas, A. O. Hero, III, R. L. Moses, and N. S. Correal, "Locating the nodes: Cooperative localization in wireless sensor networks," *IEEE Signal Process. Mag*., vol. 22, pp. 54-69, Jul. 2005.
[115] H. Lu, P. Martinez and H. Nikookar, "Cooperative TDOA Estimation with Trigger Relay," *Proc. IEEE International Symposium on Personal, Indoor and Mobile Radio Communications (PIMRC 2011)*, Toronto, Canada, pp. 1309-1313, 11-14, Sep. 2011.

List of abbreviations

ACK	Acknowledgement
AF	Amplify-and-Forward
AOA	Angle-of-Arrival
AP	Access Point
APAS	All Participate All Sub-carrier
AP-RS	All Participate Rate Splitting
ARQ	Automatic Repeat re-Quest
AvgBRS	Average Best Relay Selection
AWGN	Additive White Gaussian Noise
BER	Bit-Error Rate
BFSK	Binary Frequency Shift Keying
BPSK	Binary Phase Shift Keying
CDF	Cumulative Density Function
CF	Compress-and-Forward
CFOs	Carrier Frequency Offsets
CP	Cyclic Prefix
CR	Cognitive Radio
CSI	Channel State Information
DF	Decode-and-Forward
DPS	Digital Phase Sweeping
DSSS	Direct Sequence Spread Spectrum
ECMA	European Computer Manufacturers Association
FFT	Fast Fourier Transform
FIR	Finite Impulse Response
GPS	Global Positioning System
HPA	High-Power Amplifier
ICI	Inter-Carrier Interference
IFFT	Inverse Fast Fourier Transform
ISI	Inter-Symbol Interference
LEs	Linear Equalizers
LOS	Line-of-Sight
LS	Least-Squares
LTV	Linear Time-Varying
MB	Multi-Band
MGF	Moment Generating Function
MIMO	Multiple-Input-Multiple-Output
MLEs	Maximum-Likelihood Equalizers
MMSE	Minimum Mean Square Error
MRC	Maximal Ratio Combiner
M2M	Machine-to-Machine
NLOS	Non Line-of-Sight
od	orthogonality deficiency

OFDM	Orthogonal Frequency Division Multiplexing
OLA	Overlap and Add
OWDM	Orthogonal Wavelet Division Multiplexing
PAPR	Peak to Average Power Ratio
PDF	Probability Density Function
PP	Peak Power
PSBRS	Per Sub-carrier Best Relay Selection
PSD	Power Spectral Density
PSK	Phase Shift Keying
QAM	Quadrature Amplitude Modulation
QPSK	Quadrature Phase Shift Keying
RBS	Random Based Selection
RFID	Radio-Frequency Identification
RSS	Received-Signal-Strength
RTOA	Round-trip Time-of-Arrival
SD	Sphere Decoding
SFC	Space Frequency Coding
SINR	Signal-to-Interference plus Noise Ratio
SNR	Signal-to-Noise Ratio
STC	Space Time Coding
STFC	Space Time Frequency Coding
TDOA	Time Difference of Arrival
TOA	Time of Arrival
UWB	Ultra Wide Band
V2V	Vehicle-to-Vehicle
ZF	Zero-Forcing
ZP	Zero Padding

Notations

Symbol	*Description*
$(\cdot)^T$	transpose of $(\cdot)$
$(\cdot)^*$	conjugate of $(\cdot)$
$(\cdot)^H$	Hermitian of $(\cdot)$
$(\cdot)^{-1}$	inverse of $(\cdot)$
$(\cdot)^\dagger$	pseudo inverse of $(\cdot)$
$\forall$	for all
$\in$	is a element of
$\lvert\cdot\rvert$	absolute value of a scalar or cardinality of a set
$\lVert\cdot\rVert$	2-norm of a vector/matrix
$\equiv$	congruence relation
$:=$	definition
$\sum$	summation
$\prod$	product
∂	partial derivative
$\mathrm{argtan}(\cdot)$	inverse tangent function of $(\cdot)$
$\arg\min(\cdot)$	argument of minimum of $(\cdot)$
$\arg\max(\cdot)$	argument of maximum of $(\cdot)$
$\mathrm{diag}(\cdot)$	diagonal matrix with main diagonal $(\cdot)$
$\det(\cdot)$	determinant of $(\cdot)$
$\exp(\cdot)$	exponential function of $(\cdot)$
$\mathrm{Im}(\cdot)$	imaginary part of $(\cdot)$
$\lim(\cdot)$	limit of $(\cdot)$
$\log(\cdot)$	logarithm with base 10
$\log_2(\cdot)$	logarithm with base 2
$\ln(\cdot)$	logarithm with base e
$\min(\cdot)$	minimum of $(\cdot)$
$\max(\cdot)$	maximum of $(\cdot)$
$od(\cdot)$	orthogonality deficiency of matrix $(\cdot)$
$O(\cdot)$	Landau notation
$\mathrm{Prob}(\cdot)$	probability of $(\cdot)$

$\mathrm{rank}(\cdot)$	rank of $(\cdot)$
$\mathrm{Re}(\cdot)$	real part of $(\cdot)$
$\mathrm{sign}(\cdot)$	sign function of $(\cdot)$
$\sup(\cdot)$	supremum of a set $(\cdot)$

Acknowledgements

First and foremost, I owe my deepest gratitude to my daily supervisor Dr. Nikookar. You guided and supported me with care and promptness, and always patiently encouraged and helped me to come up with new ideas and cope with difficulties. Your cooperation and enthusiasm made me regard you as my friend, who I appreciate sincerely from heart.

Furthermore, I am also most grateful to Prof. Ligthart, my promotor during the Ph. D. study. You provide always help and concern to me and spent a lot of effort to improve my research quality. Without your support, finishing my Ph. D. journey would have been impossible.

I would like to express my special thanks to Prof. Yarovyi for your financial support and spiritual encouragement.

I would like to thank Chinese Scholarship Council for funding my research work in The Netherlands.

I would like to deliver my most sincerely thanks to Mrs Mia van der Voort-Kester, Ms.Wendy Murtinu, Ms. Jerney van Ooijen, Ms. Stefanie van Gentevoort, Ms. Dominique Meijer, Ms. Marjon Verkaik, Ms. Laura Bauman, for your tireless cooperation. You helped me to deal with all the administration affairs.

My heartiest appreciations go to my lab mates and peers in IRCTR/MS3 Xiaohua Lian, Madan K. Lakshmanan, Dr. Galina Babur, Zongbo Wang, Bill Yang, Xiaodong Zhuge, Yuan He, Venkat Roy, Ibrahim Budiarjo, Pascal Aubry, Johan Zijderveld, D. Penkin, Dr. Diego Caratelli. The interesting discussions with you made my research life enjoyable. I would like to acknowledge my master students in IRCTR: Pablo Martinez Grande，Wahyu Adhi Prasetyo. Special thanks to Tao Xu from the Circuit and System (CAS) group, for the cooperative research on signal processing.

I would like to express my special gratitude to Richard Mendes for helping me to translate my thesis summary into Dutch.

Finally, I would like to dedicate this thesis to my family, for your

endless love, support and concern; I would have never undertaken my doctoral study without your encouragement.

Hao Lu
Den Haag, 6 February 2013

About the author

Hao Lu was born in 1981, in Longyan City, Fujian Province, China. He received the B. Eng. and M. Eng. degrees in communication engineering from the Jilin University, China, and was granted with the Outstanding Graduate Student Award in 2004. In 2004, he won the Third Prize in the National Instruments (NI) Graduate Design National Contest (China).

In 2007, he received a grant from the China Scholarship Council for a Doctoral Scholarship, and started his PhD studies at the International Research Center for Telecommunications and Radar (IRCTR) / Microwave Sensing, Signal and System (MS3) of Delft University of Technology (TU Delft), where he is currently conducting researching on cooperative Orthogonal Frequency Division Multiplexing (OFDM) communication, ultra wideband communication and wireless localization technology.

Publications by the author

Book chapter

[1] H. Lu, T. Xu and H. Nikookar, "Cooperative Communication over Multi-scale and Multi-lag Wireless Channels", book chapter in "*Ultra Wideband*", InTech publisher, ISBN 978-953-51-0781-1. Oct. 2012.
[2] H. Lu, H. Nikookar and T. Xu, "OFDM Communications with Cooperative Relays", book chapter in "*Communications and Networking*", Sciyo publisher, ISBN 978-953-307-114-5. Sep. 2010.

Journal paper

[3] H. Lu, T. Xu, H. Nikookar and L. P. Ligthart, "Performance Analysis of the Cooperative ZP-OFDM: Diversity, Capacity and Complexity", *Springer International Journal on Wireless Personal Communications*, DOI: 10.1007/s11277-011-0470-9, Dec. 2011.
[4] H. Lu, H. Nikookar and L. P. Ligthart, "Wideband Localization using Cooperative Relays", to be submitted to IEEE Aerospace and Electronic Systems Magazine.
[5] H. Lu, H. Nikookar and L. P. Ligthart, "Cooperative TDOA Estimation with High Resolution, Low Complexity and Bandwidth Efficiency", to be submitted to IEEE Wireless Communications Letters.

Conference paper

[6] H. Lu and H. Nikookar, "Cooperative Feature-based TDOA Estimation with Multipath Diversity", *Proc. IEEE Symposium on Communications and Vehicular Technology, (SCVT '12),* Eindhoven, The Netherlands, pp. 1-5, Nov. 2012.
[7] T. Xu, Z. Tang, H. Lu and R. van Leuken, "Memory and Computation Reduction for Least-Square Channel Estimation of Mobile OFDM Systems", *Proc.IEEE International Symposium on Circuits and Systems (ISCAS 2012)*, Seoul, Korea, pp. 1259-1262, 20-23, May 2012.
[8] H. Lu, P. Martinez and H. Nikookar, "Cooperative TDOA Estimation with Trigger Relay," *Proc. IEEE International Symposium on Personal, Indoor and Mobile Radio Communications (PIMRC 2011)*, Toronto, Canada, pp. 1309-1313, 11-14, Sep. 2011.

[9] W.A. Prasetyo, H. Lu and H. Nikookar, "Optimal relay selection and power allocation using game theory for cooperative networks with interference", *Proc. European Microwave Conference (EuMC 2011),* Manchester, UK, pp. 37-40, 10-13, Oct. 2011.
[10] H. Lu, T. Xu, M. Lakshmanan, and H. Nikookar, "Cooperative wavelet communication for multi-relay, multi-scale and multi-lag wireless channels", *Proc. IEEE Vehicular Technology Conference (VTC)*, Budapest, Hungary, pp. 1-5, 15-18, May 2011.
[11] H. Lu, T. Xu and H. Nikookar, "A Cooperative Scheme for ZP-OFDM with Multiple Carrier Frequency Offsets over Multipath Channel," *Proc. IEEE Vehicular Technology Conference (VTC)*, Budapest, Hungary, pp. 1-5, 15-18, May 2011.
[12] T. Xu, R.van Leuken, H. Lu and H. Nikookar, "A Cooperative Communication with Grouped Relays for Zero-Padding MB-OFDM", *Proc. 2010 IEEE International conference on Information theory and Information security*, Beijing, China, pp. 927-931, 17-19, Dec. 2010.
[13] H. Lu, T. Xu and H. Nikookar, "Performance Analysis of the STFC for Cooperative ZP-OFDM Diversity, Capacity, and Complexity", *Proc. The 13th International Symposium on Wireless Personal Multimedia communications, (WPMC'10)*, Recife, Brazil, 11-14, Oct. 2010.
[14] H. Lu, H. Nikookar and X. Lian, "Performance evaluation of hybrid DF-AF OFDM cooperation in Rayleigh Channel", *Proc. European Wireless Technology Conference (EuWIT 2010)*, Paris, France, pp. 85-88, 27-28, Sep. 2010.
[15] H. Lu and H. Nikookar, "A thresholding strategy for DF-AF hybrid cooperative wireless networks and its performance", *Proc. IEEE Symposium on Communications and Vehicular Technology, (SCVT '09),* UCL, Louvain, Nov. 2009.
[16] H. Lu, H. Nikookar, and H. Chen, "On the potential of ZP-OFDM for cognitive radio", *Proc. The 12th International Symposium on Wireless Personal Multimedia communications, (WPMC'09),* Sendai, Japan, 7-10, Sep. 2009.

Relationship of chapters with publications

The following table indicates the relevance of the publications to the chapters

publication	chapter 1	chapter 2	chapter 3	chapter 4	chapter 5	chapter 6
1				√		√
2		√		√		√
3	√	√	√			√
4	√	√			√	√
5					√	√
6					√	√
7			√			
8	√				√	√
9		√		√		√
10	√			√		√
11			√			√
12			√			
13			√			√
14	√			√		√
15		√		√		√
16		√	√			√